Modelling colloidal facilitated radionuclide filtration in porous media

Thesis submitted in accordance with the requirements of the University of Liverpool for the degree of Doctor in Philosophy

By Daniel Richard Tudor

February 2020

Abstract

The behaviour of colloidal particles within porous media is an active area of intense study within the nuclear industry, as colloidal particles can act as vectors for the transportation of radionuclides. Thus, modelling the behaviour of these particles helps better understand the likelihood of radionuclide transportation as well as, exploring the principle mechanisms that result in deposition and what conditions are required to retain colloidal particles within a porous media matrix. There are a number of different modelling conditions explored both macro, whereby porous media dynamics are investigated from a continuum point of view, and a more microscopic system where individual particles are modelled and their behaviours understood. These models allow for a full picture of particle behaviour and bed dynamics to be developed. The aim of this research is to analyse the use of agent based modelling method as an alternative way to further understand particle deposition and aggregation within porous media

Within the model, colloidal behaviours were simplified into key statements addressed as rules, where particle interactions with each other, were maintained within the parameters set by these rules. This allowed for a large number of particles to be modelled in comparison to current microscopic techniques, and addressing shortcomings of some of these techniques, such as the use of the primary minimum well depth from the standard DLVO equation.

This model was validated against both current experimental values and analytical solutions, where it was found to perform well in the estimation of colloidal aggregation rates and sizes. Furthermore, it was found that the behaviour of colloidal aggregation is not just limited to irreversible aggregation but indeed can be found to be influenced by the introduction of reversible aggregation, the rate of which was established by analysing the likelihood of aggregation under varying chemical conditions. Extensions of the models were then produced, in which a lattice Boltzmann flow field was constructed and validated along with particle trajectory equations. Allowing for particles to be investigated within an advective-diffusive environment.

The behaviour of particle deposition within varying chemical regimes was analysed where the ability for particles to deposit is heavily influenced by the role of the secondary minima. Without the incorporation of the secondary minima, particles where rejected from the system in opposition to the same experimental conditions. With the introduction of the secondary minima, breakthrough and deposition behaviour more closely matched experimental observations. Finally, the influence of surface chemistry and flow dynamics were addressed in which growth size and rates were seen to change dramatically under differing flow and surface conditions implying an inherent sensitivity to these parameters.

The behaviour of colloidal dynamics both in aggregation and deposition was accurately represented within the agent-based model allowing for an alternative modelling paradigm to be used in exploring the behaviours of colloidal particles within porous media.

Acknowledgements

I would like to thank the EPSRC and Sellafield Ltd for funding the research within this thesis along with NNL for offering supervision to the research. I would also like to thank the Next Generation Nuclear Centre for Doctoral Training without which, I would not have gained the skills needed to undertake this research. I am also extremely grateful to my supervisory team, Professor Karl Whittle, Dr Jonathan Bridge, Dr Mark Bankhead and Mr Peter Rand for their inputs on the direction the thesis should take. I would also like to extend a thanks to Dr Ming Li who regularly indulged my random discussions on fluid dynamics in his office.

Within the Next Generation Nuclear CDT, I would like to express specific thanks to Lee, Kevin, and Alex whose nights out in Manchester helped overcome the often stressful and intense periods of research. I also would like to thank the whole NGN CDT cohort 1. Within the School of Engineering, I would like thank my colleague Peyman for always being there to have a conversation on any part of colloidal sciences and other scientific discussions, as well as introducing me to Kurdish cuisine.

Finally, I would like to thank my family and friends for supporting me through the whole process. In particular, my parents and grandparents for their kind words. I would also like to express a deep heartfelt thanks to my partner Amy who spent the last 4 years offering every kind word and bit of support imaginable, whilst always pushing me.

Contents

Table of Figures

Nomenclature and abbreviations

Symbol	Definition
A	Cross-sectional area
A_H	Hamaker constant
a_p	Particle radius
B_x	Stokes-Einstein diffusion coefficient
C	Concentration
c	Lattice Boltzmann lattice speed
C_o	Initial particle concentration
C_D	Drag coefficient
C_L	Lift coefficient
D	Dispersion coefficient
d	Particle diameter
D_f	Fractal dimension
e	Elementary charge
$\overrightarrow{\boldsymbol{e_t}}$	Microscopic velocity
E_{born}	Born interaction energy
E_{elec}	Electrostatic interaction energy
E_k	Particle kinetic energy
E_{LJ}	Lennard-Jones interaction energy
E_{tot}	Total interaction energy between two particles
E_{vdw}	Van Der Waals interaction energy
f	Bed porosity
F^b	Buoyancy force
F^B	Brownian motion force
F^c	Interaction force
F^{drag}	Viscous drag force
F^G	Gravitational body force
$f_i(\vec{\boldsymbol{x}}, \vec{\boldsymbol{e}}_{\boldsymbol{i}}, \boldsymbol{t})$	Discrete probability distribution function
F_x	Force in the x direction
F_y	Force in the y direction
g	Gravitational acceleration
h	Separation distance
I	Ionic strength
j	Particle flux
k	Deposition coefficient
K	Aggregation collision kernel
k_o	Fractal prefactor
K_a	Attachment coefficient
k_B	Boltzmann constant
K_d	Detachment coefficient
k_{DLVO}	Aggregation rate with potential barrier
k_{fast}	Aggregation rate without potential barrier
K_r	Attachment coefficient during ripening
l	Thickness of the flow area
l_o	LBM characteristic length scale

L_x	Lever arm which the torque is applied to
Ma	Mach number
m_p	Mass of the colloid
N	Length of LBM domain
n	Particle size number
N_a	Avogadro's constant
N_{iter}	Total number of LBM time steps
n_k	Aggregate size
N_{tot}	Total number of particles
N_u	Zero-mean Gaussian distribution for the velocity
N_x	Zero-mean Gaussian distribution for the displacement
Pe	Peclet number
Q	Keesom, Debye, London energy constant
Q_f	Flow rate
r_{com}	Centre of mass of aggregate
Re	Reynolds number
R_g	Radius of gyration
r_k	Vector location of particle from reference point
Sec_{well}	Secondary minima depth
t	Time
T	Temperature
t_o	LBM characteristic time scale
$T_{adhesive}$	Adhesive Torque
$T_{applied}$	Applied torque from hydrodynamic forces
$\mathbf{u}(\mathbf{x},t)$	Macroscopic fluid velocity
U_{max}	Maximum fluid veloity
U_p	Particle velocity
U_r	Instantaneous velocity
u_s	Local fluid velocity
ν	Fluid kinematic viscosity
V_o	Upstream velocity
v_p	Velocity of the colloid
W	Stability ratio
x	Domain length
x_p	Particle displacement
y_{max}	Maximum width of two plates in Poiseuille flow
z_i	Ionic valence
α	Attachment efficiency
β	Collision percentage
ΔP	Pressure driven force
δt	Discrete time interval
δx	Discrete space interval
ε	Permittivity of a vacuum
ε_o	Dielectric constant
ε_{well}	Well depth

η	Collector efficiency
κ	Debye constant
μ	Fluid dynamic viscosity
ν_{lb}	LBM fluid viscosity
ν_{pore}	Average pore velocity
ξ_1 and ξ_2	Zeta potentials
ξ_x and ξ_v	Random number sampled from Zero-mean Gaussian distribution
$\rho(x,t)$	Macroscopic fluid density
ρ_1 & ρ_2	Particle number density
ρ_f	Fluid density
ρ_p	Particle density
ρ_z	Particle charge density
σ	Specific deposit
σ_c	Collision diameter
σ_r	Transient specific deposit
σ_u	Final specific deposit
τ	Rate of reaction relaxation time
τ_{lbm}	LBM single relaxation time
τ_p	Particle relaxation time
τ_p	Particle relaxation time
ϕ	Volume fraction
ψ	Electric potential
ω	Velocity gradient
ω_i	Weighting functions

Abbreviation	Definition
ABM	Agent based modelling
CAS	Complex adaptive systems
CCC	Critical coagulation constant
CFD	Computational fluid dynamics
CFT	Colloid filtration theory
DLA	Diffusion limited aggregation
DLVO theory	Derguin-Landua-Verwey-Overbeek theory
DNS	Direct numerical solution
FDM	Finite difference method
FEM	Finite element method
FVM	Finite volume method
HPC	High performance computing
LBM	Lattice Boltzmann method
LES	Large eddy simulation
LPT	Lagrangian particle tracking
MSP	Magnox Storage Pond
RANS	Reynolds-averaged Navier-Stokes
RLA	Reaction limited aggregation
SGC	Stern-Guoy-Chapman
SIXEP	Site Ion Exchange Effluent Plant
X-DLVO theory	Extended Derguin-Landua-Verwey-Overbeek theory
SDE	Stochastic differential equation
IS	Ionic Strength

Chapter 1. Introduction

1.1 Motivation

The processes required to remove colloidal particles from effluent streams are of particular importance when describing both industrial and environmental systems, where emphasis is placed on the effective removal of colloidal particles. The use of porous media is an active area of research in understanding and optimising their removal from effluent streams. Active research has been undertaken since the mid-1950's developing the necessary analytical and experimental models required to fully understand this problem (Bradford and Torkzaban, 2008).

It has been established that the filtration of colloidal particles within a porous media bed can be considered a many body problem in which numerous processes are being undertaken by the depositing particles (Auset and Keller, 2006). These processes are often complex to characterise and as such, are usually neglected for more simplified assumptions (Kulkarni, Sureshkumar and Biswas, 2005). In which case, bed dynamics can be poorly described by current modelling techniques when compared to their experimental counterpart (Kulkarni, Sureshkumar and Biswas, 2003). It is understood that colloidal dynamics within porous media relies on a complete understanding of the various processes undertaken, in particular, the particle-fluid, particle-particle, particle-collector interfaces all offer varying degrees of complexity which are usually ignored or simplified when predicting the bed dynamics (Bradford, Torkzaban and Simunek, 2011). Each of these processes can be described dynamically and offer clarity on the processes being undertaken within the porous media.

The behaviour of bed dynamics is particularly important when predicting filtration rates, saturation rates, and subsequent pressure loss across the porous media due to clogging (Bradford, Torkzaban and Simunek, 2011). Each of these offers an understanding on the performance on the porous media bed and how efficient the removal process is. In particular, current descriptions of monolayer deposition within the porous media under predicts the rate of head loss (Veerapaneni and Wiesner, 1997). When a critical threshold is met contaminant breakthrough can occur directly affecting purification processes further downstream (Adin and Rajagopalan, 1989). By including multi-layer deposition of colloidal particles, a more accurate understanding of the bed dynamics can be predicted.

Multi-layer deposition is a process which is extremely sensitive to both surface chemistry, flow conditions and particle transportation within the porous media. It is now understood that including multilayer interactions a more complete picture of the bed dynamics can be formed in which three fundamental processes occur (Henry, Minier and Lefèvre, 2012):

1. Initial monolayer deposition onto the collector surface
2. Ripening of the deposition (secondary particle deposition on previously deposited particles)
3. Clogging (pore structures are completely blocked by deposited particles)

Stage 1 of this processes is traditionally described as particles being deposited directly onto the collector surface and as such, only collector-particle surface chemistry is analysed. Stage 2, offers the ability for multi-layer deposits to grow along with particles being released back into the flow and removed from the porous media. Finally, stage 3, describes the point at which bed saturation occurs and particles are removed from the porous media (Figure 1.1).

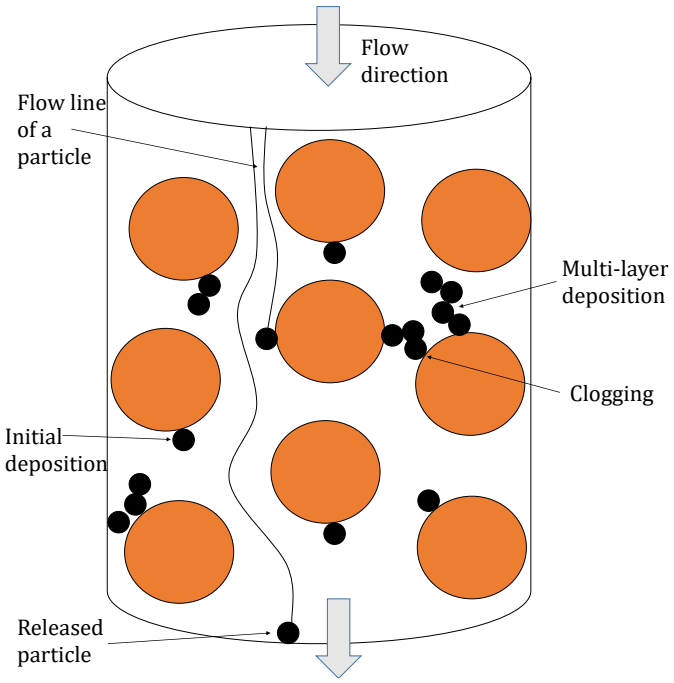

Figure 1.1 Key mechanisms within porous media for particle transportation and deposition with key processes highlighted such as initial deposition, multilayer deposition and clogging

Though, the use of a multi-layer deposition model has offered some refinement to the colloid filtration problem there are still a number of issues which need to be addressed. The behaviour of colloidal deposits on the collector surface have been understood to be associated with the force balance between the adhesive surface and shear forces along the surface of the collector (Torkzaban, S. A. Bradford and Walker, 2007a). By analysing these forces it is now understood that deposition on the collector surface is not irreversible and particles can be removed from the collector surface with the relevant shear flow.

In addition, these removed or re-entrained particles may not solely exist as individual particles, but are more likely to be collections of particles or "flocs". Traditionally, this was an area which had received less focus than other attachment mechanisms (Veerapaneni and Wiesner, 1997). Recently, there has been an increase in research on how geometry and size of particle deposits effect pore space geometry and performance

(Chen *et al.*, 2009). Consequently, the standard use of purely attachment and collector efficiency coefficients when modelling colloidal filtration can underestimate the breakthrough of materials (Nathalie Tufenkji and Elimelech, 2004). By addressing the floc size which grew due to variations in flow and surface chemistry, and incorporating this within the standard colloid filtration theory, it will allow for a more accurate understanding of the bed dynamics.

An issue which has been overlooked until recently, is the numerous attachment mechanisms which occur when colloids are deposited either, onto the collector surface or already deposited particles. Commonly within the literature, the DLVO (Derjaguin-Landau-Verwey-Overbeek) theory is used to approximate the force balance between two interacting surfaces (Torkzaban *et al.*, 2015). The most commonly applied version of this theory is to assume an infinite primary minimum which describes complete, irreversible deposition. However, it is understood that the secondary minima is more important in understanding colloidal deposition, in particular, its role in the re-entrainment of deposited colloidal particles (Tufenkji and Elimelech, 2005; Shen *et al.*, 2007). Though this is important, the likelihood of a particle being deposited in the secondary minima and the sensitivity to this deposition is still poorly understood. Extensions to the DLVO theory exists, referred to as X-DLVO, where other mechanisms associated with the force balance are incorporated, within the standard equation. The introduction of a Born potential within the equation removes the infinite primary well approximation and produces a more realistic energy balance between the two surfaces (Shen *et al.*, 2010). When addressing the problem of particulate breakthrough within porous media, this is important to not underestimating the likelihood of removal for particles which were previously assumed to be irreversibly attached.

Finally, when compared to the experimental analysis of breakthrough and attachment of colloidal particles, there can be significant discrepancy between the approximated results from colloidal filtration theory and that of the experimentally derived results (Saiers, Hornberger and Liang, 1994). Such uncertainty surrounding the results attributed to the colloidal filtration theory is particularly important across a number of industrial applications where a guarantee of removal is expected to meet strict environmental requirements. In particular, within the UK's nuclear industry it is an imperative that an accurate representation of the removal of colloidal particles is captured as these particles offer a vector for radionuclides to translate through the environment.

1.2 Industrial relevance– Nuclear waste

The majority of the nuclear waste is from the decommissioning of nuclear plants, legacy wastes, and research and development facilities (World Nuclear Association, 2017). Removal of radionuclides from effluents streams are of utmost importance when processing nuclear waste. As such, large scale industrial reprocessing plants are used to ensure that adequate volumes of liquid waste are processed and cleaned before discharge back into the natural environment. At the Sellafield Nuclear Site, this process is captured using the Site Ion Exchange Effluent Plant (SIXEP) which focuses on the reduction and removal of radionuclides.

1.2.1 Site Ion Exchange Effluent Plant

The Site Ion Exchange Effluent Plant is the main reprocessing plant for radioactive liquid effluents produced by the Magnox Storage Ponds (MSP) and is vitally important in ensuring a reduction in environmental impact. SIXEP is predominately designed to

remove radionuclide's (mainly Cs-137 & Sr-90) along with other alpha emitting particulates before sea discharge into the Irish Sea (Dyer *et al.*, 2018).

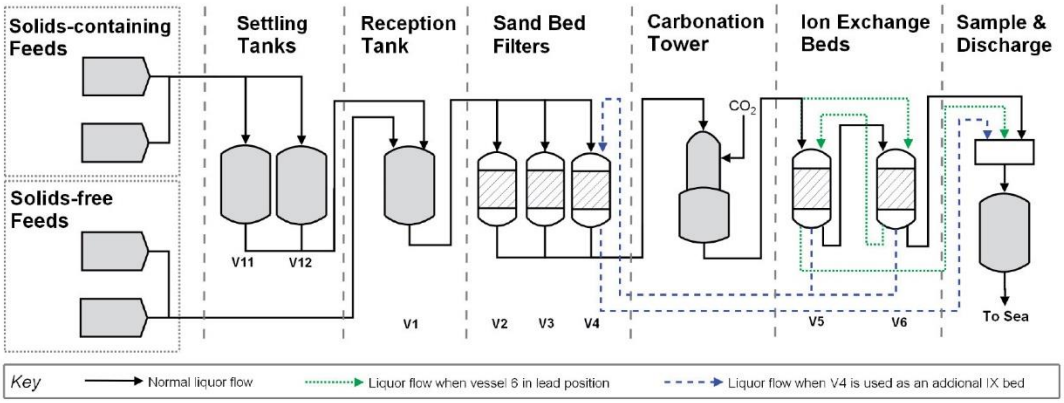

Figure 1.2 The SIXEP flow sheet (taken from Dyer et al., 2018).

The processing procedure is shown in Figure 1.2, however, a brief outline follows: initially the effluent is allowed to settle to reduce the number of large particulates within the solution, the effluent then enters two parallel sand beds which remove the finer colloidal matter via filtration (both organic and inorganic), the effluent then enters carbonation towers to reduce the pH of the solution from 11 to 7 protecting the ion exchange beds (clinoptiloite). Finally, the effluent is processed in the ion exchange tower removing the Cs and Sr, and allowing for the safe discharge into the Irish sea (Dyer *et al.*, 2018).

The SIXEP plant waste was designed to undertake the removal of colloidal particles and radionuclide's, originally it was predicted that the particles in question were homogeneous in nature. However, as modelling approaches have increased and a further understanding of particulate production, such as the inclusion of a biofilm layer at the entrance of the sand bed (Ranjan and Prem, 2018), are understood it has become apparent that the particles are heterogeneous in nature and as such the sand beds in

particular may significantly vary from originally predicted. Furthermore, the proposed plan for SIXEP is to increase the amount of effluent being processed and as such a larger modelling suite needs to be implemented to ensure that the behaviour of SIXEP can be predicted and a continuity of assurance on the relative risks can be kept.

1.2.2 Sand bed filters

Predominately the sand beds within SIXEP focus on the removal of colloidal particles from the effluent. This process is complex due to the nature of the effluent feed stream and the uncertainty in the chemical and physical make up of these streams. This adds extra uncertainty in the quality of the effluent stream and as such the efficiency in the sand beds. As such, a large volume of research has recently been undertaken in quantifying the uncertainties surrounding the sand bed and optimising the refresh and renewal stage to ensure that the relevant environmental regulations are being adhered too.

To add further complexity, materials quantification of the influent stream entering the bed is unknown due to a number of biological and inorganic colloidal particles, arising from the Magnox ponds being open to the environment. As a consequence the colloidal particles can safely be described as heterogeneous in nature, offering added complexity when trying to model the sand bed, as traditional techniques for modelling sand bed efficiencies may not be adequate to confidently assess the bed change parameters, arising from the heterogeneity of the feed stream. Alternative modelling stratagems are thus required to offer insight into the sand bed, on both the micro and macro scale. By applying alternative or novel simulation and modelling ideas to the problem, confidence within the modelling technique can be increased whilst also offering cost and efficiency optimisation of the sand bed itself.

1.3 Aims and Objectives

The aim of this research is to analyse the use of agent based modelling method as an alternative way to further understand particle deposition and aggregation within porous media. This aim is split into the following key objectives:

1. Analysing the current literature on particle dynamics within porous media along with current agent based modelling methods and addressing the most suitable agent based modelling simulation suite
2. Implementing the lattice Boltzmann model within agent based modelling and analysing its uses as a suitable fluid solver in approximating fluid flow within porous media
3. Choosing a suitable particle trajectory equation and using this equation to address the suitability of agent based modelling in the role of understanding particle aggregation
4. Integration of both the particle tracking equation and lattice Boltzmann fluid solver to understand particle deposition within porous media and analyse the key behaviours which result in successful deposition

1.4 Organisation of thesis

This thesis is organised into the following sections which aim to answer the objectives above:

- Chapter 2 – the current theoretical concepts for modelling colloidal deposition within porous media with particular focus given on the use of colloid filtration theory and DLVO theory
- Chapter 3 - the current computational techniques required to model colloidal deposition and their relative advantages and dis-advantages. This section then comprises a brief history of agent-based modelling and its applicability to the problems posed within traditional colloidal filtration modelling
- Chapter 4 – implements the lattice-Boltzmann method within an agent based modelling context. The model is validated against traditional 2D fluid dynamic problems, with a particular emphasis on the validation of the method within NetLogo on flow around a circle in 2D
- Chapter 5 – describes the use of agent based modelling and develops a suitable choice in particle trajectory equation. Validation of the particle trajectory method is undertaken by modelling colloidal aggregation in a purely diffusive system. The model is then extended to understand sensitivity of key variables when modelling colloidal aggregate growth
- Chapter 6 - integrates both the particle trajectory and lattice-Boltzmann models to investigate particle transportation and deposition on a single collector. The development of growth size and location in varying chemical and physical conditions are simulated to understand the sensitivities of key parameters within colloidal filtration theory

- Chapter 7 – this acts as a conclusion, where the key findings of the work and conclusions are summarised, with a number of a future directions in which the work can be extended discussed.

1.5 References

Adin, A. and Rajagopalan, R. (1989) 'Breakthrough Curves in Granular Media Filtration', *Journal of Environmental Engineering*, 115(4), pp. 785–798. doi: 10.1061/(ASCE)0733-9372(1989)115:4(785).

Auset, M. and Keller, A. A. (2006) 'Pore-scale visualization of colloid straining and filtration in saturated porous media using micromodels', *Water Resources Research*, 42(12), pp. 1–9. doi: 10.1029/2005WR004639.

Bradford, S. A. and Torkzaban, S. (2008) 'Colloid Transport and Retention in Unsaturated Porous Media: A Review of Interface-, Collector-, and Pore-Scale Processes and Models', *Vadose Zone Journal*, 7(2), p. 667. doi: 10.2136/vzj2007.0092.

Bradford, S. a., Torkzaban, S. and Simunek, J. (2011) 'Modeling colloid transport and retention in saturated porous media under unfavorable attachment conditions', *Water Resources Research*, 47(10), pp. 1–12. doi: 10.1029/2011WR010812.

Chen, C. *et al.* (2009) 'Temporal evolution of pore geometry, fluid flow, and solute transport resulting from colloid deposition', *Water Resources Research*. John Wiley & Sons, Ltd, 45(6). doi: 10.1029/2008WR007252.

Dyer, A. *et al.* (2018) 'The use of columns of the zeolite clinoptilolite in the remediation of aqueous nuclear waste streams', *Journal of Radioanalytical and Nuclear Chemistry*. Springer International Publishing, 318(3), pp. 2473–2491. doi: 10.1007/s10967-018-6329-8.

Henry, C., Minier, J. P. and Lefèvre, G. (2012) 'Towards a description of particulate fouling: From single particle deposition to clogging', *Advances in Colloid and Interface Science*, 185–186(October), pp. 34–76. doi: 10.1016/j.cis.2012.10.001.

Kulkarni, P., Sureshkumar, R. and Biswas, P. (2003) 'Multiscale simulation of irreversible deposition in presence of double layer interactions', *Journal of Colloid and Interface Science*, 260(1), pp. 36–48. doi: 10.1016/S0021-9797(02)00236-9.

Kulkarni, P., Sureshkumar, R. and Biswas, P. (2005) 'Hierarchical approach to model multilayer colloidal deposition in porous media', *Environmental Science and Technology*, 39(17), pp. 6361–6370. doi: 10.1021/es0500557.

Ranjan, P. and Prem, M. (2018) 'Schmutzdecke- A Filtration Layer of Slow Sand Filter', *International Journal of Current Microbiology and Applied Sciences*, 7(07), pp. 637–645. doi: 10.20546/ijcmas.2018.707.077.

Saiers, J. E., Hornberger, G. M. and Liang, L. (1994) 'First- and second-order kinetics approaches for modeling the transport of colloidal particles in porous media', *Water Resources Research*. John Wiley & Sons, Ltd, 30(9), pp. 2499–2506. doi: 10.1029/94WR01046.

Shen, C. *et al.* (2007) 'Kinetics of coupled primary- and secondary-minimum deposition of colloids under unfavorable chemical conditions', *Environmental Science and Technology*, 41(20), pp. 6976–6982. doi: 10.1021/es070210c.

Shen, C. *et al.* (2010) 'Predicting attachment efficiency of colloid deposition under unfavorable attachment conditions', *Water Resources Research*. John Wiley & Sons, Ltd, 46(11). doi: 10.1029/2010WR009218.

Torkzaban, S. *et al.* (2015) 'Colloid release and clogging in porous media : Effects of solution ionic strength and fl ow velocity', *Journal of Contaminant Hydrology*. Elsevier B.V., 181, pp. 161–171. doi: 10.1016/j.jconhyd.2015.06.005.

Torkzaban, S., Bradford, S. A. and Walker, S. L. (2007) 'Resolving the coupled effects of hydrodynamics and DLVO forces on colloid attachment in porous media',

Langmuir, 23(19), pp. 9652–9660. doi: 10.1021/la700995e.

Tufenkji, N. and Elimelech, M. (2004) 'Deviation from colloid filtration theory in the presence of repulsive electrostatic interactions: Implications to microbial transport', (21), p. ENVR-095.

Tufenkji, N. and Elimelech, M. (2005) 'Breakdown of colloid filtration theory: Role of the secondary energy minimum and surface charge heterogeneities', *Langmuir*, 21(3), pp. 841–852. doi: 10.1021/la048102g.

Veerapaneni, S. and Wiesner, M. R. (1997) 'Deposit morphology and head loss development in porous media', *Environmental Science and Technology*, 31(10), pp. 2738–2744. doi: 10.1021/es960979h.

Chapter 2. A review of the literature surrounding fouling of porous media

Within colloidal sciences the process of fouling can be described as the behaviour of colloidal particles when they come into contact with the surface of porous media. This behaviour is widely studied across a number of different disciplines; wastewater engineering, food manufacturing, automotive industries, and environmental sciences. The rate at which fouling occurs can directly influence the behaviour of the porous media, in which case captured nanoparticles can be re-released in the environment causing issues (Tian *et al.*, 2010). Within the wastewater industry, porous media are used to capture biological, synthetic, and natural nanoparticles (Stevik *et al.*, 2004) . These particles are then removed from effluent and captured either within storage facilities or re-processed.

Nanoparticles can exist within the environment for a number of different reasons. Naturally occurring nanoparticles, such as colloidal or biological particles can be a consequence of environmental changes, whereas, synthetic nanoparticles may be released due to industrial processes, or environmental disaster (Nowack and Bucheli, 2007). In either case, the behaviour of these particles once released within a porous media is of utmost importance and hence, well studied. Though the behaviour of these systems is both highly complex and dynamical, there are a number of underlying principles which connect them all. The most commonly applied theory is colloidal filtration theory which gives a first approximation to the porous media dynamics.

2.1. Colloid filtration theory

Colloid filtration theory focuses on the removal mechanisms within porous media. In particular, the mechanisms under which optimal removal can occur and when the removal efficiency decays. This can be important when producing filtration systems

where saturation of the bed can cause breakthrough of undesirable products. The majority of colloidal filtration theory is based upon clean bed theory (Logan *et al.*, 1995), which dictates that the behaviour of the porous media can be predicted by advection-diffusion equations along with deposition coefficients (Tong and Johnson, 2006).

$$\frac{\partial C}{\partial t} = D\frac{\partial^2 C}{\partial x^2} - V_0\frac{\partial C}{\partial x} - kC \qquad 2.1$$

Where C is the particle concentration, t the time, D the dispersion coefficient, x is the distance, V_0 is the upstream fluid velocity and k is the deposition coefficient.

Initially, it was believed that the behaviour of colloidal materials within a filtration medium could be captured solely by describing the transport and attachment steps as two independent steps (Yao, Habibian and O'Melia, 1971). Within the transportation procedure, the importance is laid upon the hydrodynamic forces being exerted upon the particle (Mays and Hunt, 2004). A conceptual understanding of the transport behaviour of colloidal particles was produced, which solely focused on three mechanisms which results in an interception between the particle and the collector surface (Yao, Habibian and O'Melia, 1971). Firstly, if the density of the particle is significantly greater than the fluid phase, inertial effects are important. In this case the influence of the gravitational force on the particle can allow for the particle to leave the fluid and interact with the collector surface. Secondly, if the density difference between the particle and fluid phase is close to zero, then inertial effects can be ignored. In this situation the particle can be treated as a "tracer" particle where its trajectory follows the streamlines of the flow exactly. For interception to occur the particle size must be large enough for capture (Figure 2.1). Finally, diffusion may influence the behaviour of the particle, in particularly slow flow regimes the diffusive force may be greater than

that of the advective force (Elimelech and O'Melia, 1990a). As such particle collision is a consequence of the random motion of the particle. Further analysis of these forces will be undertaken later within this review.

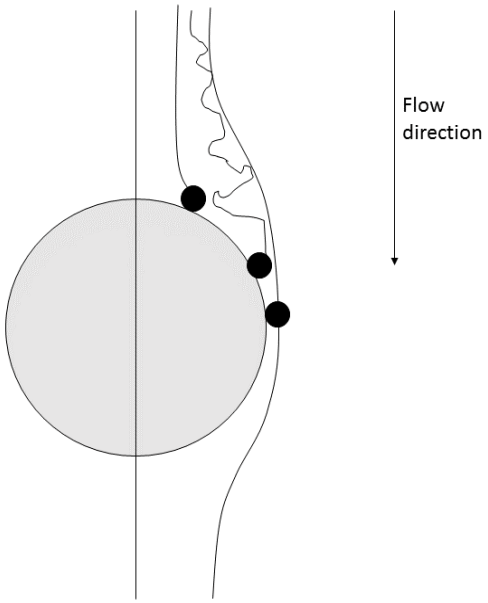

Figure 2.1 The various mechanisms in which colloidal interception with a collector can occur, sedimentation, diffusion, interception. Re-drawn from Yao et al, 1967.

By analysing the likelihood of a collision occurring with the collector, the following equation can be found (Rajagopalan and Tien, 1976):

$$\eta = \frac{rate\ at\ which\ particles\ strike\ the\ collector}{V_0 C_0 \left(\frac{\pi d^2}{4}\right)} \qquad 2.2$$

Where d is the particle diameter, V_o and C_o are the upstream velocity and initial particle concentration

By understanding the total number of forces applied to the particle near the collector surface equation 2.2 can be used to successfully predict the collector efficiency (η). Commonly, this term along the attachment efficiency (α) is used to describe the

deposition rate (kC) within equation 2.1. By capturing both the transport step (η) and attachment step (α) the following concentration equation can be derived (Yao *et al*, 1975):

$$k = -\frac{\frac{3}{2}(1-f)}{d}\alpha\eta \qquad 2.3$$

Where f is the bed porosity, α is the attachment efficiency

However, by simplifying the behaviour of the flow conditions around the collector (ignoring the impact of neighbouring collectors) the overall collector efficiency can underestimate the number of collisions (Logan *et al.*, 1995).

The behaviour of the flow around a collector within porous media is well understood and a conceptual geometric model has been developed by Happel (1958). This model relates localised fluid behaviour to that of porosity, in effect creating a fluid envelope where the fluid flow can be analytically solved (Nelson and Ginn, 2005).The size of this fluid envelop can be directly related to that of the porosity of the system (Nelson and Ginn, 2005). Rajagopalan and Tien (1976), utilised this method to produce more informative geometric and analytical solution to the collector efficiency problem. Furthermore, by producing a semi-implicit equation computing time is significantly reduced.

This new efficiency equation is a function of a number of forces, as previously mentioned the initial colloid filtration behaviour was depicted within the Yao model as being within three fundamental areas, sedimentation, interception, and diffusion. In relation to this, the approach set forward by Ragajopalan and Tien, introduces a further influential force, surface interaction, upon the particle trajectories. In this case the application of surface forces also influences the trajectory behaviour of the particles

and subsequently the interception efficiency of the collector. In effect, all of these systems rely on a collection of fundamental forces being analysed and predicted using analytical or experimental data.

2.2. Colloid-surface interactions

Colloid filtration theory assumes that once a contact is made between the surface of the collector and the particle, attachment occurs. The particle is then attached to the surface of the collector and assumed to be removed from the solution (Elimelech and O'Melia, 1990a). By assuming irreversible removal of colloids form the solution, incorrect estimation of removal efficiencies may occur (Torkzaban, Scott A., Bradford and Walker, 2007).

The behaviour of colloids which are attached are not only subjected to continual hydrodynamic influences, but are also introduced to surface chemistry conditions which significantly varies both spatially and temporally. Thus, an attached colloid is unlikely to be attached indefinitely.

2.2.1 Derjaguin-Landau-Verwey-Overbeek theory (DLVO)

DLVO theory allows for a simplified prediction of the surface interaction energies between the collector and the particle. Furthermore, it can be used to predict colloid-colloid and plate-plate interactions. Due to the size difference between the colloid and the collector being orders of magnitude apart, this section will focus mainly on colloid-plate interactions.

This theory uses an additive approach to calculate the interaction energy between the particle and the collector as the distance between them diminishes. Combining these energies allows for the total interaction energy to be predicted (Hiemenz and Rajagopalan, 1997). By assessing the attractive (van Der Waals) and repulsive

(electrostatic) components of the equation it is possible to predict the likelihood of aggregation or sticking occurring between the two interacting particles (in this case the collector and the particle).

$$E_{tot}(h) = E_{vdw}(h) + E_{elec}(h) \qquad 2.4$$

Where E_{vdw} is the energy attributed to the van Der Waals interaction, E_{elec} is the energy attributed to the electrostatic interaction, E_{tot} is the total energy, and h is the separation distance (nm)

By solving equation 2.4, the total energy can be calculated. In recent studies there has been a significant move towards also capturing the Born interaction, the interatomic forces, between the particle and the collector surface (van Oss, Giese and Costanzo, 1990; Assemi, Nalaskowski and Johnson, 2006). There are also some simplifying equations which can be used instead of the Born profile such as Lennard-Jones hard and soft sphere potentials or deep well potentials (Guzmán and de Pablo, 2003). This introduces a hard "cut-off", stopping any likelihood of the particle effectively passing through the collector. The new equation then becomes:

$$E_{tot}(h) = E_{born}(h) + E_{vdw}(h) + E_{elec}(h) \qquad 2.5$$

Where E_{born} is the energy attributed to the Born interaction

2.2.2 Van Der Waals Interaction

The behaviour of two approaching colloids are such that when they are an appreciable distance from each other the influence of the fluctuating dipoles are negligible. When the particles are within a set distance from each other, the behaviour of the dipoles play an integral part in influencing the force balance between them. As the dipoles start

fluctuating, they lose phase and as a consequence of this action become more attractive, retarded van Der Waals (Israelachvili and Tabor, 1972).

By assuming an additive approach to the intermolecular energies applied, the following equation for the van Der walls interaction for sphere-plate can be found (Elimelech, 1998):

$$E_{vdw}(h) = -\frac{A_H}{6}\left[\frac{a_p}{h} + \frac{a_p}{h+2a_p} + \ln\left(\frac{h}{h+2a_p}\right)\right] \quad 2.6$$

Where A_H is the Hamaker constant, a_p is the particle radius, h is the separation distance.

It is possible to approximate the Hamaker constant for two interacting particles (Cosgrove, 2010):

$$A_H = \pi^2 \rho_1 \rho_2 Q \quad 2.7$$

Where $\rho_{1\,\&\,2}$ are the respective number densities, Q is the constant from the Keesom energy, Debye energy and London dispersion energy.

2.2.3 Electrostatic Interaction

According to the Stern-Guoy-Chapman (SGC) theory, the behaviour of two particles as they come into contact with each other is directly related to the behaviour of their counter-ion layer and how diffused this layer is. The concentration and behaviour of the ions within the diffuse layer is related to the concentration of the electrolyte (Cosgrove, 2010). The Helmholtz layer (compact) is charge neutral and can be described using atomic dimensions in comparison to that of the diffuse layer, which can be described using Poisson and Boltzmann equation (Oldham, 2008).The Boltzmann description implies an exponential decay of the concentration of the ions

across the diffuse layer, in this case the width of the diffuse layer can be described as infinite. The influence this has on the colliding colloidal particles is only felt within a few hundred nm (Oldham, 2008).

The original Guoy-Chapman model implies that the ions are a diffused layer, where they exhibit point like properties, however, Stern concluded that the behaviour of the ions is finite (Elimelech, 1998).

The electrostatic interaction relies upon the surrounding diffused ion cloud being negatively charged, in this case as the two interacting particles or interacting particle-collector come together the overwhelming energy is repulsive. This behaviour can be described using the Stern-Gouy-Chapman theory, which states that there are two layers known as the electric double layer. The first layer being highly compact and existing as a near surface energy, known as the Helmholtz layer (Hiemenz and Rajagopalan, 1997), whilst the secondary layer is more diffused, known as the Stern-Gouy layer. Originally, this behaviour was considered to be point source, however, later extensions to the model by Chapman introduced a discrete modelling style instead.

The thickness of this double layer can be calculated using the Debye length which can be quantified by applying the Poisson equation for the electric static surface potential:

$$\epsilon\epsilon_0 \frac{(d^2\psi(h))}{dh^2} = -\rho_p(h) \qquad 2.8$$

Where ρ_p the charge density, ε is permittivity of the vacuum, ε_o the dielectric constant, ψ is the electrical potential.

The application of a Debye-Hückel linearization of exponentials leads to the following equation which can be approximated from the Poisson equation (Polte, 2015):

$$\epsilon\epsilon_0 \frac{d^2\psi(h)}{dh^2} = \sum_i \frac{z_i^2 e^2 n_{i_\infty}^2 \psi(h)}{k_B T} = \kappa^2 \psi(h) \qquad 2.9$$

Where z_i is the ionic valence, n_{i_∞} is the concentration of the ions at $h = \infty$, e is the elementary charge and κ is the Debye constant, which equals:

$$\kappa = \left[\sum_i \frac{z_i^2 e^2 n_{i_\infty}^2}{k_B T} \right]^2 \qquad 2.10$$

Where k_B is the Boltzmann constant and T is the temperature

The diffuse layer thickness can be calculated using the reciprocal of the Debye length. As the thickness of the diffusive layer increases, the rate at which the interacting surfaces also increases, as such the repulsive energy is felt significantly earlier than that of the attractive van Der Waals energy (Elimelech, 1998) . The distribution in concentration of the ions are linked directly to the Poisson equation, furthermore, the concentration of the ions can be calculated using the ionic strength of the solution. In this case the Debye constant equation can be stated:

$$\kappa = \sqrt{\frac{2000 N_a I e^2 z_i^2}{\epsilon\epsilon_0 k_B T}} \qquad 2.11$$

Where N_a is Avogadro's constant, I the ionic strength

It is common within the literature to approximate the surface potential by using the ξ potential which in this case describes the total amount of mobile ions within the diffusive layer (Elimelech, 1998). It has been stated that this approximation does not

capture the surface potential at high surface charges or high ionic strengths (Ryan and Gschwend, 1994). Alternative, techniques are available which capture the surface potential at higher surface charges and higher ionic strength.

By utilising the infinite plate-plate equation:

$$E_{elec}(h) = \epsilon\epsilon_0\kappa\zeta_1\zeta_2\left[\frac{\zeta_1^2+\zeta_2^2}{2\zeta_1\zeta_2}(1-\coth\kappa h)+\frac{1}{\sinh\kappa h}\right] \quad 2.12$$

Where ξ represents the zeta potentials of the plates

There are numerous methods to find and approximate analytical solution to sphere-plate interaction, such as the Derjaguin or linear superposition method which gives the following:

$$E_{elec}(h) = \pi\epsilon\epsilon_0 a_p\left[2\zeta_1\zeta_2\ln\left(\frac{1+exp(-\kappa h)}{1-exp(-\kappa h)}\right) + (\zeta_1^2+\zeta_2^2)\ln[1-\exp(-2\kappa h)]\right] \quad 2.23$$

2.2.4 Born Interaction

Though DLVO theory captures the electrostatic and van Der Waals energy, it usually neglects the short-range repulsion which exists when particles or particle-grains start to interpenetrate each other (Ryan & Gschwend, 1994). The interaction of colloidal particles as they start to interpenetrate each other introduces Born repulsion, due to the electronic orbital interacting with each other and inducing short range repulsion. Though the behaviour of this system is quantum in nature, there are a number of

current techniques which aim to approximate the repulsive properties. For a sphere-interaction the Ruckenstein and Prieve equation gives the following (Elimelech, 1998):

$$E_{born}(h) = \frac{A_H \sigma_c^6}{7560}\left[8a_p + \frac{h}{(2a+h)^7} + \frac{6a_p - h}{h^7}\right] \quad 2.14$$

Where σ_c is the collision diameter which is usually around the order of 0.5 nm (Elimelech, 1998).

There are a number of analytical solutions which approximates the interaction potentials between the Born and van Der Waals solutions. The most commonly used approximate solution is the Lennard-Jones, which utilises a short range repulsive term to capture the Born repulsion and a long range attractive term to capture the van Der Waals term:

$$E_{LJ} = 4\epsilon_w\left[\left(\frac{d}{h}\right)^{12} - \left(\frac{d}{h}\right)^{6}\right] \quad 2.35$$

Where E_{LJ} is the Lennard-Jones interaction energy ϵ_w is the well depth

The first power term can be seen to rapidly change as a function of the distance from the centre, this term is a consequence of the Pauli exclusion principle (Tomilov *et al.*, 2013). The second term equates the long tail of the attractive forces derived from the van Der Waals equation.

Though the Lennard-Jones equation offers an analytical solution, it loses any physical meaning in terms of input parameters, however, it does capture the behaviour of the energy profile well.

2.2.5 DLVO profiles

The full description of the terms within the DLVO equation will be addressed later however, it is worth noting that the behaviour of the energy profile is a consequence of the solution and surface chemistry of the system.

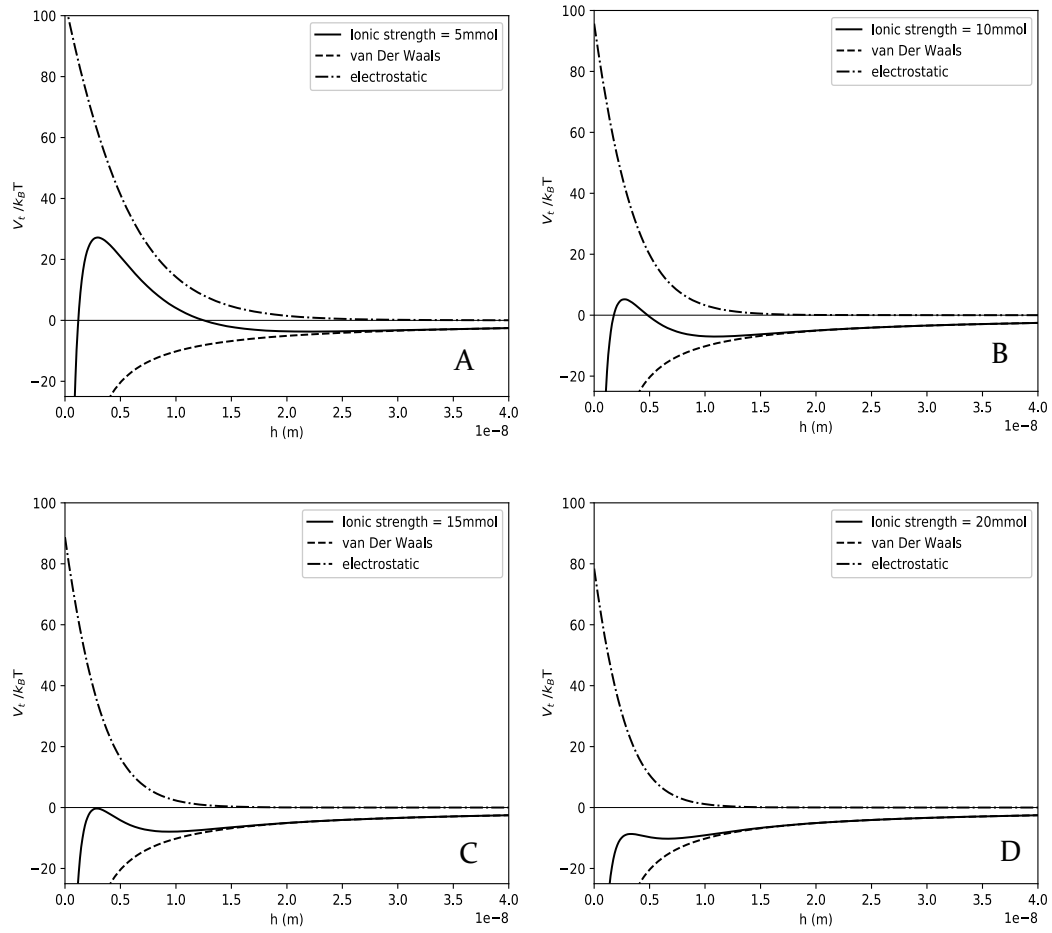

Figure 2.2 The DLVO profiles for equation 2.1. A, highlights a highly repulsive regime at low ionic strength, 5 mmol. B, highlights a slightly repulsive regime at 10 mmol. C, a slightly attractive regime at 15 mmol. D, shows an extremely attractive regime at 20 mmol

In this case, as the zeta potential, ionic strength and pH of the system varies so does the colloid-collector interaction energy profile (Figure 2.2). As such, the behaviour of the system can become radically different, even by minor changes in these three

parameters. As a consequence of this action, the system can tend from highly attractive to highly repulsive regime at low ionic strength.

When the system is highly repulsive the particle will be caught in one of two profiles, the first being a secondary minimum and the second being the primary minimum (Shen *et al.*, 2007). Though the likelihood of being caught within the primary minimum is calculated by understanding the hydrodynamic forces exerted upon the particle (Torkzaban, S. A. Bradford and Walker, 2007b).

The primary minimum without the Born terms represents the infinitely deep attractive well, where the particle is infinitely attracted to the wall, and as previously discussed this result in unrealistic. Figure 2.2, highlights the behaviour of the interaction energy and it can be seen to tend to negative infinity. However, with the Born repulsion term the primary well has a finite depth, and as such the particle may be captured but a number of external forces may allow for the release. Though unlikely, this results in a more realistic prediction of the attachment of the particle to the collector surface and the likelihood of detachment from the collector surface (Ryan & Gschwend, 1993).

As a relationship with colloid filtration theory (CFT), it can be stated that the attachment efficiency is directly related to the height of the interaction energy barrier. As the barrier increases, the attachment efficiency tends to zero, however, as the system becomes dominated by attractive only energies (Figure 2d), the attachment efficiency becomes equal to 1.

It has been argued that a secondary minimum is the more important energy minimum, due to its easier access (Shen *et al,* 2007). In this case the colloidal particle may appear bound to the surface of the collector, however, in response to small changes in the solution and surface chemistry can easily become detached. Furthermore, these particles are more easily detached via hydrodynamic forces and as such cannot be

assumed to be fully "removed" from the system (Torkzaban *et al*, 2007). There has been some research into the likelihood of colloids being removed from the primary minimum via hydrodynamic forces, however, the high fluid velocities were found to be unrealistic (Torkzaban *et al,* 2007*)*. As such it can be stated the when particles are bound within the secondary minimum they are influenced by both the hydrodynamic forces, and the depth of the secondary minimum. As a consequence, the attachment efficiency is greatly reduced due to a percentage of colloidal particles interacting with the surface of the collector with enough inertial energy to escape from the secondary minimum (Torkzaban *et al,* 2007*)*.

Furthermore, particles which are caught in the secondary minimum due to a lack of inertia may escape through a number of other routes. Firstly, a percentage of the captured particles may find an increase in kinetic energy due to the diffusive properties of the colloid. Secondly, a change in the fluid flow, hence, an increase in the shear may allow for the particles to be removed from the collector surface. Finally, kinetic collisions with passing colloidal particles may allow for the removal of the colloid from the secondary minimum (Ryan & Gschwend, 1994).

2.2.6 Colloid-colloid interaction

Though the previous section predominately focused upon the colloid-collector surface/solution chemistry, colloid-colloid interactions also occur within the solution. The initial deposition of particles upon the surface collector can be argued to be monotonic, and until the surface area is covered, the controlling surface interaction can be stated as surface-colloid (Henry, Minier and Lefèvre, 2012). Once the collector surface is covered, this role reverses colloid-colloid interactions become predominate. In this case the behaviour of the particle is linked to the surface chemistry of the particles.

In homogenous depositions this can result in a single layer of colloidal coverage on the collector, if the colloid-colloid energy profile is highly repulsive (Henry, Minier and Lefèvre, 2012). In this case there would be a large percentage of colloid particles passing deeper into the porous media, and saturation would occur much quicker. If the colloid-colloid energy profile is highly attractive larger aggregates develop which may result in clogging and subsequent particle straining occurring within the pore structure (Chen *et al.*, 2009).

2.2.7 Extended-DLVO

The standard DLVO equation (equation 2.4) takes into account only the electrostatic and van Der Waals energies, though Born repulsion has been added in the above section it is rarely incorporated within the equation. There are, however, a number of other interaction energies which influence the rate of deposition and the rate of aggregation between interacting particles. These new energies can be incorporate into the standard DLVO, this new equation is then referred to as X-DLVO or Extended-DLVO. Due to the additive manner in which the DLVO equation works new potentials can be introduced easily and the overall potential energy can be estimated from this new equation.

Biological colloidal materials are influenced by the impacts arising from hydrogen bonding interactions between the two surfaces immersed in a polar solvent, in which case the acid-base interaction potential needs to be incorporated within the DLVO equation (Bayoudh *et al.*, 2009). Furthermore, magnetic colloidal particles can be influenced by the magnetic energy which interact with the electrostatic double layer, can influence aggregation by introducing the magnetic dipolar contribution to

equation the influence of the magnetic energy can be approximated (Campos *et al.*, 2009).

Without these extensions to the standard DLVO equation, incorporation of biological and magnetic colloids would produce errors when predicting aggregation and deposition. In the majority of the literature, only the standard DLVO equation was utilised as idealised systems were modelled. In situations such as filtration, however, the colloidal population is highly heterogeneous ranging from biological to artificial colloidal materials which interact with each other and other species. As such, the behaviour of these heterogeneous samples need to be considered when utilising any of the DLVO equations.

2.3. Hydrodynamic effects

Hydrodynamics are important in both the transport and attachment phases of CFT. Microscopic flow can vary drastically from the macroscopic flow, for example whereas macroscopic flow exhibits creep flow, microscopic flow may be highly shearing, and induce straining (Yiantsios and Karabelas, 2003).

After colloidal particles are attached to the surface of the collector or form a deposit they are subjected to varying levels of shear force (Ryan and Elimelech, 1996). The behaviour of this shearing influences the likelihood of the particle remaining deposited. As such, torque balance analysis has been undertaken to calculate the threshold levels to induce either shearing of the deposition from the collector surface both partial or full, as well as, understanding the likelihood of the colloidal particle rolling into an area of low shear (Ryan & Elimelech, 1996).

$$T_{adhesive} = E_{tot} L_x$$

2.16

With E_{tot} corresponding to the DLVO energy profile, and as a consequence related to the amount of energy needed to overcome the adhesive force, L_x relates to the lever arm under which the torque is applied.

In comparison the hydrodynamic drag and lift forces applied to a hard sphere attached to the surface

$$F_L = \frac{81.2 \mu a_p^2 \omega^{0.5} v_{pore}}{v^{0.5}}$$

2.17

$$F_D = (1.7009)(6\pi a_p v_p)$$

2.18

Where ω is the velocity gradient a_c is the collector radius, v_{pore} is the pore water velocity, a_p is particle radius, v is the fluid kinematic viscosity, μ is the fluid dynamic viscosity

The fluid velocity can be calculated from the flow rate:

$$v_{pore} = \frac{6 Q_f a_p}{Al}\left(1 - \frac{a_p}{l}\right)$$

2.19

Where Q_f is the flow rate, A is the cross-sectional area and l is the thickness of the flow area. Ryan & Elimelech, state that these parameters can be adapted towards porous media by using Q_f/A as the approximated pore velocity and l equates to the pore diameter.

As such for attachment to occur the adhesive forces must overcome the repulsive and hydrodynamic forces. The influence of rolling and lifting can cause the colloidal particles to be removed from the collector. Within creep flow conditions the

predominant mechanism for removal is rolling, in this case the colloidal particles move to an area of low shear stress and is removed from the collector surface.

For rolling to occur the applied torque from the hydrodynamic force must be greater than that of the adhesive torque calculated as a function of the attachment and frictional forces.

$$T_{applied} = 1.4 a_p F_D \tag{2.20}$$

By applying equations 2.17, 2.18, 2.19, Ryan & Elimelech concluded that the critical velocity needed for detachment could be estimated using:

$$v_{pore}^{crit} = \frac{F_A l_x}{2.38\left(6\pi\mu a_p^2\right)} \tag{2.21}$$

As such as the level arm l_x increases in height and enters the flow channel fully the critical velocity increases proportionally. However, the attachment force reduces and the torque applied to the full-length increases. In this case aggregates are likely to be removed. As such, there is a criterion where $T_{applied} >> T_{adhesive}$ which will result in constant removal from the deposit. Finally, equation 2.21, implies that as the adhesive force is reduced the likelihood of reaching the critical velocity is increased and rolling initiated.

These equations are based predominately on the assumption that the particles are either deformable or that the surface of the collector is rough. Both of these are realistic assumptions, however, the Happel sphere-in-cell model implies a smooth surface as well as CFT assuming smooth colloidal particles (Bradford and Torkzaban, 2008).

2.4. Time dependent effects

The majority of the review so far has concentrated upon CFT and as a function of this has neglected to analyse the time dependent changes. In reality, the behaviour of a porous media is dictated by time dependent effects, such as the rate of deposition, rates of clogging and rates of re-entrainment (Henry, Minier and Lefèvre, 2012). The rate at which clogging occurs upon a collector surface, influences the likelihood of pore closure and increases the pressure drops throughout the system. Furthermore, removal efficiency of porous media is purely a time dependent input which relates to the rate at which colloidal particles are deposited onto the surface (Sallès, Thovert and Adler, 1993).

The behaviour of a porous media can be described in 3 stages: Ripening, operable and breakthrough (Gitis *et al.*, 2010). Each of these stages are influenced by a number of parameters which dictate the behaviour of the system. Furthermore, traditional techniques applied to CFT have focused on irreversible accumulation, which dictates that once the colloid has been captured it cannot be removed. However, as previously mentioned the behaviour of deposits are highly dynamical and sensitive to variations in both hydrodynamic and adhesive forces. As a consequence of this behaviour, particles which are deposited cannot be stated to be irreversibly bound to the surface.

Henry, Minier and Lefèvre (2012), simplified this further by analysing two stages of fouling (deposition), the early stages and later stages of fouling. Where the early stages of fouling introduce the likelihood of single-particle deposition and re-entrainment, the later stages of fouling concentrates on multi-layer deposition and the behaviour of the porous media in response to this.

2.4.1 Clogging, blocking, ripening

Ripening is predominately associated with the earlier stages of fouling, in this case attachment between the collector surface and the colloid surface is the primary mechanism. CFT relies upon the clean bed theory, assuming that initially the porous media is free of any fouling. In which case the only interaction occurring within a dilute system is between the collector and the colloidal particle. As such, a single monomer layer of particles is developed on the surface, the spread of this layer is dictated by the local hydrodynamic and chemical forces.

Once, a single layer of colloids are deposited upon the surface of the collector the primary mechanism switches from colloid-collector to colloid-colloid (Henry, Minier and Lefèvre, 2012).As such, the behaviour of the system is predominately controlled by colloidal interactions and their inherent physico-chemical forces. The behaviour of this system is particularly susceptible to changes in hydrodynamic forcing and as a consequence shearing affects can be heightened (Ng and Elimelech, 2004).

Clogging and blocking can occur for numerous reasons, though the most common is related to the detachment of deposited particle complexes (Sallès, Thovert and Adler, 1993). In this case particles which were previously attached break free due to a build-up of hydrodynamic forces upon the structure. Straining occurs when particles which otherwise would be captured along the collector surface are exposed to high fluid stresses and as such, are strained between the collector surfaces (Figure 2.3) (Johnson, Li and Yal, 2007). Consequentially particles can then travel much further into the porous media than previously predicted by CFT. This can result in the original CFT equation (equation 2.1) not predicting the correct development of the deposition profile.

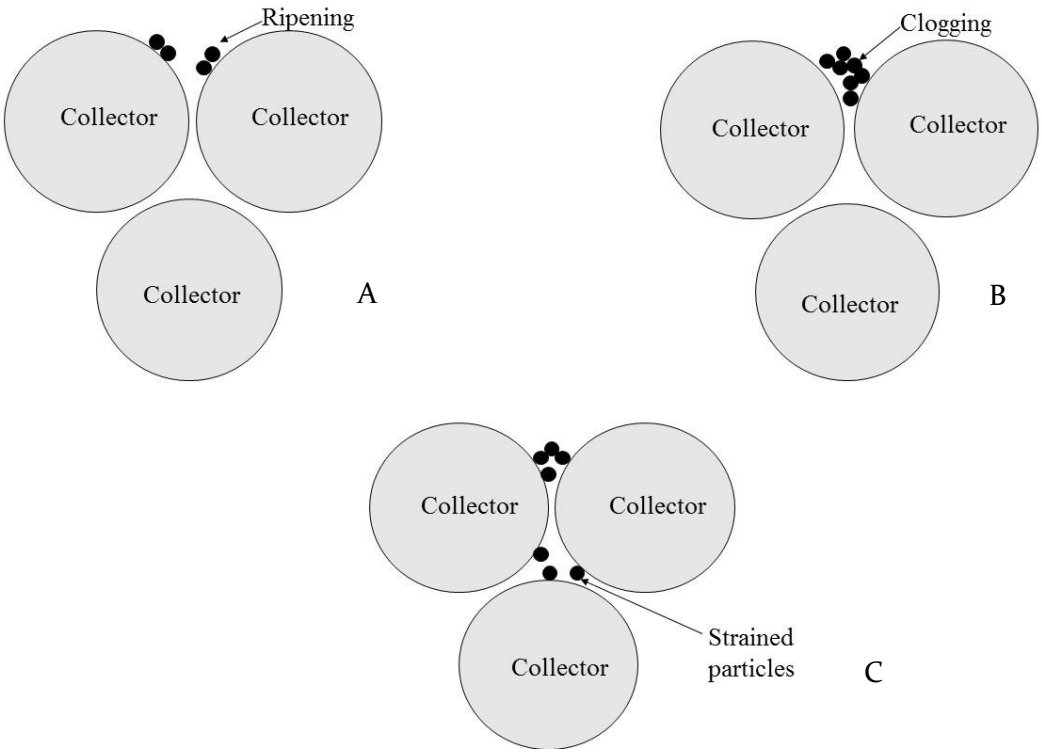

Figure 2.3 The various stages of colloid deposition. A, highlights the initial ripening stage where single particles are deposited on the collector surface. B, highlights the development of a clogged collector pore. C, highlights the strained particles within the pore space

The application of the 3 stage process introduced by Gitis *et al*, assumes that after ripening the porous media is at its operable stage, where the profile of deposition is moving away from an exponential towards a linear function. Within this stage the behaviour of the bed is dictated by the dynamic interaction between the colloid particles and the collector surface (Henry, Minier and Lefèvre, 2012). This system, uses both an attachment efficiency along with a detachment efficiency to calculate the likelihood of removal from the collector surface occurring (Gitis *et al.*, 2010). The detachment efficiency is usually arbitrarily chosen, though certain analytical forms along with experimental results are used to calculate the removal efficiency (Logan *et al.*, 1995). The behaviour of these deposits, however, are influenced by a number of compounding factors, firstly, the hydrodynamics of the local pore system changes.

These change arise due to clogging, giving rise to a localised pore velocity considerably higher than predicted using the average Darcy velocity of the system. As a consequence of this the detachment efficiency may be greater than calculated (Kretzschmar *et al.*, 1997). Secondly, the geometry of the deposited particles is important inducing detachment, as colloidal particles which are tightly bound together are less likely to be removed than loosely bounded particles (Waite *et al.*, 1999). Though the Gitis *et al.* (2010) approach offers some improvement on CFT and at least captures some spatial and temporal aspect of the porous bed system, it can still under or over-estimate the system as it neglects a number of key parameters. In particularly, the geometric shape of the deposition. Furthermore, CFT assumes that the collector surface is perfectly smooth and the geometry is spherical, though this assumption aids in computation of system it neglects the high level of heterogeneity within the porous media (Nathalie Tufenkji and Elimelech, 2004).

4.4.2 Pore space geometry

The commonly applied, Happel sphere-in-cell model, neglects to take into account inter-region pore zones, as such localised changes in flow are ignored. As a consequence of this the colloidal deposition dynamics are also ignored. At its simplest the collector surface can be assumed to act as a sink (Elimelech, 1998), where colloidal particles once captured are assumed removed and irreversibly attached to the collector surface. Adding a layer of complexity allows for the colloidal particles to become detached by some detachment rate (Gitis *et al*, 2010), however, this detachment is arbitrarily chosen and usually re-adjusted to match experimental data. Neither of these techniques utilise the pore geometric behaviour as way of describing the dynamics of the system and as a consequence of this information on the internal workings of the system are neglected or lost.

Collector geometry and pore space geometry are areas which are neglected within traditional CFT, however, in reality these geometries are highly complex. The behaviour of flow within pores can directly affect the rate of deposition. The behaviour of colloidal deposition as a whole is predicted using the CFT equation (advection-dispersion), however, this neglect the internal pore structure and its ability to release captured colloidal deposits. It has been well understood that the behaviour within a pore space is highly complex and dynamical (Kretzschmar *et al.*, 1997; Bradford and Torkzaban, 2008; Chen *et al.*, 2009), relating to both colloidal deposition rates, along with flow velocity. The pore geometry itself is constantly evolving as a consequence of both the hydrodynamic and chemical forces within the region.

2.5. Conclusions

The behaviour of colloidal particles within porous media are dictated by numerous parameters, both physical and chemical in nature. The literature surrounding this area is both wide and extensive, with particular concentration placed upon the behaviour of the porous media as a function of hydrodynamic forces and chemical forces described using DLVO or Extended DLVO theory. Further, emphasis can be placed upon the deposition geometry and collector surface geometry. These behaviours can be seen to be both temporal and spatial, and as such, these systems can be hard to quantify due to their inherent complexity.

Current techniques, such as colloidal filtration theory along with associated hydrodynamic models such as Happel sphere-in-cell, utilise a number of highly simplifying assumptions to approximate porous media bed dynamics. Thus, the majority of the theoretical knowledge surrounding porous media and colloidal interactions are approximated to the macroscopic scale (i.e. how the bed behaves is a function of the summation of the processes applied). The so called "collector efficiency" along with the attachment efficiencies, are the two fundamental efficiencies which are currently being analysed for numerous conditions within the colloidal sciences. There is scope within the colloidal filtration theory, to go beyond the current macroscopic understanding and start to model the meso and micro-scale interactions which affect the bed performance locally. By extrapolation of these processes to the macro-scale adjustments to the current CFT equation can be applied. One area which can be seen to be lacking within the colloidal filtration field is the deposition profiles of the colloidal particles. Further analysis of this behaviour could be incorporated within CFT to increase the accuracy of the bed dynamics being modelled.

2.6. References

Assemi, S., Nalaskowski, J. and Johnson, W. P. (2006) 'Direct force measurements between carboxylate-modified latex microspheres and glass using atomic force microscopy', *Colloids and Surfaces A: Physicochemical and Engineering Aspects*. Elsevier, 286(1–3), pp. 70–77. doi: 10.1016/J.COLSURFA.2006.03.024.

Bayoudh, S. *et al.* (2009) 'Assessing bacterial adhesion using DLVO and XDLVO theories and the jet impingement technique', *Colloids and Surfaces B: Biointerfaces*. Elsevier, 73(1), pp. 1–9. doi: 10.1016/J.COLSURFB.2009.04.030.

Bradford, S. A. and Torkzaban, S. (2008) 'Colloid Transport and Retention in Unsaturated Porous Media: A Review of Interface-, Collector-, and Pore-Scale Processes and Models', *Vadose Zone Journal*, 7(2), p. 667. doi: 10.2136/vzj2007.0092.

Campos, A. F. C. *et al.* (2009) 'X-DLVO Interactions between nanocolloidal magnetic particles: the quantitative interpretation of the pH-dependent phase diagram of EDL-MF', *Brazilian Journal of Physics*. Sociedade Brasileira de Física, 39(1a), pp. 230–235. doi: 10.1590/S0103-97332009000200018.

Chen, C. *et al.* (2009) 'Temporal evolution of pore geometry, fluid flow, and solute transport resulting from colloid deposition', *Water Resources Research*. John Wiley & Sons, Ltd, 45(6). doi: 10.1029/2008WR007252.

Cosgrove, T. (Terence) (2010) *Colloid science : principles, methods and applications*. Wiley. Available at: https://www.wiley.com/en-gb/Colloid+Science%3A+Principles%2C+Methods+and+Applications%2C+2nd+Edition-p-9781444320206 (Accessed: 8 August 2019).

Elimelech, M. (Menachem) (1998) *Particle deposition and aggregation : measurement,*

modelling, and simulation. Butterworth-Heinemann.

Elimelech, M. and O'Melia, C. R. (1990) 'Kinetics of Deposition of Colloidal Particles in Porous Media', *Environmental Science and Technology*, 24(10), pp. 1528–1536. doi: 10.1021/es00080a012.

Gitis, V. *et al.* (2010) 'Deep-bed filtration model with multistage deposition kinetics', *Chemical Engineering Journal*. Elsevier B.V., 163(1–2), pp. 78–85. doi: 10.1016/j.cej.2010.07.044.

Guzmán, O. and de Pablo, J. J. (2003) 'An effective-colloid pair potential for Lennard-Jones colloid–polymer mixtures', *The Journal of Chemical Physics*. American Institute of Physics, 118(5), pp. 2392–2397. doi: 10.1063/1.1533787.

Happel, J. (1958) 'Viscous flow in multiparticle systems: Slow motion of fluids relative to beds of spherical particles', *AIChE Journal*. John Wiley & Sons, Ltd, 4(2), pp. 197–201. doi: 10.1002/aic.690040214.

Henry, C., Minier, J. P. and Lefèvre, G. (2012) 'Towards a description of particulate fouling: From single particle deposition to clogging', *Advances in Colloid and Interface Science*, 185–186(October), pp. 34–76. doi: 10.1016/j.cis.2012.10.001.

Hiemenz, P. C. and Rajagopalan, R. (1997) *Principles of Colloid and Surface Chemistry*. Taylor & Francis Group, 6000 Broken Sound Parkway NW, Suite 300, Boca Raton, FL 33487-2742: CRC Press. doi: 10.1201/9781315274287.

Israelachvili, J. N. and Tabor, D. (1972) 'The Measurement of Van Der Waals Dispersion Forces in the Range 1.5 to 130 nm', *Proceedings of the Royal Society A: Mathematical, Physical and Engineering Sciences*. The Royal SocietyLondon, 331(1584), pp. 19–38. doi: 10.1098/rspa.1972.0162.

Johnson, W. P., Li, X. and Yal, G. (2007) 'Colloid retention in porous media:

Mechanistic confirmation of wedging and retention in zones of flow stagnation', *Environmental Science and Technology*, 41(4), pp. 1279–1287. doi: 10.1021/es061301x.

Kretzschmar, R. *et al.* (1997) 'Experimental determination of colloid deposition rates and collision efficiencies in natural porous media', *Water Resources Research*. John Wiley & Sons, Ltd, 33(5), pp. 1129–1137. doi: 10.1029/97WR00298.

Logan, B. E. *et al.* (1995) 'Clarification of Clean-Bed Filtration Models', *Journal of Environmental Engineering*, 121(12), pp. 869–873. doi: 10.1061/(ASCE)0733-9372(1995)121:12(869).

Mays, D. C. and Hunt, J. R. (2004) 'Hydrodynamic Aspects of Particle Clogging in Porous Media'. American Chemical Society. doi: 10.1021/ES049367K.

Nelson, K. E. and Ginn, T. R. (2005) 'Colloid filtration theory and the happel sphere-in-cell model revisited with direct numerical simulation of colloids', *Langmuir*, 21(6), pp. 2173–2184. doi: 10.1021/la048404i.

Ng, H. Y. and Elimelech, M. (2004) 'Influence of colloidal fouling on rejection of trace organic contaminants by reverse osmosis', *Journal of Membrane Science*. Elsevier, 244(1–2), pp. 215–226. doi: 10.1016/J.MEMSCI.2004.06.054.

Nowack, B. and Bucheli, T. D. (2007) 'Occurrence, behavior and effects of nanoparticles in the environment', *Environmental Pollution*. Elsevier, 150(1), pp. 5–22. doi: 10.1016/J.ENVPOL.2007.06.006.

Oldham, K. B. (2008) 'A Gouy–Chapman–Stern model of the double layer at a (metal)/(ionic liquid) interface', *Journal of Electroanalytical Chemistry*. Elsevier, 613(2), pp. 131–138. doi: 10.1016/J.JELECHEM.2007.10.017.

van Oss, C. J., Giese, R. F. and Costanzo, P. M. (1990) 'DLVO and Non-DLVO Interactions in Hectorite', *Clays and Clay Minerals*. Springer International Publishing,

38(2), pp. 151–159. doi: 10.1346/CCMN.1990.0380206.

Polte, J. (2015) 'Fundamental Growth Principles of Colloidal Metal Nanoparticles - a new Perspective', *CrystEngComm*, 17(5), pp. 6809–6830. doi: 10.1039/C5CE01014D.

Rajagopalan, R. and Tien, C. (1976) 'Trajectory analysis of deep-bed filtration with the sphere-in-cell porous media model', *AIChE Journal*. John Wiley & Sons, Ltd, 22(3), pp. 523–533. doi: 10.1002/aic.690220316.

Ryan, J. N. and Elimelech, M. (1996) 'Colloid mobilization and transport in groundwater', *Colloids and Surfaces A: Physicochemical and Engineering Aspects*, 107(95), pp. 1–56. doi: 10.1016/0927-7757(95)03384-X.

Ryan, J. N. and Gschwend, P. M. (1994) 'Effects of Ionic Strength and Flow Rate on Colloid Release: Relating Kinetics to Intersurface Potential Energy', *Journal of Colloid and Interface Science*. Academic Press, 164(1), pp. 21–34. doi: 10.1006/JCIS.1994.1139.

Sallès, J., Thovert, J. F. and Adler, P. M. (1993) 'Deposition in porous media and clogging', *Chemical Engineering Science*. Pergamon, 48(16), pp. 2839–2858. doi: 10.1016/0009-2509(93)80031-K.

Shen, C. *et al.* (2007) 'Kinetics of coupled primary- and secondary-minimum deposition of colloids under unfavorable chemical conditions', *Environmental Science and Technology*, 41(20), pp. 6976–6982. doi: 10.1021/es070210c.

Stevik, T. K. *et al.* (2004) 'Retention and removal of pathogenic bacteria in wastewater percolating through porous media: A review', *Water Research*, 38(6), pp. 1355–1367. doi: 10.1016/j.watres.2003.12.024.

Sugimoto, T. (2001) *Monodispersed particles*. Elsevier.

Tian, Y. *et al.* (2010) 'Transport of engineered nanoparticles in saturated porous

media', *Journal of Nanoparticle Research*, 12(7), pp. 2371–2380. doi: 10.1007/s11051-010-9912-7.

Tomilov, A. *et al.* (2013) 'Aggregation in colloidal suspensions: Evaluation of the role of hydrodynamic interactions by means of numerical simulations', *Journal of Physical Chemistry B*, 117(46), pp. 14509–14517. doi: 10.1021/jp407247y.

Tong, M. and Johnson, W. P. (2006) 'Excess colloid retention in porous media as a function of colloid size, fluid velocity, and grain angularity', *Environmental Science and Technology*, 40(24), pp. 7725–7731. doi: 10.1021/es061201r.

Torkzaban, S., Bradford, S. A. and Walker, S. L. (2007) 'Resolving the coupled effects of hydrodynamics and DLVO forces on colloid attachment in porous media', *Langmuir*, 23(19), pp. 9652–9660. doi: 10.1021/la700995e.

Torkzaban, S., Scott A., Bradford, A. and Walker, S. L. (2007) 'Resolving the Coupled Effects of Hydrodynamics and DLVO Forces on Colloid Attachment in Porous Media'. American Chemical Society. doi: 10.1021/LA700995E.

Tufenkji, N. and Elimelech, M. (2004) 'Deviation from colloid filtration theory in the presence of repulsive electrostatic interactions: Implications to microbial transport', (21), p. ENVR-095.

Waite, T. D. *et al.* (1999) 'Colloidal Fouling of Ultrafiltration Membranes: Impact of Aggregate Structure and Size', *Journal of Colloid and Interface Science*, 212(2), pp. 264–274. doi: 10.1006/jcis.1998.6040.

Yao, K., Habibian, M. T. and O'Melia, C. R. (1971) 'Water and Waste Water Filtration: Concepts and Applications', *Environmental Science & Technology*, 5(11), pp. 1105–1112. doi: 10.1021/es60058a005.

Yiantsios, S. G. and Karabelas, A. J. (2003) 'Deposition of micron-sized particles on

flat surfaces: Effects of hydrodynamic and physicochemical conditions on particle attachment efficiency', *Chemical Engineering Science*. Elsevier Ltd, 58(14), pp. 3105–3113. doi: 10.1016/S0009-2509(03)00169-6.

Chapter 3. Modelling and simulation techniques for colloidal deposition within porous media

Within the literature two types of modelling take precedence when understanding colloidal filtration and sand bed dynamics. Two systems, Eulerian and Lagrangian, apply to different length scales; Eulerian concentrates on the continuum basis of the system, i.e. modelling the mass or concentration balances at the macro-scale, whereas, Lagrangian focuses on the micro-scale and explicit tracking of individual or collections of particles to single or multiple collectors (Molnar *et al.*, 2015). Though fundamentally different, recently both Lagrangian and Eulerian techniques have been used in conjunction to increase the accuracy of both modelling techniques (Nelson and Ginn, 2005).

3.1 Eulerian modelling

Eulerian techniques (or continuum modelling) can be understood to describe the behaviour of colloidal transportation within porous media offers the distinct advantage of allowing for concurrent modelling of various mechanisms irrespective of spatial scale (Babakhani *et al.*, 2017). This behaviour is commonly captured using the following advection dispersion equation (ADE) which can either be constructed using the mass balance or the population balance of the system (Tufenkji, 2007):

$$\frac{\partial C}{\partial t} = D\frac{\partial^2 C}{\partial x^2} - V_0\frac{\partial C}{\partial x} - kC \qquad 3.1$$

Where C is the particle concentration, D is the dispersion coefficient and V_o is the upstream fluid velocity, x is the domain length and k is the deposition coefficient

This behaviour is dependent on the necessary rate coefficients attached to the advection-diffusion equation (ADE). Originally within the literature, emphasis was

placed upon a single kinetic retention coefficient, which captured the deposition of colloidal particles at the surface of collector using a combination of average deposition efficiency and collector interception efficiency, with implication that the behaviour of this coefficient was independent of the bed depth. Within the confines of idealised particle deposition, i.e., when a particle makes contact with the collector surface irreversible deposition occurs, a single rate coefficient can be seen to fit well the breakthrough data (Kretzschmar *et al.*, 1997). Recently, the behaviour of the rate coefficient has been shown to depend on the bed depth along with a number of other parameters and as such, dual-deposition rates have been applied to the ADE in which the deposition of particles can be captured more accurately as a function of fluid velocity within the porous media (Chatterjee, Pratap and Abdulkareem, 2011).

Though dual-deposition rate coefficients offer a more suitable extension to the standard ADE, they still offer an underestimation of breakthrough due to neglecting both colloidal particle-particle aggregation and reversible deposition. By extending the modelling criteria to include these, a coupled differential equation can be used to model a full multi-stage kinetic system in which deposition occurs in 3 fundamental stages (Gitis *et al.*, 2010):

1. Ripening stage – assumed to deposition onto the surface of the collector is irreversible and monolayer of particles is produced
2. Operable stage – reversible deposition can occur, nominally due to variations in surface chemistry and flow velocity
3. Breakthrough stage – the point where maximum bed saturation occurs and the system is assumed to undergo significant particulate breakthrough

By application of these three stages the mass balance equation (3.1) is extended to incorporate porosity as a time dependent function, producing the following:

$$\frac{\partial fC}{\partial t} + \frac{\partial \sigma}{\partial t} = -\frac{\partial}{\partial x} j \qquad 3.2$$

Where f is the porosity of the system, x is the domain length, C is the concentration, σ is the specific deposit, where j is the particle flux of the system:

$$j = V_0 C - \epsilon D \frac{\partial C}{\partial z} \qquad 3.3$$

Where D, is the dispersion coefficient, V_o is the fluid velocity and finally, the kinetic coefficients for each stage are captured using the following equations:

$$\frac{\partial \sigma^{\mathrm{def}}}{\partial t} = \begin{cases} K_r uC & 0 < \sigma \leq \sigma_r \\ K_a uC - K_d \sigma & when\ \sigma_r < \sigma < \sigma_u \\ 0 & \sigma = \sigma_u \end{cases} \qquad 3.4$$

Where K_r is the attachment coefficient during ripening, K_a is the attachment coefficient, K_d is the detachment coefficient, σ_r transient specific deposit, σ_u final specific deposit

It can be seen that each stage of the kinetic retention relies on the attachment rate and detachment rate, which are experimentally derived coefficients. An alternative attachment coefficient and detachment coefficient can be modelled using a variety of different techniques or fitted against various experimental data sets. By choosing suitable coefficients from the literature or by experimental observation, it can be seen that the above method captures the breakthrough and deposition concentration within porous media (Figure 3.1).

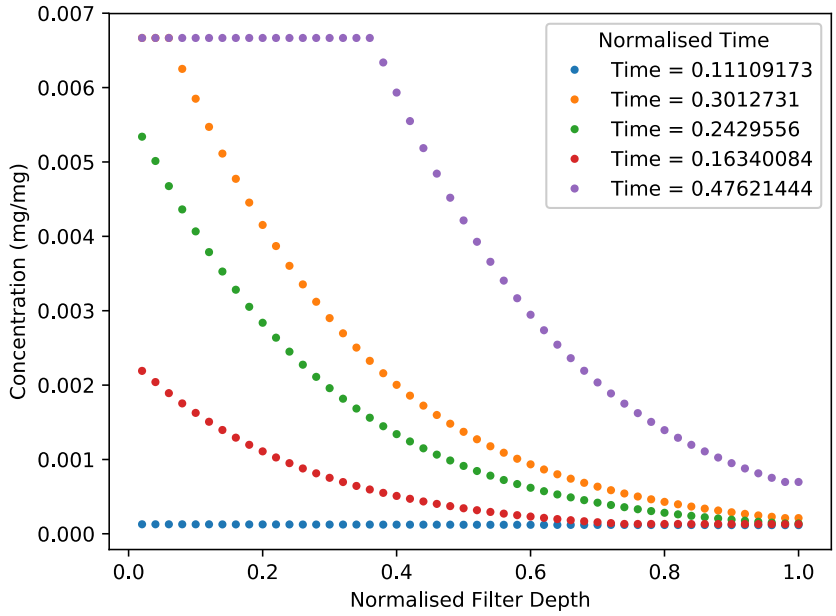

Figure 3.1 Particle concentration profile along the length a porous medium column when equation 3.2 is solved within the gProms modelling suite.

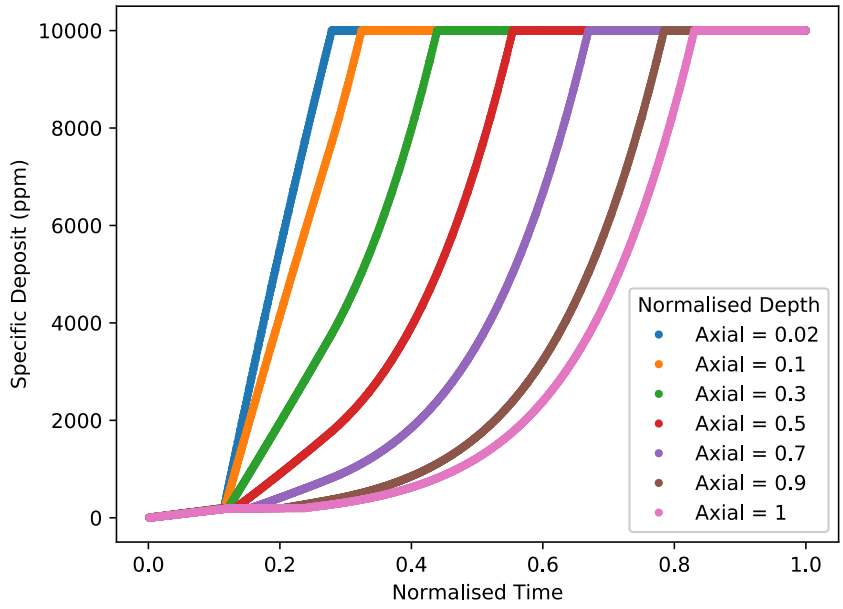

Figure 3.2 The specific deposit of particles as a function of time at varying bed depths within the gProms simulation suite.

As such, it can be inferred that these coefficients are fundamentally sensitive to variations within the porous media (equation 3.4).Recently, a review of the sensitivity

of the K_d and K_a coefficients to differing physical and chemical processes was undertaken; which concluded that these coefficients are inherently sensitive to variations to the chemistry and physics of the system (Babakhani *et al.*, 2017). By introducing these parameters the uncertainty in the solution is increased, particularly when introducing DLVO interactions wherein the change in concentration can be assumed to be a function of the surface chemistry of the system. In the DLVO case there is a significant sensitivity to the zeta (ξ) potential of the collector surface, however, solving the zeta potential analytically is complex and in most cases unattainable. With this increasing complexity it is regularly found that Eulerian techniques utilise experimental zeta potentials, however, any experimental error is then carried over into the continuum model.

Furthermore, the column length was found to significantly affect the breakthrough profile (Foppen, van Herwerden and Schijven, 2007). This implies that the behaviour within the column is a function of the length, along with the mixing capability of the colloids in flow and the interaction with the collector surfaces. In traditional Eulerian modelling, the domain is usually simplified to a 1D assumption and utilises the Happel sphere-in-cell method, in which only a single collector is modelled and the behaviour of the system is extrapolated (Nelson and Ginn, 2005). Extrapolation of this system may thus cause inherent instabilities within the macro-scale model, as functions which are highly sensitive are smoothed out or ignored.

Apart from the previous example of issues with the Eulerian approach there are also a number of other disadvantages associated with the use of this method, at the increase in speed and spatial domain accessibility there is a reduction in resolution (Clement *et al.*, 2002). This reduction can significantly reduce the accuracy of the solution and offers a large amount of uncertainty. By introducing the coefficient terms within the

equation the behaviour of the colloids are neglected and averages, however, these coefficients neglect the geometry of the deposits, location on the surface, and pore throat geometry even though this is well established within the literature to influence the rate at which pressure drop and breakthrough occurs (Song and Elimelech, 1993; Ko, Bhattacharjee and Elimelech, 2000; Benamar *et al.*, 2007).

Finally, the behaviour of fluid flow is neglected, it is common practice within Eulerian methods to utilise the Happel-sphere-in-cell or hemispheres-in-cell to capture the flow profile around a smooth collector (Boccardo, Marchisio and Sethi, 2014). By using this technique the fluid is split into two phases the near surface phase in which interactions with the collector (sand grain) can occur and the fluid phase in which the fluid is undisturbed by the collector. Though this offers speed in calculation it makes a large number of assumptions which can rapidly introduce errors within the model. Firstly, the collector surface is idealised and usually assumed to be spherical, though some recent work has sort to introduce surface roughness to the procedure (Ma *et al.*, 2009). Secondly, the influence of the surrounding collectors are captured within the porosity term. Finally, the behaviour of the colloids are considered to be influenced by three terms: sedimentation, diffusion and interception (Nelson and Ginn, 2005). Whilst the introduction of rolling and collection of colloids in the wake of the collector is neglected. Furthermore, the use of localised collection rate is used and then averaged for the area of the bed to ensure that any inherent local heterogeneity is smoothed out to produce global homogeneity.

3.2 Lagrangian particle tracking

An alternative approach to solving sand bed performance issues is to use a Lagrangian particle tracking (LPT) method. This approach uses localised interactions between the particles and the fluid phase, to predict the likelihood of aggregation between particles

and also interception and sedimentation of the particles on the collector (Johnson, Li and Yal, 2007). Lagrangian particle tracking methods are well established techniques, commonly found when dealing with deformable, highly mobile particle structures (Ansell and Dickinson, 1986). These techniques are well established in terms of engineering based problems, for example when dealing with the degradation of various materials under high stresses. Within the nuclear industry this could be, fuel rod degradation in the reactor core or the degradation of the pipelines within the wastewater processing procedure. They have also been used to study the re-entrainment of deposited materials in highly mobile areas, i.e. fluid flows which undergo turbulent regimes (Re > 100) (Sefrioui *et al.*, 2013). These studies show the versatility and the application of Lagrangian particle tracking methods for studying the behaviour of particles and particle complexes within highly complex flows (Tsuji, Kawaguchi and Tanaka, 1993). Further, they also offer an insight in how the flow field itself behaves with the introduction of high concentrations or volumes of particles within the flow (Tartakovsky, Tartakovsky and Meakin, 2008). By using these techniques, predictions can be made on the likelihood of deposition at wall boundary phases and also how turbulence may affect deposition and re-entrainment rates.

It is understood that volumetric flow rate within the sand bed conforms to Stokes flow (Re << 1), though pore flow rates may break this in highly confined channels (i.e. semi-blocked pore space). This behaviour implies that the flow around the collector surface is laminar, however, in reality the flow would exhibit some micro-turbulence behaviour particle in areas of high surface roughness either induced by the crystalline structure of the collector or the deposition of the colloidal particles onto the surface structure. Furthermore, from a nanoparticle point of view the behaviour of the particle deposition and further re-entrainment rates are heavily influenced by these systems. In particular, it is well established that deposited particles on the surface of collectors exhibit a

rolling motion as a function of the forces being exerted upon them (Molnar *et al.*, 2015). This rotational motion can significantly affect the fluid behaviour after a long time period, particular in regions of initial high deposition in which the deposited aggregate slowly grows into the main fluid flow channel, in this case the overall shearing effect may become pronounced enough for the aggregate to break off and block a pore deeper within stream (Torkzaban, S. a. Bradford and Walker, 2007). By using a Eulerian approach to this problem, these effects are captured within the attachment and detachment criteria within the parameters, however, these parameters neglect to incorporate that detachment may only be a function of the colloidal particle rolling along the surface until it reaches an area of reduced shear force at which point the colloidal is effectively re-attached. In comparison, by using a Lagrangian technique this is taken into account due to the force balances which are continually being calculated upon the particle. These forces balances are explicitly calculated from the equations of motions:

$$m_p \frac{dv_p(t)}{dt} = F^{drag} + F^b + F^g + F^B + F^c \qquad 3.5$$

In which m_p is the mass of the colloid, $v_p(t)$ is the velocity of the colloid, F^{drag} is viscous drag, F^b is the buoyancy, F^G is the gravitational body force, F^B is the Brownian motion force, F^c is the interaction force

By using a suitable integration technique and utilising a fluid solver it is possible to predict the trajectory of the particles within porous media, allowing for a more detailed understanding of the deposition on the collector surface.

There are some disadvantages to using LPT, particularly when dealing with large scale systems such as, a full-scale sand bed plant. The major limiting factor, is the cost in computing power, as the spatial and temporal scalability are limited. Though with the use of parallelisation in high performance computing, much larger dataset are now

being analysed. Furthermore, the concentration of the particles need to be chosen carefully as a significant proportion of the technique relies upon the necessary tracking algorithm (Wang *et al.*, 2012). As well as, the concentration needing to be chosen carefully, the number of parameters within this model also need to be chosen with consideration. In particularly, when dealing with particle-particle collisions and particle-collector collisions. Some of this issue are addressed when dealing with a suitable mesh for domain as well as the most suitable numerical technique. When dealing with LPT it is common to use computational fluid dynamic (CFD) techniques (RANS, DNS, LES etc.) as well as numerical discretization techniques (FDM, FEM, FVM). These techniques are used to simplify the Navier-Stokes equation and in particular calculate the forces in which the particles are introduced too. For higher Reynold number flows, these techniques are well suited and are well cited within the literature, however, at lower Reynold number flows i.e. creep, the efficiency of these techniques quickly reduces. Furthermore, the complexity of domain being studied quickly increases run time (Wang *et al.*, 2012).

3.4 Agent based modelling for colloid facilitated transport

The use of agent based modelling (ABM) offers an alternative way to understand colloidal particle deposition within porous media whilst utilising the techniques produced within the Lagrangian particle tracking method. Within the traditional particle tracking methods when particles undergo aggregation or deposition the potentials between the particles are explicitly calculated, ABM offers an alternative method in which the aggregation and deposition is broken down into a rule based collision utilising similar ideas to LPT without the need for excessive computation. Within this context the particles are represented as agents undergoing autonomous interactions. Over time these interactions result in emergent behaviour forming, in the case of particle-particle interaction aggregation and in particle-collector interaction

deposition. Furthermore, as agents are considered autonomous, sensitivities to different parameters can be tested without the need to change the fundamental equations or systems in which the agents reside.

3.41 History of agent based modelling

The emergence of complex adaptive systems (CAS) was developed allowing for the inherent complexity of a system to be captured by describing the individual behaviour of the elements within the system and their interactions with each other.

An example, is the traditional swarm system, this system is readily observable in nature (bird flocking, bee swarms, and fish shoaling). By modelling this system as collection of individual elements which interact with each other it is possible to capture complexity of the system (Railsback, 2001). Furthermore, by understanding the individual processes which comprise the system dynamics it is possible to capture the emergence of the system. This emergence in nature produces the traditional flocking (Figure 3.3) in which the collective behaviour produces complex and constantly adapting shapes, however, if the individual motion of the element was traced the behaviour would appear chaotic.

Figure 3.3 The system dynamics of a starling swarm which shows the emergent collective behaviour from individual interactions between starlings (Kjaer, 2011).

This leads to an ability to define a CAS in two ways using the following definitions (Ahmed, Elgazzar and Hegazi, 2005):

1. The system consists of a number of interacting heterogeneous agents, who are capable of adapting
2. Emergence is exhibited at the system level which is not recognised at the individual agent level

Though this is the definition chosen here, it is currently a highly contentious issue with complexity modellers choosing their own definitions to describe a complex system. In general, however, all complex models behave as described above. This can be seen by the quote by (Dent, 1999)

"*Complexity science is an approach to research, study, and perspective that makes the philosophical assumptions of the emerging worldview"*

Though (Holland, 2006) expanded upon this definition significantly by introducing two other definitions:

1. Conditional action, the agents rely on the information in which they share or receive. This information can be passed from the agent-agent interactions or agent-environment interactions
2. Modularity, each of the agents exists within their own or shared sub-routines which allow for the generation of the system as a whole. These sub-routines constitute the agents rules within the environment

This in turn formalised the use of agent based modelling as a way to solve complex adaptive systems, when using an agent-based model the use of solvable equations is greatly reduced and instead replaced with the use of a collection of if-then logic questions. This allows for the reduction of differential equations needing to be solved

and allows for the heterogeneity of the system to be captured, something which traditionally is lost (Holland, 2006). Using the example of multi-body interactions it is possible to produce an agent based model of a multi-celestial body system, by assuming that each of the bodies are individual elements within the system and can interact with each other using a number of simplified assumptions whilst remaining autonomous. The system behaviour would then emerge to produce a more complete model.

Effectively, the system is described as a collection of interacting agents which observe the following behaviour characteristics (Tarvid, 2016):

- Situation - The agents respond to changes in their environment and can enact change upon their environment
- Autonomy – Control their own behaviour by a series of person rules and do not need a global controller
- Flexibility - Can plan their actions from the possibility of future environmental changes
- Social – Can interact with other agents and the environment

Agent based modelling offers an alternative to the complex and sometimes unachievable process of creating a series of mathematical equations to describe the behaviour of adaptive systems. Bypassing this process and instead using a series of flow procedures, i.e. if/then constructs, it is possible to capture the essence of the problem offering an alternative way of solving the problem (Holland, 2006). Though agent based models also simplifies the system, this simplification is a function of reducing the problem down to its key components and allowing for the behaviour of the system to emerge from a series of simple interactions as a function of these rules (Holland, 2006). Finally, by not employing traditional mathematical solving techniques it allows for highly heterogeneous systems to be modelled without the need of a series of complex

differentials. By applying the necessary agent based techniques, problems which were once intractable due to their inherent heterogeneous nature are now solvable in a conceptual sense. This notion of simplifying complex systems is novel in its ability to conceive the problem; as a set of dependent interactions in which the summation of all known and unknown interactions produce emergence of large scale phenomena (Railsback, 2001).

3.42 Common simulation packages

As the use of ABM became more wide-stream so did the growth in simulation packages, each of these packages offers a different advantages when approaching an agent based problem. Within the literature there have been a number of comprehensive review of available simulation packages for a variety of different applications (Abar *et al.*, 2017; Nikolai and Madey, 2009; Railsback, Lytinen and Jackson, 2006; Tobias and Hofmann, 2004). Each of these reviews focused on different applications of simulation packages, with the reviews of Railsback and Tobias both focussing on their respective fields, whereas, the review by Nikolai and Madey covers a general review of the majority of simulation suites available. In effect all the reviews cover a similar scope of characteristics namely; the language require to programme and simulate, types of licence required to run and types of support available for the user.

There are a large number of simulation toolkits and suites available both freeware and other licenced, whilst some of these models are generic simulation toolkits with a large range of applications others are predominately aimed at specific environments (Hofmann, 2004; Madey, 2009). Each of these simulation packages are developed within the intention of offering specific modelling environments which fit the user's needs, as a consequence of this it is common to find a large amount of commercial and freeware simulations being developed or based around either Java, C or similar high

level languages, hence requiring the user to have a some experience with programming and programming languages (Abar *et al.*, 2017). Furthermore, the learning curve within these simulation environments can be relatively steep and can be off putting for a number of researchers who are more interested in modelling the system rather than learning a programming language.

As such, a number of simpler languages have been developed which allow for basic agent based models to be developed without the need for a programming background (Table 3.1). These models offer an easier inception, however, with limitations on scalability. A full review of these relative merits of each simulation on scalability and simplicity of learning was produced by Abar *et al*, with Figure 3.3 showing a simplified version of this.

	Ease of Implementation →		
Scalability ↑	Easy	Moderate	Hard
Large-scale	SeSaM	AnyLogic FLAME	FLAME GPU Repast Symphony
Medium-Scale	NetLogo	GAMA	MASON
Small-scale	AgentScript Scratch	SEAS	

Figure 3.4 Comparison of different agent based modelling packages (adapted from Abar et al., 2017)

The majority of agent based modelling simulation packages are built to provide easier modelling capabilities from either a laptop or desktop. However, some of the toolkits offer the added advantage of allowing for high performance computing (HPC), in particular, FLAME and RePast are specifically developed for this use (Collier and North, 2012; Kiran *et al.*, 2011). By offering large scale parallelisation, a much more scalable model can be created which allows for the influence of a large number of agents to be

tested with long run times. Though the obvious advantage of using HPC ABM is the scalability, both of these modelling suites require the knowledge of C++ to run along with knowledge of HPC processes and how to parallelise the model without affecting the outcome.

Models	**Implementation language**
Swarm	Objective-C
NetLogo	Logo
Gama	GAML
Cormas	SmallTalk
Repast Symphony	Java

Table 3.1 Commonly cited ABM suites and the language they use

3.43 NetLogo

When compared to other agent based modelling simulation suites NetLogo was the obvious choice due to the large number of cited literature associated with the model along with its relative ease in learning. Furthermore, it offers a large dictionary of terms along with a model library allowing for a more rapid learning curve in comparison to the alternative modelling suites available. Finally, when compared to other models which are easy to implement NetLogo stands alone for its scalability along with the length in which it has been available as an ABM tool (Tisue and Wilensky, 2004). As the popularity of NetLogo has increased so have the options for further extensions within the modelling environment, there are number of key extensions which are useful when dealing with large datasets or models, such as the R, Python and Mathematica extensions (Thiele and Grimm, 2010). As well as this, there a number of

tools online which accept NetLogo built models such as the OpenMole tool, which allows for a rapid sensitivity analysis of models to be undertaken. Finally, other modelling suites such as RePast are now accepting NetLogo built models, offering the easy learning curve of the Logo with the power of more C++. By accepting NetLogo models within RePast the advantages of both modelling suites to be combined.

The NetLogo interface can be seen in Figure 3.5, the tabs denote the location of the user within the simulation suite. The interface tab shows the current model being run with the procedural buttons outlined, the code tab is where the main body of code is inputted and variables are created and stored, finally, the info tab allows for an explanation of the model to be created along with suitable suggestions for extensions (this is due to NetLogo's original purpose as a simulation tool) (Tisue and Wilensky, 2004).

One of the major advantages of NetLogo compared to other simulation suites is the interface tab in which the current model being run can be easily monitored within live reporting of outputs being made available (Figure 3.5). Furthermore, global variables, local variables and constants can all be set within this interface by the use of NetLogo's in built input criteria. This allows for a models variables to be easily changed and extended without the need for excessive coding in comparison, to other simulation suites require explicit coding to produce a graphical interface.

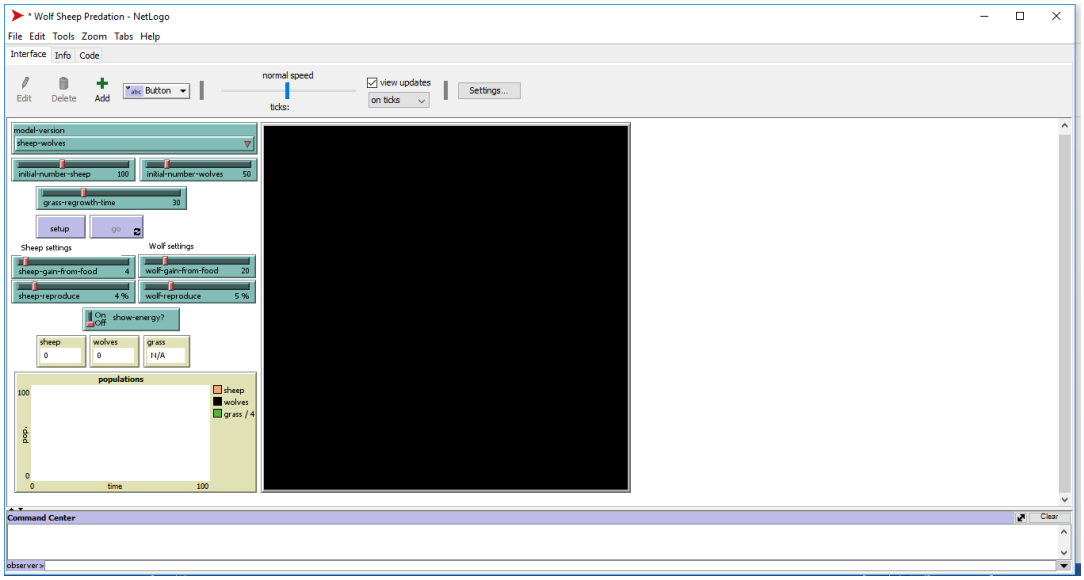

Figure 3.5 Shows the Wolf-Sheep predation model within NetLogo where the graphical output screen, plots, run commands and input variables are shown (Wilensky, 1999)

Within NetLogo the term “world” is used to define the domain in which the model is run over (Figure 3.5), within this world exists three agent structures; patches, turtles, links. The patch agent is an immovable object which can interact with other patches and turtles. The turtle agent is a moveable agent which can interact with both other turtles, patches and links. Finally, link agents connect turtles allowing for transfer of information to occur, links cannot occur without a turtle (Wilensky, 1999).

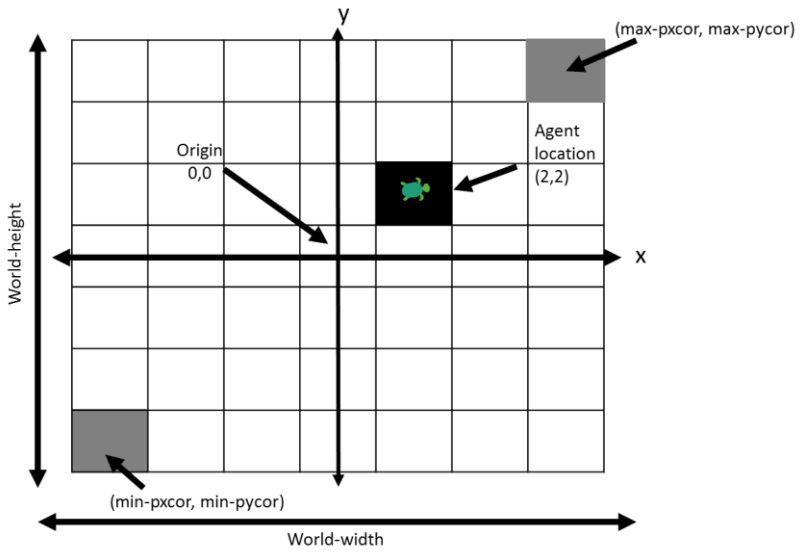

Figure 3.6 Schematic of the NetLogo world with the key agents highlighted

Another advantage of using NetLogo is the in-built behaviour space system, this allows for parameter sweeping to occur in which the key variables within the model can be varied systematically. This allows for a range of sensitivity analysis to occur. Behaviour space can run on multiple processors meaning that a large range of variables can be tested for sensitivity without the need for the user to run multiple models themselves, hence reducing the time needed for large datasets to be produced. Furthermore, multiple variables can be run in combinations allowing for large scale parameter sweeping to occur, resulting in a more optimised run time. Finally, the results are outputted either in table or text format allowing for easy analysis to occur within a number of scientific tools (Wilensky, 1999).

Though NetLogo offers a distinct advantage than the majority of ABM suites available it does have some inherent issues due to the audience at which it is aimed. The setup of the code tab requires that all code is inputted within a single file in which procedures are called from other procedures within this file, this can result in a long block of code. This can cause excessively long file sheets if complex systems within multiple

procedures are being run. Furthermore, in a recent review of the 5 major ABM suites available when compared to higher language programming the scale of the models are limited along with run times (Abar *et al.*, 2017). These run times are also function of the simplicity of the language, as the programming uses the Pseudo-language Logo where the NetLogo code is converted into Java before running. Hence, a limitation on the memory usage, though recent iterations of the simulation suite have been produced which optimise the memory usage and allow for larger memory allocation to be set from the command line (Railsback *et al.*, 2017). The language limitation also means that it is not possible to run NetLogo models on HPC facilities, however, as previously mentioned RePast now accepts NetLogo models and converts them to RePast code which can run on HPC facilities. Finally, though the debugging within NetLogo allows for quick and easy access within the coding tab, it does not offer a more detailed error checker usually associated with IDE's with some error messages going unlogged or else with no explanation, usually associated with a Java error within the compiling of the model. Table 3.1, gives a comparison of the advantages and disadvantages of using NetLogo as the agent based modelling suite. It can be seen that though there are a number of disadvantages, there are considerably more advantages in using NetLogo. This is especially the case when modelling is the priority rather than learning a new programming language.

Advantages	Disadvantages
Large amount of literature surrounding NetLogo, as well as, a well validated and cited simulation package	Currently un-able to perform high performance modelling, though this is an active area of research
Offers an easier learning curve	Limitation of memory usage
Does not assume user has any previous knowledge of traditional modelling languages (C++, Java, Fortran)	Can be issues with debugging
Has a large dictionary and training module database to aid in learning	
Can support number of extensions for data analysis (Python, Mathematica)	
Has inbuilt functionality for easy parameter sweeping by using the "behaviour space" module	
The interface tab allows for "live" monitoring and graphical output	

Table 3.2 The advantages and disadvantages to using NetLogo as an agent based modelling suite

3.44 Applicability of agent based modelling to colloid filtration

Application of an agent based model to colloidal filtration can offer extended information on the sensitivity of aggregate morphology and deposition processes within porous media. Colloidal particles can easily be described as agents, they behave within a strict set of rules which exhibit self-similar behaviour and behave with autonomy within this environment. Even when aggregate or deposited on the collector surface if particles have significant thermal energy they can be released particle into the flow. Therefore, it could be argued that these environments fit the nature of agent based modelling, in particular, with their complex nature and natural emergency depending on a number of key variables such as, surface chemistry, particle size, shape, and flow velocity.

With the use of the particle tracking method discussed within the Lagrangian section (3.2) it can be seen to offer a suitable method when describing the system in a set of

fundamental rules. Colloidal particles undergo transportation as a function of the forces applied to them, however, the behaviour of the particles is fundamental to their own variables, i.e. in the case of large particles within a flow domain they exhibit less diffusive property than that of smaller particles in the exact same domain. The behaviour of these particles is purely autonomous and irrespective of what other particles are doing within the system. The application of agent based modelling with particle tracking methods and fluid dynamics was previously undertaken by Fullstone *et al.*, 2015, in which the behaviour of red blood cells in the vicinity of a porous membrane. This technique can be seen to be directly comparable to the process of deposition on the surface of collector.

Furthermore, particle interactive behaviour can be decomposed into a simple set of rules; in the case of particle aggregation or deposition the likelihood of depositing can be described in a simple if/or statement rather than explicitly calculating the total potential energies thus exhibiting an easier model to simulate with less computational constraints. Naturally, within the NetLogo environment the behaviour of particles interacting and aggregating can be captured utilising the linking procedures in which particles remain autonomous but share information which allows them to update their relative position whilst following the fundamental requirements of the system.

Finally, within the role particle deposition, the emergence of geometry along with deposition location can be studied as a simple function of the solution to the particle trajectory location along with the "rules" attributed to deposition upon the particle surface. Hence, allowing for an interrogation of the particle geometric profile as a function of different variables. By approximating colloidal systems, as an agent based model the fundamental deposition behaviour and aggregation behaviour can be deconstructed into its key components. This in turns allow for more refined

experiment and modelling to occur in areas that show significant sensitivity within the agent based model. By allowing for agent based modelling to occupy the meso-scale region of simulation it can allow for an invaluable link to be formed between the kinetic coefficients used within the continuum based modelling and the micro-scale temporal and spatially limited solutions offered within the micro-scale.

3.5 Conclusions

It can be seen that the standard models for understanding colloidal transportation and deposition within porous media are lacking in detail, in particular, the key issues surrounding attachment and detachment coefficients used to solve the ADE. The standard approach to solving these coefficient are to fit from experimental datasets, however, it has been established that undertaking this approach ignores a number of key parameters. Furthermore, these coefficients have shown to be highly sensitive to physical and chemical variations within the modelling domain, which as such, implies that a better understanding of the mechanisms which produce these coefficients is needed. Common microscale modelling techniques approach the problem analysing these coefficients by explicitly solving the forces applied to the individual particles and understanding the consequences of this in the deposition structure and location. However, there are a number of issues of scalability associated with these modelling techniques in particular the spatial and temporal scaling can be an issue.

Alternative methods are needed to analyse this problem which offer a bridge between microscale and macroscale modelling, allowing for some of the issues to be negated. Agent based modelling offers an alternative insight into these processes by breaking down the problem into its fundamental characteristics and understanding how these characteristics result in the emergent behaviour seen within colloidal deposition.

Within the agent based modelling community there are a number of simulation suites and toolkits which could be utilised when approaching this problem, however, a review of the advantages and limitations shows that NetLogo is the most applicable simulation suite available (Table 3.2). Furthermore, there is a large amount of literature already associated with NetLogo both the modelling suite being verified along with implementation of agent based models for a number of scientific and economic fields. The simulation suite comes with a large learning toolkit and allows for an easy learning curve making it the optimal choice for analysing the colloidal aggregation and deposition problems outlined within this thesis.

3.5 References

Abar, S. *et al.* (2017) 'Agent Based Modelling and Simulation tools: A review of the state-of-art software', *Computer Science Review*. Elsevier Inc., 24, pp. 13–33. doi: 10.1016/j.cosrev.2017.03.001.

Ahmed, E., Elgazzar, A. S. and Hegazi, A. S. (2005) 'An Overview of Complex Adaptive Systems'. Available at: http://arxiv.org/abs/nlin/0506059 (Accessed: 22 July 2019).

Ansell, G. C. and Dickinson, E. (1986) 'Sediment formation by Brownian dynamics simulation: Effect of colloidal and hydrodynamic interactions on the sediment structure', *The Journal of Chemical Physics*, 85(7), pp. 4079–4086. doi: 10.1063/1.450879.

Babakhani, P. *et al.* (2017) 'Parameterization and prediction of nanoparticle transport in porous media: A reanalysis using artificial neural network', *Water Resources Research*, 53(6), pp. 4564–4585. doi: 10.1002/2016WR020358.

Benamar, A. *et al.* (2007) 'Particle transport in a saturated porous medium: Pore structure effects', *Comptes Rendus Geoscience*. Elsevier Masson, 339(10), pp. 674–681. doi: 10.1016/J.CRTE.2007.07.012.

Boccardo, G., Marchisio, D. L. and Sethi, R. (2014) 'Microscale simulation of particle deposition in porous media', *Journal of Colloid and Interface Science*. Elsevier Inc., 417, pp. 227–237. doi: 10.1016/j.jcis.2013.11.007.

Chatterjee, J., Pratap, S. and Abdulkareem, S. (2011) 'Dual-deposition rates in colloid filtration caused by coupled heterogeneities in a colloidal population', *Journal of Colloid and Interface Science*. Elsevier Inc., 356(1), pp. 362–368. doi: 10.1016/j.jcis.2010.12.029.

Clement, T. P. *et al.* (2002) 'Modeling Bacterial Transport and Accumulation

Processes in Saturated Porous Media: A Review', in *Advances in Nuclear Science and Technology*. Boston: Kluwer Academic Publishers, pp. 59–78. doi: 10.1007/0-306-47088-8_3.

Dent, E. B. (1999) 'Complexity Science : A Worldview Shift', *Emergence*, 1(4), pp. 5–19. doi: 10.1207/s15327000em0104_2.

Foppen, J. W., van Herwerden, M. and Schijven, J. (2007) 'Measuring and modelling straining of Escherichia coli in saturated porous media', *Journal of Contaminant Hydrology*. Elsevier, 93(1–4), pp. 236–254. doi: 10.1016/J.JCONHYD.2007.03.001.

Fullstone, G. *et al.* (2015) 'Modelling the Transport of Nanoparticles under Blood Flow using an Agent-based Approach', *Scientific Reports*. Nature Publishing Group, 5, p. 10649. doi: 10.1038/srep10649.

Gitis, V. *et al.* (2010) 'Deep-bed filtration model with multistage deposition kinetics', *Chemical Engineering Journal*. Elsevier B.V., 163(1–2), pp. 78–85. doi: 10.1016/j.cej.2010.07.044.

Hofmann, R. T. and C. (2004) 'Evaluation of free Java-libraries for social-scientific agent basedsimulation'. JASSS. Available at: http://jasss.soc.surrey.ac.uk/7/1/6.html (Accessed: 23 July 2019).

Holland, J. H. (2006) 'Studying Complex Adaptive Systems', *Journal of Systems Science and Complexity*. Kluwer Academic Publishers, 19(1), pp. 1–8. doi: 10.1007/s11424-006-0001-z.

Kiran, M. *et al.* (2011) 'FLAME: A platform for high performance computing of complex systems, applied for three case studies', *Acta Physica Polonica B, Proceedings Supplement*, 4(2), pp. 201–216. doi: 10.5506/APhysPolBSupp.4.201.

Kjaer, D. (2011) 'A spectacular murmuration of starlings', 9 February. Available at:

https://www.telegraph.co.uk/news/earth/agriculture/farming/8314014/Starlings-like-swarm-of-locusts-say-farmers.html (Accessed: 23 July 2019).

Ko, C.-H., Bhattacharjee, S. and Elimelech, M. (2000) 'Coupled Influence of Colloidal and Hydrodynamic Interactions on the RSA Dynamic Blocking Function for Particle Deposition onto Packed Spherical Collectors', *Journal of Colloid and Interface Science*. Academic Press, 229(2), pp. 554–567. doi: 10.1006/JCIS.2000.7062.

Kretzschmar, R. *et al.* (1997) 'Experimental determination of colloid deposition rates and collision efficiencies in natural porous media', *Water Resources Research*. John Wiley & Sons, Ltd, 33(5), pp. 1129–1137. doi: 10.1029/97WR00298.

Ma, H. *et al.* (2009) 'Hemispheres-in-Cell Geometry to Predict Colloid Deposition in Porous Media', *Environmental Science & Technology*. American Chemical Society, 43(22), pp. 8573–8579. doi: 10.1021/es901242b.

Madey, C. N. and G. (2009) 'Tools of the Trade: A Survey of Various Agent Based Modeling Platforms'. JASSS. Available at: http://jasss.soc.surrey.ac.uk/12/2/2.html (Accessed: 23 July 2019).

Molnar, I. L. *et al.* (2015) 'Predicting colloid transport through saturated porous media: A critical review', *Water Resources Research*, 51(9), pp. 6804–6845. doi: 10.1002/2015WR017318.

Nelson, K. E. and Ginn, T. R. (2005) 'Colloid filtration theory and the happel sphere-in-cell model revisited with direct numerical simulation of colloids', *Langmuir*, 21(6), pp. 2173–2184. doi: 10.1021/la048404i.

Railsback, S. *et al.* (2017) 'Improving Execution Speed of Models Implemented in NetLogo', *Journal of Artificial Societies and Social Simulation*. JASSS, 20(1), p. 3. doi: 10.18564/jasss.3282.

Railsback, S. F. (2001) 'Concepts from complex adaptive systems as a framework for individual-based modelling', *Ecological Modelling*. Elsevier, 139(1), pp. 47–62. doi: 10.1016/S0304-3800(01)00228-9.

Railsback, S. F., Lytinen, S. L. and Jackson, S. K. (2006) 'Agent-based Simulation Platforms : Review and Development Recommendations', *SIMULATION*, 82(9), pp. 609–623. doi: 10.1177/0037549706073695.

Sefrioui, N. *et al.* (2013) 'Numerical simulation of retention and release of colloids in porous media at the pore scale', *Colloids and Surfaces A: Physicochemical and Engineering Aspects*. Elsevier B.V., 427, pp. 33–40. doi: 10.1016/j.colsurfa.2013.03.005.

Song, L. and Elimelech, M. (1993) 'Dynamics of colloid deposition in porous media: Modeling the role of retained particles', *Colloids and Surfaces A: Physicochemical and Engineering Aspects*. Elsevier, 73, pp. 49–63. doi: 10.1016/0927-7757(93)80006-Z.

Tartakovsky, A. M., Tartakovsky, D. M. and Meakin, P. (2008) 'Stochastic Langevin Model for Flow and Transport in Porous Media', *Physical Review Letters*. American Physical Society, 101(4), p. 044502. doi: 10.1103/PhysRevLett.101.044502.

Tarvid, A. (2016) 'Complex Adaptive Systems and Agent-Based Modelling', in. Springer, Cham, pp. 23–38. doi: 10.1007/978-3-319-26539-1_2.

Thiele, J. C. and Grimm, V. (2010) 'NetLogo meets R: Linking agent-based models with a toolbox for their analysis', *Environmental Modelling & Software*. Elsevier, 25(8), pp. 972–974. doi: 10.1016/J.ENVSOFT.2010.02.008.

Tisue, S. and Wilensky, U. (2004) 'NetLogo: A simple environment for modeling complexity', *IN INTERNATIONAL CONFERENCE ON COMPLEX SYSTEMS*, pp. 16--21. Available at: http://citeseerx.ist.psu.edu/viewdoc/summary?doi=10.1.1.117.949 (Accessed: 23 July 2019).

Torkzaban, S., Bradford, S. a. and Walker, S. L. (2007) 'Resolving the coupled effects of hydrodynamics and DLVO forces on colloid attachment in porous media', *Langmuir*, 23(17), pp. 9652–9660. doi: 10.1021/la700995e.

Tsuji, Y., Kawaguchi, T. and Tanaka, T. (1993) 'Discrete particle simulation of two-dimensional fluidized bed', *Powder Technology*. Elsevier, 77(1), pp. 79–87. doi: 10.1016/0032-5910(93)85010-7.

Tufenkji, N. (2007) 'Modeling microbial transport in porous media : Traditional approaches and recent developments', 30, pp. 1455–1469. doi: 10.1016/j.advwatres.2006.05.014.

W. P. Johnson, Xiqing Li, A. and Yal, G. (2007) 'Colloid Retention in Porous Media: Mechanistic Confirmation of Wedging and Retention in Zones of Flow Stagnation'. American Chemical Society. doi: 10.1021/ES061301X.

Wang, H. *et al.* (2012) 'Numerical simulation of particle capture process of fibrous filters using Lattice Boltzmann two-phase flow model', *Powder Technology*. Elsevier, 227, pp. 111–122. doi: 10.1016/J.POWTEC.2011.12.057.

Wilensky, U. (1999). NetLogo. http://ccl.northwestern.edu/netlogo/. Center for Connected Learning and Computer-Based Modeling, Northwestern University, Evanston, IL.

Chapter 4. The implementation and validation of the lattice Boltzmann method within NetLogo

4.1 Modelling of fluid flow in porous media

It is common to simulate the majority of flow problems via a finite class of discretisation methods, i.e finite difference. Through these methods a number of systems have been successfully investigated, however, the use of these techniques can become complicated when solving flow through porous media (Shu, Liu and Chew, 2007). An alternative approach is to apply the lattice-Boltzmann method (LBM) when solving complex boundaries, such as, porous media(Spaid and Phelan, 1997). The ability of LBM to capture fluid flow in complex geometry is well addressed in the literature(Succi, Foti and Higuera, 1989; Manz, Gladden and Warren, 1999; Pan, Hilpert and Miller, 2004; Jeong, Choi and Lin, 2006; Aidun and Clausen, 2010). Furthermore, LBM has been used in a variety of other non-trivial fluid problems, such as, multicomponent flow (Kang, Lichtner and Zhang, 2006), flow of non-Newtonian fluids (Gabbanelli, Drazer and Koplik, 2005) and diffusion-convective systems (He, Li and Goldstein, 2000). The application of LBM focuses on a statistical approach to the behaviour of the fluid particles, however, instead of modelling each particle as in molecular dynamics particles are fixed to a lattice which allows for the Boltzmann equation to be simplified (Chen and Doolen, 1998). The ability of LB to capture fluid flow is based predominately on the collective behaviour of these particles producing macroscopic flow behaviour.

4.1.1 Lattice Boltzmann method

Traditionally, a fluid can be considered a collection of particles which are constantly undergoing diffusion due to thermal and pressure gradients. By assuming that a fluid

can be modelled as a collection of particles undergoing several exchanges of momentum and energies, such exchanges are a result of the random motions of the particle (Guo and Shu, 2013), it can therefore be assumed that each of these exchanges behave as an elastic collision. Modelling such processes can cause numerous issues in terms of temporal and spatial scalability, traditionally these systems are modelled using a molecular dynamics based approach, concentrating on the microscopic behaviour of the fluid. In comparison, the lattice gas automaton (LGA) approach utilises a statistical approach which relies on the fluid being simplified to a system of particles which can stream and collide in a specific direction(D'humières and Lallemand, 1986). Frisch, Hasslacher and Pomeau (1986), first associated the lattice gas automaton and then subsequently recovered the Navier-Stokes equation via the Chapman-Enskonig expansion. Though the focus of this approach is still based on the behaviour of the fluid particle, the outcome is to approximate this to model macroscopic flow (McNamara and Zanetti, 1988). One of the major issues with LGA is the statistical noise associated with the solution, hence, a large number of simulations are needed to reduce the inaccuracy of the system (Chen, Chen and Matthaeus, 1992). In comparison, the lattice Boltzmann (LB) model minimises the noise associated with the LGA by applying the fixed lattice model to square lattices (Benzi, Succi and Vergassola, 1992).

LBM simplifies traditional gas dynamics by reducing the number of particle distributions to a fixed point on a lattice(Guo and Zhao, 2002). With the choice of lattice depending on the problem, however, for 2D systems the most common lattice is the D2Q9, which has 8 particles which can stream and a central point for the rest particle (Figure 4.1).

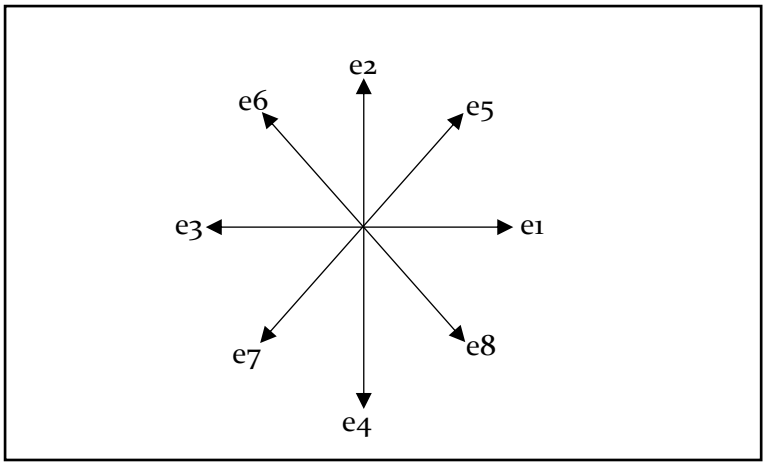

Figure 4.1 The orientation of the 9 lattice particles on a D2Q9 lattice. The central particle is the rest particle.

Each of these particles have a set particle microscopic velocity (e_a) and are defined by:

$$\overrightarrow{e_i} = \begin{cases} (0,0)\,, & i = 0 \\ \cos\left(\frac{\pi}{2(i-1)}\right), \sin\left(\frac{\pi}{2(i-1)}\right) & i = 1 \dots 4 \\ \sqrt{2}\cos\left(\frac{\pi}{2(i-1)} + \frac{\pi}{4}\right), \sqrt{2}\sin\left(\frac{\pi}{2(i-1)} + \frac{\pi}{4}\right) & i = 5 \dots 8 \end{cases} \quad 4.1$$

Each particle in the lattice is then associated with a discrete probability distribution function, $f_i(\vec{x}, \vec{e}_i, t)$. This describes the probability of the particle streaming in a specified direction. By applying a uniform lattice to the system it can be stated that $\delta x = \delta y$. Furthermore, the lattice speed $c = \frac{\delta x}{\delta t} = 1\ lu/ts$ in non-dimensionalised form then the $\delta x = \delta t$ and hence they both equate to unity. Applying, this simplifying assumption the lattice Boltzmann equation is simplified. Finally, the primary lattice particles will have a speed of 1 lu/ts, whereas, the angular particles will have a velocity magnitude of $\sqrt{2}$ lu/ts.

From the probability distribution functions, it is then possible to produce the macroscopic fluid density (ρ), which is described as the summation of the particle distribution functions:

$$\rho(\vec{x}, t) = \sum_{i=0}^{8} f_i(\vec{x}, t) \quad 4.2$$

Furthermore, the macroscopic velocity ($\vec{u}(\vec{x}, t)$) is a geometric average of the microscopic velocities weighted against the distribution functions:

$$\vec{u}(\vec{x}, t) = \frac{1}{\rho}\sum_{i=0}^{8} f_i(\vec{x}, t)\vec{e_i} \quad 4.3$$

These two equations allow for the discrete microscopic velocities which make up LBM to be related back to the continuum of the macroscopic velocities which represent the fluids motion (Sukop and Thorne, 2007).

4.1.2 Non-dimensionalisation of the system

The inherent applicability of the LB simulation to modelling complex flow behaviour is primarily due to its relatively simple implementation. By making some simplifying assumptions, such as assuming that the lattice spacing and lattice time-step are placed at unity, simplifies the equation considerably. However, it is important that the system being modelled is accurately portrayed within the lattice Boltzmann framework. This can be challenging when dealing with complex systems and being constrained by the terminology used within the LB approach, in particular, the lattice variables and lattice units.

To capture this, the physical parameters of the system are non-dimensionalised and converted into lattice Boltzmann units. Non-dimensionalisation of any physical system can be reduced using a characteristic time (t_o) and length scale (l_o). Furthermore, to ensure that the system being simulated is accurately conserving the physical system a

dimensionless quantity is used. Commonly, it is the Reynold's number which can be used to calculate the relevant dimensional and non-dimensional forms (Krüger *et al.*, 2017).

By choosing a suitable time and length scale, the dimensional length and time can be converted by the following expressions:

$$t_{nd} = \frac{t}{t_0} \; ; \qquad x_{nd} = \frac{x}{l_0} \tag{4.4}$$

From this the physical velocity of the system can be calculated by the following expression:

$$u_{phys} = \frac{x_{phys}}{t_{phys}} = \frac{x_{nd}}{t_{nd}} . \frac{l_0}{t_0} = \frac{l_0}{t_0} . u_{nd} \tag{4.5}$$

From these descriptors it is then possible to discretize the dimensionless space and the time using the following expressions:

$$\delta x = \frac{1}{N} \tag{4.6}$$

$$\delta t = \frac{1}{N_{iter}} \tag{4.7}$$

Where here δx is the discrete space interval and δt is the discrete time interval, N is the length of the domain and N_{iter} is the total number of time steps.

From here we can express the rest of the parameters using the non-dimensionlised Reynolds number:

$$Re = \frac{x_{phys} \cdot u_{phys}}{\nu_{phys}} = \frac{N \cdot N / N_{iter}}{\nu_{lb}} = \frac{\delta t}{(\delta x)^2 \nu_{lb}} \tag{4.8}$$

Where,

$$u_{nd} = \frac{\delta x}{\delta t} u_{lb} \tag{4.9}$$

Hence,

$$\nu_{lb} = \frac{\delta t}{\delta x^2} \nu_{nd}$$

One of the issues associated with the lattice Boltzmann method is that of the constraint imposed by the Mach number, due to the technique only able to model incompressible flow there is a compressibility limit (Krüger *et al.*, 2017). To ensure that this limit is not met, the Mach number must be << 1, where the Mach number is expressed as:

$$Ma = \frac{\boldsymbol{u}}{c_s} \qquad 4.10$$

Where **u** is the LB velocity and c_s is the speed of sound = $1/\sqrt{3}$

4.1.3 Implementation of the lattice Boltzmann equation

To implement the lattice Boltzmann equation it is common to split the equation into its two fundamental procedures; streaming and collision.

$$\underbrace{f_i(\vec{x} + \vec{e_i}\Delta t, t + \Delta t) = f_i(\vec{x}, t)}_{streaming} - \underbrace{\frac{[f_i(\vec{x},t) - f_i^{eq}(\vec{x},t)]}{\tau_{lbm}}}_{collision} \qquad 4.11$$

Where τ_{lbm} is the single relaxation time and f^{eq} is the equilibrium function

Here the LHS of the equation along with the first term on the RHS equate to the streaming step with the second term on the RHS solving the collision step.

Firstly, the collision step will be focused on, in particular, the use of the single relaxation time also known as the Bhatnagar-Gross-Krook method (BGK). Though there are other techniques to solve the collision equation, the BGK method is the simplest to implement and most widely cited within the literature (Sukop and Thorne, 2007).

The collision of the particles is treated as relaxation towards an equilibrium and this is defined by the equilibrium distribution function ($f_i^{eq}(\vec{x}, t)$) (Kruger *et al*, 2017):

$$f_i^{eq}(\vec{x},t) = \omega_i \rho(\vec{x}) \left[1 + 3\frac{\vec{e_i}\vec{u}}{c^2} + \frac{9}{2}\frac{(\vec{e_i}\vec{u})^2}{c^4} - \frac{3}{2}\frac{\vec{u}^2}{c^2}\right] \quad 4.12$$

Where, ω_i are the weighting functions:

$$\omega_i = \begin{cases} \frac{4}{9} & i = 0 \\ \frac{1}{9} & i = 1 \dots 4 \\ \frac{1}{36} & i = 5 \dots 8 \end{cases} \quad 4.13$$

C is the basic speed of the lattice (usually set to 1 lu ts^{-1})

Finally, the fluid kinematic viscosity of 2D lattice is:

$$\nu = \frac{1}{3}\left(\tau_{lbm} - \frac{1}{2}\right) \quad 4.14$$

A suitable choice in relaxation time is important as this significantly influences the rate at which the equilibrium is met. The simplest solution to this is to set $\tau_{lbm} = 1$, when the distribution function equates to the equilibrium distribution function, furthermore, setting $\tau_{lbm} > 1$ results in an exponential decay in the distribution function and when $1/2 < \tau_{lbm} < 1$ the solution oscillates around the equilibrium function (Kruger *et al*, 2017). It should be stated that though the optimal configuration is set to the relaxation time = 1, in practice this may not be achieved due to the physical constraints of the system being studied.

Optimising the choice in τ_{lbm} is an area of active research, with the fundamental properties of the BGK approach being analysed. There are a number of alternative values which have been proposed within the literature which offer a reduction in the error (Holdych *et al.*, 2004; Krüger, Varnik and Raabe, 2008; Zhao, 2013). Holdych *et al,* analysed the errors associated with the Taylor series expansion when applying the finite difference method to the lattice Boltzmann equation. Here it was found that for low Reynolds number flow setting the relaxation time to <1 was optimal and in the limiting case of steady shear flow a definite root appears at $\tau_{lbm} \approx 0.9082$. This implies that the

system is to be optimally modelled then a suitable choice in domain size is needed to ensure that τ_{lbm} approaches 0.9082. Although, once again this is limited to the physical system and the computational availability.

Predominately the focus of the above section has been on the classical implementation of the lattice Boltzmann method in which a single relaxation time and the BGK method is used to calculate the collision step. In recent years different approaches have been analysed to improve the accuracy and stability of the method in which multiple relaxation time methods have been utilised. One of the fundamental issues with the single relaxation time method is its inability to calculate high Re numbers, by assuming that a single relaxation time can be applied across the whole domain. Alternative approaches, utilise the multiple relaxation time (MRT) in which each node is assigned an individual relaxation time which can be adjusted to maintain the stability of the system (d'Humières, 2002). Though MRT offers an extension into higher Reynold numbers and greater accuracy, it increases the computational cost and at lower Reynold numbers does not offer a significant increase in accuracy (Du, Shi and Chen, 2006).

Finally, streaming the distribution functions which have been calculated in the collision step are propagated to their nearest neighbour.

4.3.1 Boundary Conditions

The use of boundary conditions within lattice Boltzmann are what makes this style of modelling unique. Bounce-back boundary and Zou-He velocity and pressure boundaries will be discussed below, however there are a number of boundary conditions which can be used to increase the order of accuracy.

When dealing with boundary conditions in lattice Boltzmann the boundary surface is treated separately in the collision criteria than the rest of the flow. This boundary surface is treated with the bounce-back technique. The simplicity of the bounce-back technique is what makes lattice Boltzmann modelling such a powerful tool for porous media and complex boundaries.

4.3.1.1 Bounce back boundaries

As previously mentioned, the bounce back boundaries are treated separately to the collision procedure within the flow. There are several bounce back treatments available, however, the two focused on here are: on-grid and mid-plane.

On-grid bounce back is the simpler of the two and works by reversing the incoming streamed particles on the boundary node (figure 4.2). This allows for a 1st order of accuracy to be achieved within the model (Sukop and Thorne, 2007).

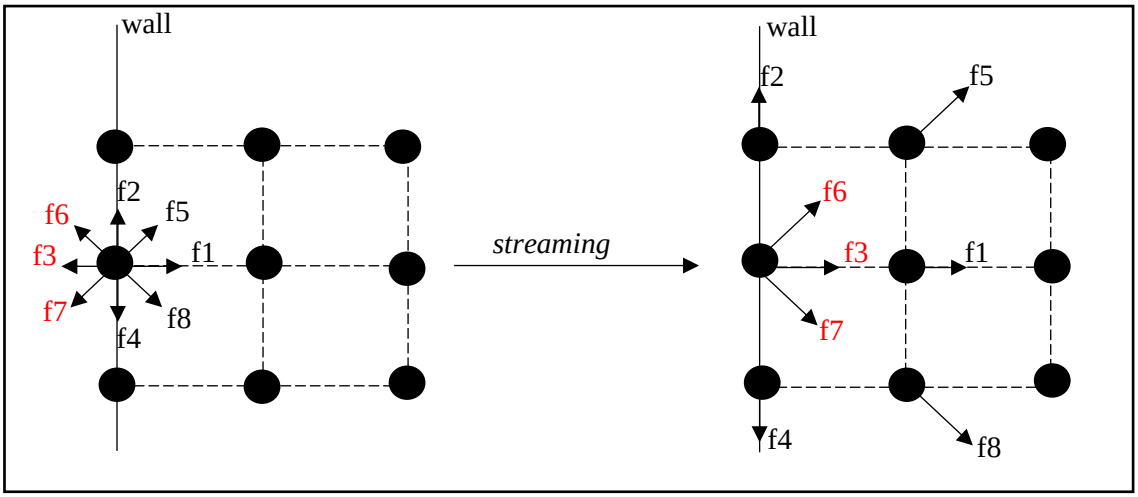

Figure 4.2 The on-grid bounce-back boundary with the density specific functions shown

Mid-grid bounce back assumes that there are pseudo-nodes to account for the boundary nodes and the wall is situated between the pseudo-nodes and the boundary nodes of the fluid. This technique works on the principle that within a given time step, distribution functions exist for the fluid domain that can then be temporarily held within the pseudo-nodes. They are then reflected via a collision procedure and the re-distributed back into the fluid domain (Figure 4.3).

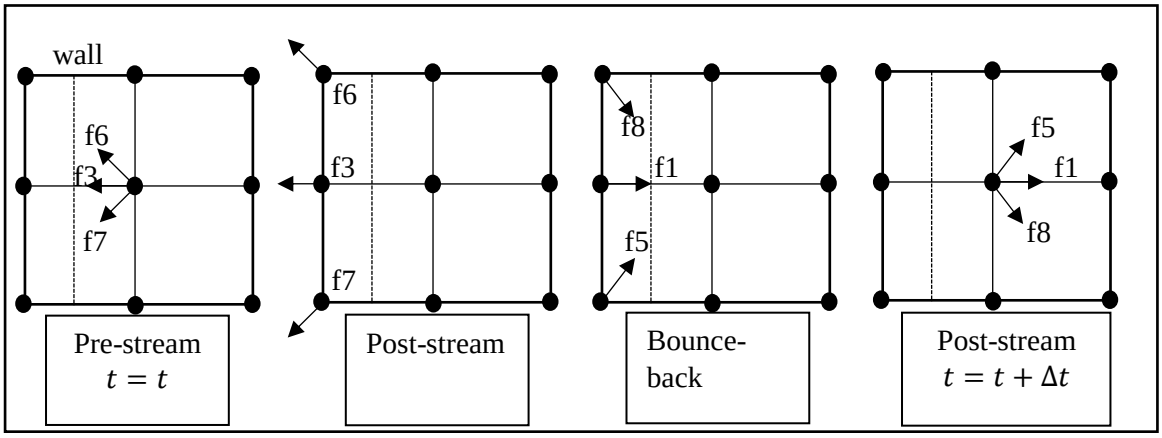

Figure 4.2 The mid-grid bounce-back boundary with directional densities show. The mid-plane wall is highlighted in the first panel.

If simplicity is required then the on-grid method offers a quick and easy way to implement boundary conditions, however, for a slight increase in complication of the code the mid-grid bounce back method offers a more accurate solution, to a second order accuracy (Chen and Doolen, 1998).

Though bounce-back is the most common applied boundary condition for the unknown distribution functions, it does have some drawbacks, particularly when dealing with circular geometries. In the case of circular geometries either a refinement of the domain is needed to reduce the influence of stair casing on the solution or an alternative higher order interpolation scheme is needed which takes into account the geometry (Guo, Zheng and Shi, 2002). There has been a number of advances in the behaviour of circular geometries and the application of specific boundary conditions to the lattice-Boltzmann method in recent years (Boyd *et al.*, 2004; Bernaschi *et al.*, 2010). Finally, corner nodes need specific treatment when dealing with square boundaries, i.e. backwards facing step or lid-driven cavity problems. In this case there is just one unknown which needs to be solved before the traditional bounce-back technique can be used, however, these nodes need to be specifically described (Krüger *et al.*, 2017).

4.3.1.2 Zou-He boundary conditions

It is important to be able to model realistic systems, as such the ability to prescribe a set density or velocity at the boundary is important. The Zou-He boundary conditions allows for the unknown distributions to be found by utilising a linear interpolation system (Zou and He, 1996). It consists of 4 equations in which the bounce back boundary holds for the non-equilibrium part of the system. By starting with a known velocity or pressure in the x or y-direction it is possible to elucidate the required equations that allow for unknown distribution functions to be formulated.

An example of solving the Zou-He boundary condition can be found using the following technique described by Zhou & He, 1997, all other cases can derived the same way (Sukop and Thorne, 2007):

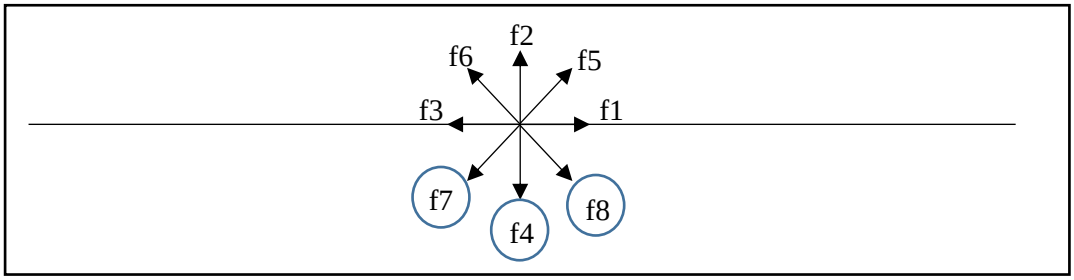

Figure 4.3 The unknown directional densities highlighted.

There are 3 unknowns in the north boundary condition, f_4, f_7, and f8, firstly it is worth considering the individual f_a's which influence the vector velocities (figure 4.4). This can be found by using equation 4.11, the individual equations are:

$$0 = f_1 - f_3 + f_5 - f_6 - f_7 - f_8 \qquad 4.15$$

&

$$\rho v_0 = f_2 - f_4 + f_5 + f_6 - f_7 - f_8 \qquad 4.16$$

By using the bounce-back boundary condition described above, it is possible to write the following equation:

$$f_2 - f_2^{eq} = f_4 - f_4^{eq} \qquad 4.17$$

Where eq is the equilibrium function

By also considering the macroscopic density, this gives the system a set of four unknowns. By re-arranging the equations to include the unknown directional densities; f_4, f_7 and f_8. By equating the right-hand sides, the following equation is derived:

$$\rho - f_0 - f_1 - f_2 - f_3 - f_5 - f_6 = f_2 + f_5 + f_6 - \rho v_0 \quad 4.18$$

Then solving for ρ:

$$\rho = \frac{f_0+f_1+f_3+2(f_2+f_5+f_6)}{1+v_0} \quad 4.19$$

From this equation, it is possible to solve f_4:

$$f_4 = f_2 - f_2^{eq} = f_2 - \frac{2}{3}\rho v_0 \quad 4.20$$

For the last two unknowns' the procedure giving:

$$f_7 = f_5 + \frac{1}{2}(f_1 - f_3) - \frac{1}{6}\rho v_0 \quad 4.21$$

And for f_8:

$$f_8 = f_6 - \frac{1}{2}(f_1 - f_3) - \frac{1}{6}\rho v_0 \quad 4.22$$

These equations are derived from the macroscopic equations along with the on-grid bounce back boundary conditions discussed earlier. It is worth noting that these boundary conditions are orientation sensitive, and that behaviour at the corner nodes take special consideration.

4.2 NetLogo and the lattice Boltzmann method

Though NetLogo has been previously described, a brief overview will be given here. The focus on NetLogo is to implement agent-based models (Wilenksy, 1999), in this case models where localised interactions of agents corresponds to emergent behaviour on the continuum scale. This modelling technique has been well used in a number of disciplines, however, the use within engineering is still relatively novel. Introducing the

lattice-Boltzmann technique to NetLogo allows for a number of further research areas which can be analysed with a solid grasp in the environmental behaviour of the system. Furthermore, lattice-Boltzmann itself can be considered an agent-based model. In its simplest form it consists of a macroscopic behaviour which can be decomposed into its most basic behaviour, in this case a set number of fluid particles which stream and collide. These collisions are dictated by the localised equilibrium value equates to continuum behaviour, in this case, momentum and density. Furthermore, by implementing the lattice-Boltzmann method within NetLogo it also highlights that it is a relevant and competitive modelling technique for complex fluid systems.

4.2.1 Implementation of lattice Boltzmann in NetLogo

The initial implementation is based on the steps outlined in the lattice Boltzmann algorithm. These are the collision steps and streaming steps, the collision step is relatively straightforward to programme, i.e. the equilibrium distribution function is calculated using equation 4.12 and then this is used to calculate the collision equation:

$$f_i(\vec{x},t) = f_i(\vec{x},t) - \frac{f_i(\vec{x},t) - f_i^{eq}(\vec{x},t)}{\tau_{lbm}} \qquad 4.23$$

This is followed by the streaming step, however, to temporarily hold the new $f_i(\vec{x},t)$ there is a distinction in terminology is needed to reduce inference of legacy coding. In NetLogo the distinction was made by, differentiating the streamed $f_i(\vec{x},t)$ from the collision $f_i(\vec{x},t)$. To this the collision function was renamed to $f_{out}(\vec{x},t)$ and the streaming function was renamed to $f_{in}(\vec{x},t)$. Hence, the new collision equation would read:

$$f_{out}(\vec{x},t) = f_{in}(\vec{x},t) - \frac{f_{in}(\vec{x},t) - f^{eq}(\vec{x},t)}{\tau_{lbm}} \qquad 4.24$$

So, within the NetLogo language, for i = 2, the collision equation is:

set f2O f2i - (f2i - feq2) / τ_{lbm}

In this case f20 is the new collision distribution function and feq2 is the equilibrium relaxation function.

As there is now a differentiation between the collision function and the streaming function it is possible to programme the streaming function as, $f_{in}(\vec{x}, t) = f_{out}(\vec{x}, t)$ of the neighbouring lattice node. Within Netlogo the following code is used:

set f2i [f20] of patch-at -1 0

Finally, the macroscopic variables can be calculated from equations 4.2 and 4.3.

4.3 Verification of the lattice Boltzmann method in NetLogo

To ensure that the lattice Boltzmann approach is working correctly within the NetLogo framework a number of verification tests were run. Firstly, the Poiseuille flow system was modelled to test both the forcing term within the LBM Equation along with the boundary conditions, both bounce back and periodic. The use of the Poiseuille flow as a suitable verification tool for CFD models is due to its simple derivation from the Navier-Stokes equation, as such a direct numerical and analytical comparison can be taken. The second test consisted of using the lid-driven cavity model, in this case a direct derivation from the Navier-Stokes equation is not possible, however there is suitable literature data to compare against. As such this allows for an analysis of the systems behaviour under the bounce back boundary condition along with a velocity driven boundary condition. Hence, allowing the applicability of the Zou-He boundary conditions to be tested. Finally, the use of a cylinder in flow is used as a test to ensure that immersed bodies are captured. This is a common approach for testing the ability

of the system to capture behaviour of the system with suitable boundary conditions at varying Reynold numbers.

4.3.1 Poiseuille Flow

Flow behaviour between two parallel plates is the most commonly applied validation model for fluid dynamics due to its simple derivation from the Navier-Stokes allowing for a direct comparison between the analytical solution and the model solution. A force is applied to the fluid either gravitationally or else pressure driven, at low Re this results in a parabolic profile forming between the two plates.

The analytical solution to the Poiseuille Flow profile is as follows:

$$u(x) = \left(-\frac{1}{2\nu}\right)\Delta P(y - y_0)(y - y_{max}) \tag{4.25}$$

Commonly, a pressure driven force (ΔP) is applied to the system which captures the pressure drop along the system. Here a force is applied to each node to capture the pressure drop by applying the following equation to the nodes in the x-direction:

$$\Delta P = \frac{8\nu u_{max}}{y_{max} - y_0} \tag{4.26}$$

To apply this within the LB procedure the forcing procedure is an extra term which is added to the x-velocity in the equilibrium code as described by Sukop & Throne (2007):

$$u^{eq} = u + \frac{\tau_{lbm} F}{\rho} \tag{4.27}$$

Where u^{eq} is, the equilibrium velocity used is equilibrium code.

Finally, the system is modelled using the half-way bounce back method discussed in the previous section and periodic boundaries at the inlet and outlet of the system. The

error between the well-known analytical solution to the Poiseuille flow and the lattice Boltzmann model is calculated using the L^2 norm (Nash *et al.*, 2014):

$$error = \sqrt{\frac{1}{N_y}\sum_i \left(\frac{u_{x,i} - u_{x,analytical,i}}{u_{max}}\right)^2} \qquad 4.28$$

The difference between the two values is calculated every 1000 time steps and the simulation is considered convergence when the error is less than 10^{-8}. To test the error associated with a variation in the grid size a number of grid sizes where produced which tested coarser meshes against finer mesh sizes.

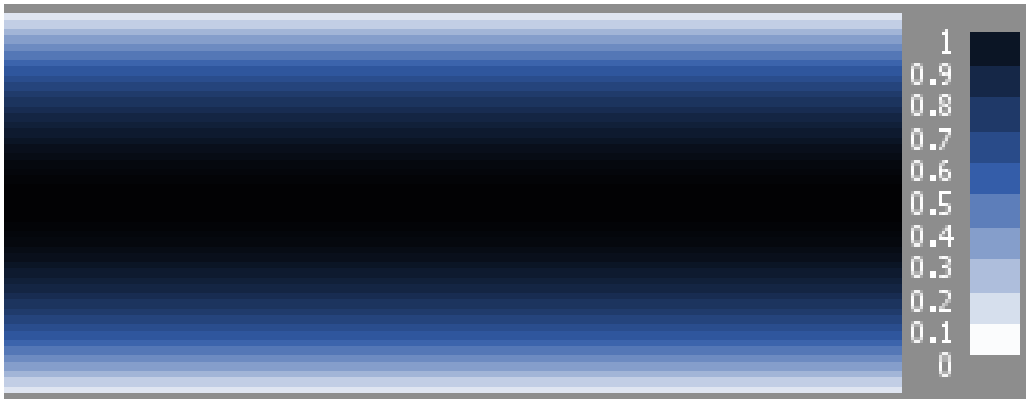

Figure 4.4 Normalised velocity flow profile from the Poiseuille flow NetLogo model with reflective boundaries and a force applied via gravity

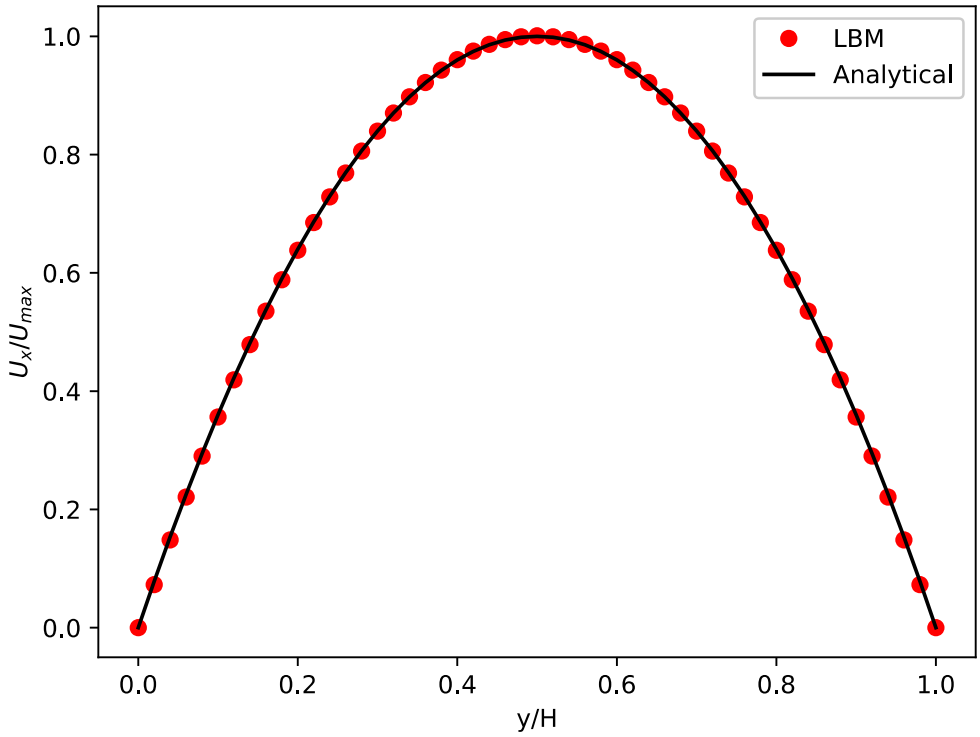

Figure 4.5 Poiseuille Flow profile showing the comparable results of the NetLogo model to the analytical solution with a mesh size of 50lu (L^2 error = 0.0064)

The forcing term within the LBM code along with the suitable choice in boundary conditions, in particularly the mid-grid bounce back method can be seen to show excellent agreement with the analytical solution (Figure 4.6). Furthermore, grid refinement can influence error within the system, with a reduction in lattice spacing there is a significant decrease in error (Figure 4.7). However, there is a pay-off between accuracy and efficiency, with the grid costing an increase in computing time. As such, it is important that a suitable choice in grid size is chosen whilst considering the computing time, this choice is entirely dependent on the problem being studied.

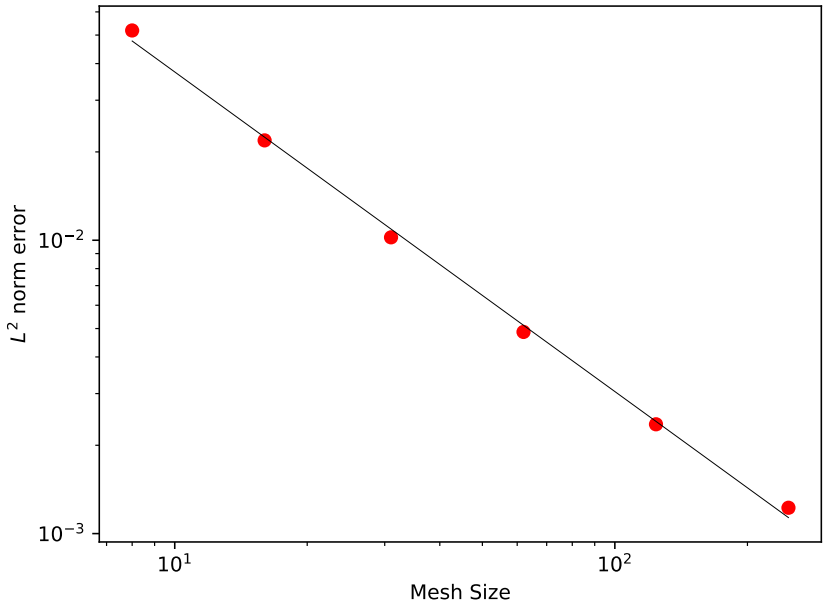

Figure 4.6 Variation in error associated with grid refinement where the line is to show linearity of data points

The error of the system can be seen to reduce significantly as the grid is refined, however, the computational cost increases significantly. As such when performing the lattice Boltzmann model it is particularly important to ensure that the grid accuracy is offset by the computational cost.

4.3.2 Lid driven cavity flow

The lid driven cavity system is simple to implement and allows for a number of areas of the lattice Boltzmann code to be tested, particularly the ability of the model to implement the Zou-He boundary conditions, in this case velocity. Though the bounce-back condition has been previously tested via the Poiseuille flow model special emphasis is given on how to implement corner nodes within this problem.

To initialise the system, all nodes are given a starting velocity of 0 and a $\rho = 1$, except the top lid boundary condition which is given a velocity of 0.1 and the density is derived from the Zou-He boundary condition (Figure 4.8). Furthermore, all walls are given a

velocity of 0 and ρ = 0. Previously, the convergence criteria was chosen by comparing two successive L^2 norms, however, due to the lack of an analytical solution this is not possible. Instead, two successive iterations of the system velocities are compared every 2000 time steps, if the difference between the velocity of the system is $>10^{-8}$ the system is considered converged.

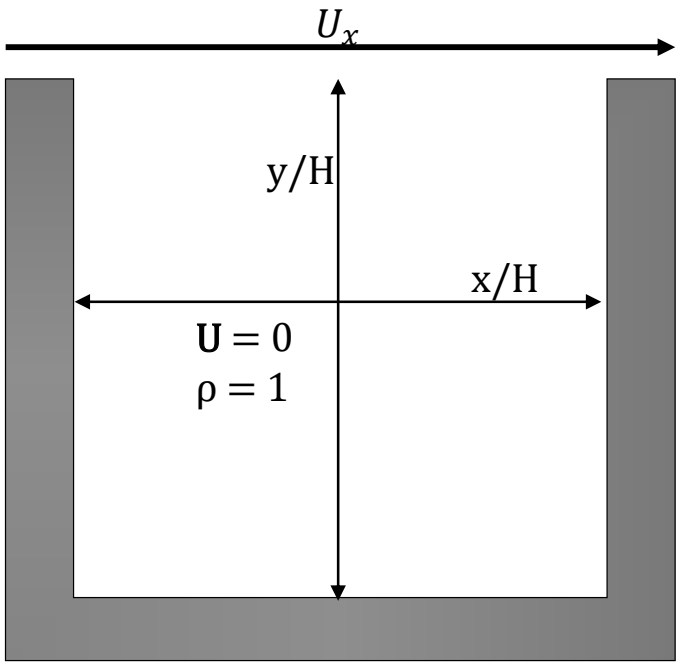

Figure 4.7 Schematic of the lid driven cavity flow

As the current implementation considers only the BGK collision technique, there is a limitation on the Re numbers being tested. This is due to the single relaxation time and the consequence of the computation time. As such, two key comparisons are made between the Ghia, Ghia and Shin (1982) data set and that of the NetLogo-LBM implementation. To test the model a Re = 100 and Re = 400 where chosen. There can be seen to be good agreement in both Re (100 & 400) cases when the LBM-NetLogo model is compared to the Ghia *et al* model. Though it should be noted that the Ghia data is not sampled across the whole computational domain and only at certain

intervals, in comparison to that of the NetLogo model which is sampled evenly across the domain (Figure 4.9).

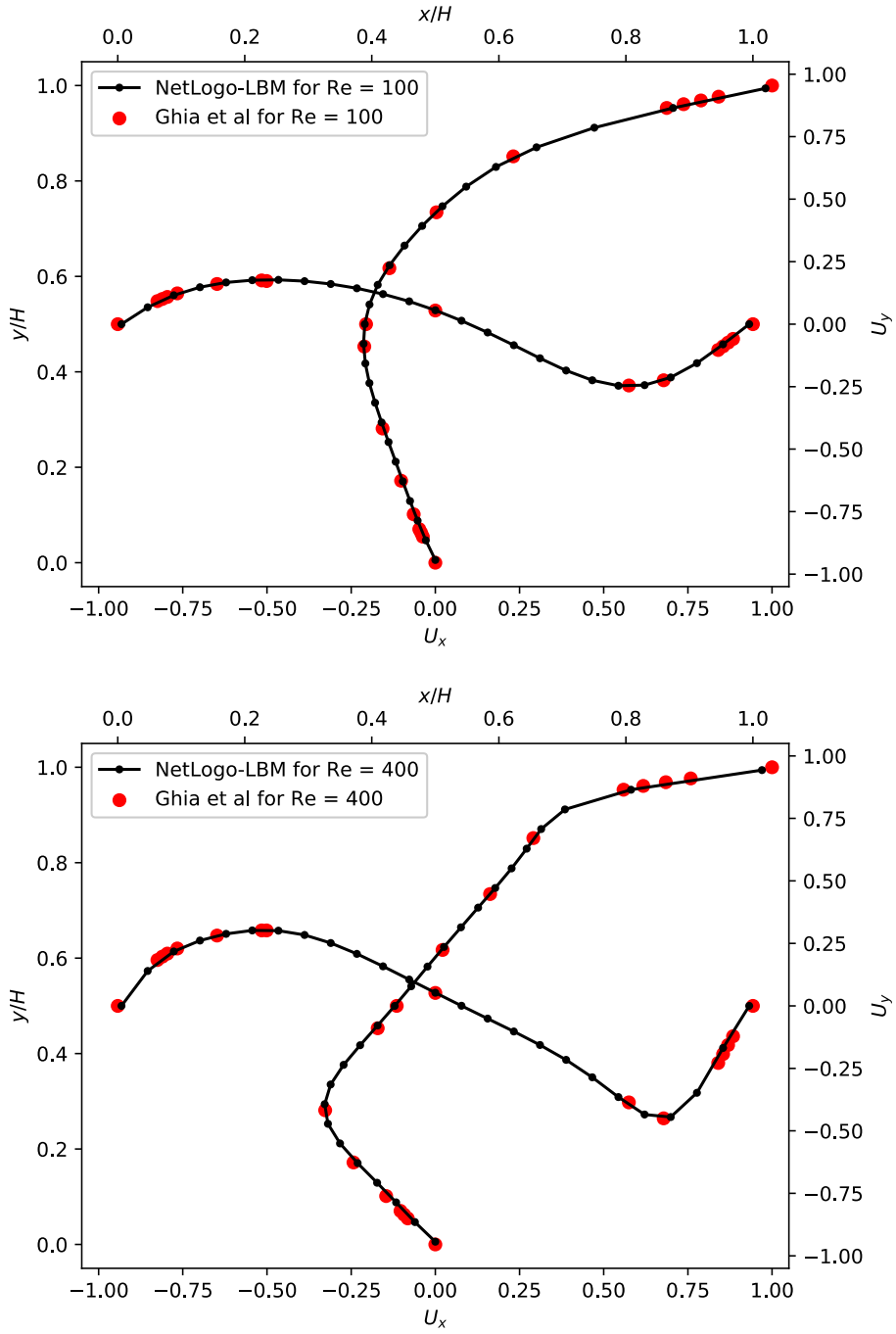

Figure 4.8 The agreement between the typical sampled points taken from the Ghia et al data set compared to the NetLogo-LBM data points sampled evenly across the domain. A) Shows the comparison of the LBM to Ghia et al for Re 100 along both the vertical and horizontal axes highlighted in Figure 4.8 B)) Shows the comparison of the LBM to Ghia et al for Re 400 along both the vertical and horizontal axes highlighted in Figure 4.8.

4.3.3 Flow around a cylinder

Flow around a cylinder is one of the most common tests for a fluid dynamics code. To test the introduction of turbulence within the model different models were run which varied the Re number from 50 to 200. Particular emphasis was placed on the transition zone from laminar flow profiles to turbulence, though some disagreement occurs within the literature, here it is assumed that turbulence occurs when the recirculation zones behind the cylinder separate to cause von Karmen vortices around Re 100.

To reduce the time needed for convergence the whole domain was initialised with a parabolic flow profile, excluding the wall and cylinder boundaries which had the half way bounce back condition applied to them. The inlet and outlet boundaries conditions were applied using the Zou-He method applied previously with the localised density at the inlet being calculated from the parabolic velocity profiles and the velocity profile at the outlet being calculated using a density set at unity.

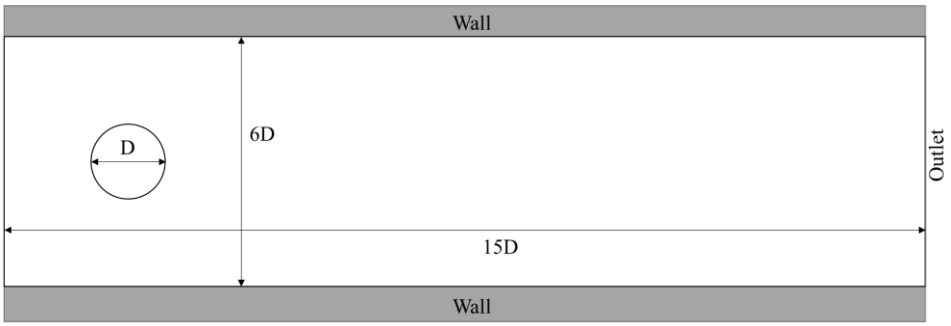

Figure 4.9 Schematic of the flow around a cylinder domain with the inlet profile being set as parabolic and the outlet at a constant density

To convert the force applied to the cylinder by the fluid, the momentum exchange method was applied to each of the boundary nodes (Ladd, 2015). This method is well cited within the literature for producing drag and lift coefficients, along with extending the model to moving boundaries, in particular, particulate flow (Chen *et al.*, 2013). By

applying this method a comparison between the various drag coefficients as a function of the Re number can be undertaken.

$$C_D = \frac{F_x}{\rho U^2 A} \quad 4.29$$

$$C_L = \frac{F_y}{\rho U^2 A} \quad 4.30$$

The LB expression for the moment exchange method is as follows (Yu *et al*, 2003):

$$F = \sum_{\text{all } x_b} \sum_{\alpha}^{N_d} e_{\bar{\alpha}} \left[\bar{f}_{\alpha}(b_b, t) + \bar{f}_{\bar{\alpha}}(x_b + e_{\bar{\alpha}}\, \delta t, t) \right] \quad 4.31$$

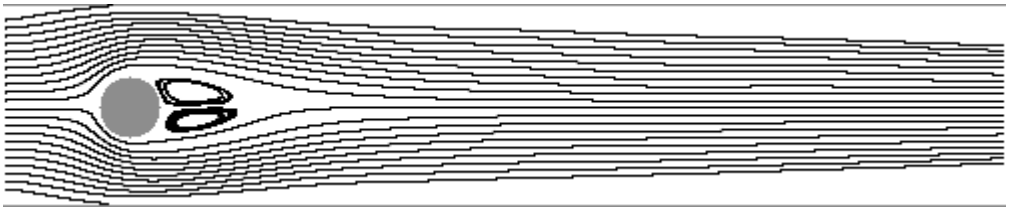

Figure 4.10 Flow lines around the collector at Re = 40 from the NetLogo model with recirculation zones visible

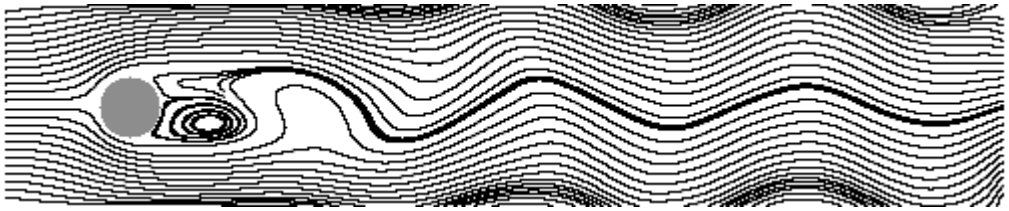

Figure 4.11 Flow lines around the collector at Re = 100 from the NetLogo Model with recirculation zones starting to break up and van Karman vortices developing

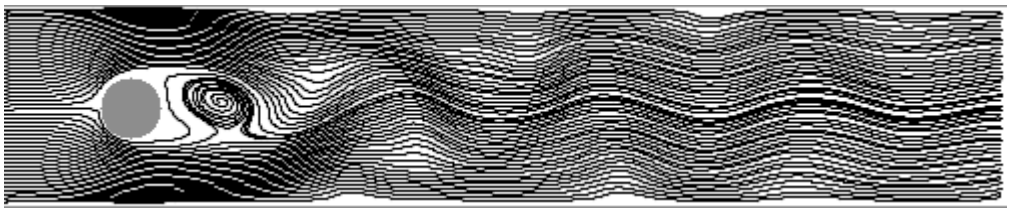

Figure 4.12 Flow lines around the collector at Re = 179 from the NetLogo model with van Karman vortices developed directly behind the rear of the collector

At lower Reynolds numbers (Re = 40) there can be seen to be clearer recirculation zones (Figure 4.11), however, at higher Reynold's number (Re >= 100) von Karman vortices

start to occur and that the behaviour of the system is indeed turbulent with the recirculation zones shedding from directly behind the cylinder (Figure 4.12 & 4.13).

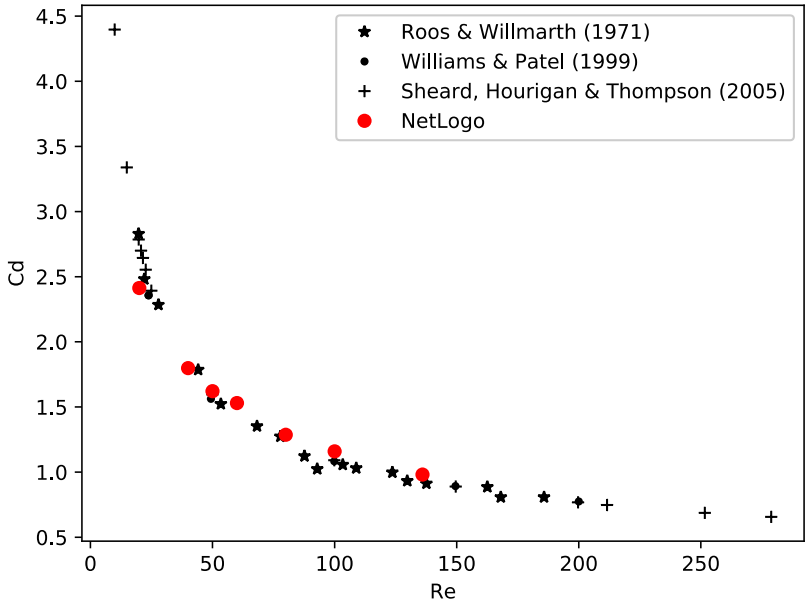

Figure 4.13 Drag coefficients for varying Re conditions

The behaviour of drag coefficient (Figure 4.14) can be seen to decay at a similar rate to other studies within the literature (Ross and Willmarth, 1971; Johnson and Patel, 1999; Sheard, Hourigan and Thompson, 2005). There can be seen to be some discrepancy between the NetLogo results and the other studies, however, this may be due to grid refinement. Here it can be seen that as the regime converts from laminar to turbulent flow there is a significant reduction in drag coefficient.

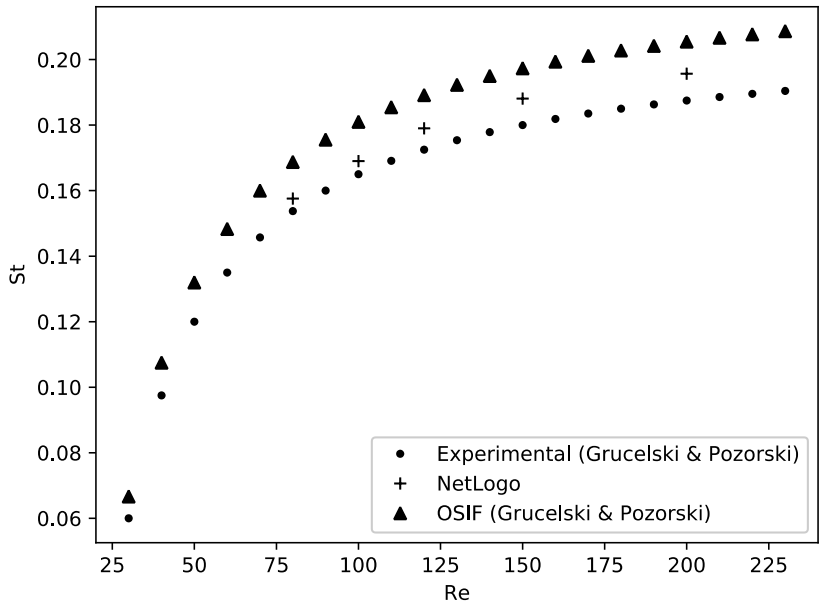

Figure 4.14 Comparison of the Strouhal number from the LBM against the analytical solution (On-site interpolation-free OSIF) and experimental solutions put forward by Grucelski and Pozorski (2013)

The Strouhal number (St) allows for comparison of the vortex shredding as a function of Re, here it can be seen to fall between the experimental (Exp) and modelling results (OSIF) produced by Grucelski and Pozorski (2013), this may be a consequence of the grid and as such refinement of this would allow for a better comparison. Limitations on the number of runs available at both higher Reynolds number and lower Reynolds numbers were experienced due to the long convergence times experienced within NetLogo.

One of the major issues with using the bounce-back method is the observed stair-casing at circular boundary conditions. This can be described as a legacy of the method due to the inherent inaccuracy of the stair-casing method in comparison to curved boundary conditions, however, the inaccuracy is marginal in comparison to the computational cost of introducing interpolation methods for boundary conditions.

Furthermore, grid refinement at the boundary condition would offer greater accuracy, however, one of the issues with NetLogo is the inability to refine areas of the world and instead full domain refinement would be needed

4.4 Conclusions

The fluid solver lattice Boltzmann method (LBM) was chosen for its ability to represent complex fluid flow, essential within porous media, along with its simple bounce back boundary conditions. Furthermore, the LBM can be considered an ABM in terms of its approach to solving fluid dynamics in an emergent way, particularly, by using microscopic variables to produce macroscopic fluid flow. By validating the LBM against a number of standard CFD benchmark tests such as; Poiseuille flow, flow around a cylinder, and lid driven cavity flow, confidence in the model can be built.

The model outputs accurate representations of Poiseuille flow whilst showing a dependence on accuracy as the grid was refined. The lid driven cavity problem shows excellent agreement with the results derived from Ghia *et al*, 1982, however, testing predominately centred around the low Re numbers due to the instability of the SRT at higher Re. Extensions to the model to incorporate MRT could be made, however, NetLogo may suffer with long run times, as it is predominately not set up to undergo matrix calculations. Finally, within the flow around a cylinder, the behaviour of the flow at higher Re numbers can be seen to induce turbulence and at low Re numbers to produce re-circulation zones behind the cylinder. Here the bounce-back method was used which resulted in some loss of accuracy in comparison to alternative approaches which interpolate the curvature of the boundary.

It is worth nothing that there are a number of disadvantages to implementing the LBM within NetLogo such as, longer run times, limited memory storage and the inability to use higher classes of relaxation times such as the multi relaxation time. Though these

can be offset by using the simplified LBM structure or else moving to alternative ABM software suites such as RePast. Within this study of work NetLogo was chosen over RePast to allow for easier cross compatibility when running both the LBM and particle trajectory models together.

In conclusion, the validation of the lattice Boltzmann method within NetLogo proves that it is a suitable modelling suite, with some caveats on long run times and more complex boundary conditions. Furthermore, LBM can be considered in its simplest form an ABM, in its ability reduce complex phenomena into base rules which produce emergent behaviour. In the case of LBM this emergent behaviour is the fluid flow produced from local particle interactions.

4.5 References

Aidun, C. K. and Clausen, J. R. (2010) 'Lattice-Boltzmann Method for Complex Flows', *Annual Review of Fluid Mechanics*, 42(1), pp. 439–472. doi: 10.1146/annurev-fluid-121108-145519.

Benzi, R., Succi, S. and Vergassola, M. (1992) 'The lattice Boltzmann equation: theory and applications', *Physics Reports*. North-Holland, 222(3), pp. 145–197. doi: 10.1016/0370-1573(92)90090-M.

Bernaschi, M. *et al.* (2010) 'A flexible high-performance Lattice Boltzmann GPU code for the simulations of fluid flows in complex geometries', *Concurrency and Computation: Practice and Experience*. John Wiley & Sons, Ltd, 22(1), pp. 1–14. doi: 10.1002/cpe.1466.

Boyd, J. *et al.* (2004) 'Application of the lattice Boltzmann method to arterial flow simulation: Investigation of boundary conditions for complex arterial geometries', *Australasian Physics & Engineering Sciences in Medicine*. Springer Netherlands, 27(4), pp. 207–212. doi: 10.1007/BF03178650.

Chen, H., Chen, S. and Matthaeus, W. H. (1992) 'Recovery of the Navier-Stokes equations using a lattice-gas Boltzmann method', *Physical Review A*. American Physical Society, 45(8), pp. R5339–R5342. doi: 10.1103/PhysRevA.45.R5339.

Chen, S. and Doolen, G. D. (1998) 'LATTICE BOLTZMANN METHOD FOR FLUID FLOWS', *Annual Review of Fluid Mechanics*. Annual Reviews 4139 El Camino Way, P.O. Box 10139, Palo Alto, CA 94303-0139, USA , 30(1), pp. 329–364. doi: 10.1146/annurev.fluid.30.1.329.

Chen, Y. *et al.* (2013) 'Momentum-exchange method in lattice Boltzmann simulations of particle-fluid interactions', *Physical Review E*, 88(1), p. 013303. doi:

10.1103/PhysRevE.88.013303.

d'Humières, D. (2002) 'Multiple–relaxation–time lattice Boltzmann models in three dimensions', *Philosophical Transactions of the Royal Society of London. Series A: Mathematical, Physical and Engineering Sciences*. Edited by P. V. Coveney et al. The Royal Society, 360(1792), pp. 437–451. doi: 10.1098/rsta.2001.0955.

D'humières, D. and Lallemand, P. (1986) 'Lattice gas automata for fluid mechanics', *Physica A: Statistical Mechanics and its Applications*. North-Holland, 140(1–2), pp. 326–335. doi: 10.1016/0378-4371(86)90239-6.

Du, R., Shi, B. and Chen, X. (2006) 'Multi-relaxation-time lattice Boltzmann model for incompressible flow', *Physics Letters A*. North-Holland, 359(6), pp. 564–572. doi: 10.1016/J.PHYSLETA.2006.07.074.

Frisch, U., Hasslacher, B. and Pomeau, Y. (1986) 'Lattice-Gas Automata for the Navier-Stokes Equation', *Physical Review Letters*. American Physical Society, 56(14), pp. 1505–1508. doi: 10.1103/PhysRevLett.56.1505.

Gabbanelli, S., Drazer, G. and Koplik, J. (2005) 'Lattice Boltzmann method for non-Newtonian (power-law) fluids', *Physical Review E*. American Physical Society, 72(4), p. 046312. doi: 10.1103/PhysRevE.72.046312.

Ghia, U., Ghia, K. . and Shin, C. . (1982) 'High-Re solutions for incompressible flow using the Navier-Stokes equations and a multigrid method', *Journal of Computational Physics*. Academic Press, 48(3), pp. 387–411. doi: 10.1016/0021-9991(82)90058-4.

Grucelski, A. and Pozorski, J. (2013) 'Lattice Boltzmann simulations of flow past a circular cylinder and in simple porous media', *Computers & Fluids*. Pergamon, 71, pp. 406–416. doi: 10.1016/J.COMPFLUID.2012.11.006.

Guo, Z. and Shu, C. (2013) *Lattice Boltzmann Method and Its Applications in*

Engineering. WORLD SCIENTIFIC (Advances in Computational Fluid Dynamics). doi: 10.1142/8806.

Guo, Z. and Zhao, T. S. (2002) 'Lattice Boltzmann model for incompressible flows through porous media', *Physical Review E*, 66(3), p. 036304. doi: 10.1103/PhysRevE.66.036304.

Guo, Z., Zheng, C. and Shi, B. (2002) 'An extrapolation method for boundary conditions in lattice Boltzmann method', *Physics of Fluids*. American Institute of Physics, 14(6), pp. 2007–2010. doi: 10.1063/1.1471914.

He, X., Li, N. and Goldstein, B. (2000) 'Lattice Boltzmann Simulation of Diffusion-Convection Systems with Surface Chemical Reaction', *Molecular Simulation*. Taylor & Francis Group , 25(3–4), pp. 145–156. doi: 10.1080/08927020008044120.

Holdych, D. J. *et al.* (2004) 'Truncation error analysis of lattice Boltzmann methods', *Journal of Computational Physics*. Academic Press, 193(2), pp. 595–619. doi: 10.1016/J.JCP.2003.08.012.

Jeong, N., Choi, D. H. and Lin, C.-L. (2006) 'Prediction of Darcy–Forchheimer drag for micro-porous structures of complex geometry using the lattice Boltzmann method', *Journal of Micromechanics and Microengineering*. IOP Publishing, 16(10), pp. 2240–2250. doi: 10.1088/0960-1317/16/10/042.

Johnson, T. A. and Patel, V. C. (1999) 'Flow past a sphere up to a Reynolds number of 300', *Journal of Fluid Mechanics*. Cambridge University Press, 378, pp. 19–70. doi: 10.1017/S0022112098003206.

Kang, Q., Lichtner, P. C. and Zhang, D. (2006) 'Lattice Boltzmann pore-scale model for multicomponent reactive transport in porous media', *Journal of Geophysical Research: Solid Earth*. John Wiley & Sons, Ltd, 111(B5), p. n/a-n/a. doi:

10.1029/2005JB003951.

Krüger, T. *et al.* (2017) *The lattice Boltzmann method : principles and practice*.

Krüger, T., Varnik, F. and Raabe, D. (2008) 'Shear stress in lattice Boltzmann simulations'. doi: 10.1103/PhysRevE.79.046704.

Ladd, A. J. C. (2015) 'Lattice-Boltzmann methods for suspensions of solid particles', *Molecular Physics*, 0(0), pp. 1–7. doi: 10.1080/00268976.2015.1023755.

Manz, B., Gladden, L. F. and Warren, P. B. (1999) 'Flow and dispersion in porous media: Lattice-Boltzmann and NMR studies', *AIChE Journal*. John Wiley & Sons, Ltd, 45(9), pp. 1845–1854. doi: 10.1002/aic.690450902.

McNamara, G. R. and Zanetti, G. (1988) 'Use of the Boltzmann Equation to Simulate Lattice-Gas Automata', *Physical Review Letters*, 61(20), pp. 2332–2335. doi: 10.1103/PhysRevLett.61.2332.

Nash, R. W. *et al.* (2014) 'Choice of boundary condition for lattice-Boltzmann simulation of moderate-Reynolds-number flow in complex domains', *Physical Review E*. American Physical Society, 89(2), p. 023303. doi: 10.1103/PhysRevE.89.023303.

Pan, C., Hilpert, M. and Miller, C. T. (2004) 'Lattice-Boltzmann simulation of two-phase flow in porous media', *Water Resources Research*. John Wiley & Sons, Ltd, 40(1). doi: 10.1029/2003WR002120.

Roos, F. W. and Willmarth, W. W. (1971) 'Some experimental results on sphere and disk drag', *AIAA Journal*, 9(2), pp. 285–291. doi: 10.2514/3.6164.

Sheard, G. J., Hourigan, K. and Thompson, M. C. (2005) 'Computations of the drag coefficients for low-Reynolds-number flow past rings', *Journal of Fluid Mechanics*. Cambridge University Press, 526, pp. 257–275. doi: 10.1017/S0022112004002836.

Shu, C., Liu, N. and Chew, Y. T. (2007) 'A novel immersed boundary velocity correction–lattice Boltzmann method and its application to simulate flow past a circular cylinder', *Journal of Computational Physics*. Academic Press, 226(2), pp. 1607–1622. doi: 10.1016/J.JCP.2007.06.002.

Spaid, M. A. A. and Phelan, F. R. (1997) 'Lattice Boltzmann methods for modeling microscale flow in fibrous porous media', *Physics of Fluids*. American Institute of Physics, 9(9), pp. 2468–2474. doi: 10.1063/1.869392.

Succi, S., Foti, E. and Higuera, F. (1989) 'Three-Dimensional Flows in Complex Geometries with the Lattice Boltzmann Method', *Europhysics Letters (EPL)*. IOP Publishing, 10(5), pp. 433–438. doi: 10.1209/0295-5075/10/5/008.

Sukop, M. C. and Thorne, D. T. (2007) *Lattice Boltzmann modeling : an introduction for geoscientists and engineers*.

Zhao, F. (2013) 'Optimal relaxation collisions for lattice Boltzmann methods', *Computers & Mathematics with Applications*. Pergamon, 65(2), pp. 172–185. doi: 10.1016/J.CAMWA.2011.06.005.

Zou, Q. and He, X. (1996) 'On pressure and velocity flow boundary conditions and bounceback for the lattice Boltzmann BGK model'. doi: 10.1063/1.869307.

Chapter 5. Implementation of particle tracking within NetLogo for the modelling of colloidal aggregation

This section focuses on the implementation of a stochastic tracking algorithm for particles in a static fluid within the NetLogo environment. Purely diffusive systems are studied with emphasis placed upon growth rates and growth geometries under varying chemical and physical conditions. A simple case study is first analysed to compare against a purely analytical solution to the problem. Finally, the system is extended for validation against both experimental and geometrically derived solutions found within the literature.

5.1 Background and previous work

Aggregation is the consequence of two processes; the transportation of the colloidal particles and the interaction between colliding particles. Transportation in static flow conditions is predominately controlled by diffusion where the particle density is equal or close to the fluid density, or else the particle size is significantly small enough for gravitational effects to be negligible (>1 μm). If the colloidal density is greater or less than the fluid density; extra transportation forces need to be taken into account namely gravitational and buoyant forces. In this case, the transportation of colloidal particles is controlled by a summation of the diffusive and gravitational forces where fluid advection influences can be ignored. The rate at which these particles diffusive or settle through the systems influences the subsequent rate of aggregation. Depending on the necessary role of the colloidal particles in the system this can be tuned to reduce or increase the rate of transportation. In controlling the rate of transportation some system optimisation can be achieved, in particular, by reducing the temperature diffusive processes can be slowed down. Though this can reduce the rate at which collisions occur the interaction between colliding colloidal particles has the most

influence on the rate of aggregation. Within purely attractive systems, the electrostatic repulsive force is effectively "switched" off and as such the controlling mechanism for aggregation is diffusion, however, in a system where electrostatic repulsion is competing against the attractive force then stability of the system is a function of the potential energy, commonly this process is modelled by using the DLVO or X-DLVO equation to calculate the potential energy between two colliding particles (Chapter 2) along with the primary minimum well.

5.2 Modelling particle motion

Modelling diffusive motion with NetLogo was achieved by applying the stochastic particle tracking algorithm developed by (Minier, Peirano and Chibbaro, 2003). The technique is Lagrangian which explicitly tracks the motion of the N particles in the domain. This technique has been well validated within the literature (Peirano *et al.*, 2006; Mohaupt, J.-P. Minier and Tanière, 2011) for a number of different domain sizes and conditions, in particular, turbulent flow near wall boundaries. Commonly transportation is modelled by using both the instantaneous fluid velocity and the Weiner process (Henry *et al.*, 2014):

$$dx_p(t) = u_s(t) + B_x dW(t) \qquad 5.1$$

Where, $B_x = \left(\frac{k_B T}{6\pi\mu a_p}\right)^{\frac{1}{2}}$, Where k_B is the Boltzmann constant, T is the temperature, μ is the dynamic fluid viscosity, a_p is the particle radius.

Here the particle trajectories can be seen to be a function of both the fluid velocity term and the diffusive force, the full equation is shown here for completeness, however, as the fluid is assumed to be static the second term in equation 1.1 can be neglected. Furthermore, the particle velocities are assumed to be fluctuating rapidly and as such,

are captured using a Gaussian term (Henry *et al.*, 2013). As such, equation 5.1 can be formulated using a first order numerical scheme into the following:

$$x(t + \Delta t) = x(t) + u_s(t)\Delta t + B_x\sqrt{\left(\frac{1}{\Delta t}\right)}\ N \qquad 5.2$$

$$u(t + \Delta t) = u_s(t) + B_x\sqrt{\frac{1}{2\tau_p}}N \qquad 5.3$$

Where Δt is the time step and τ_p is the particle relaxation time, calculated using the following:

$$\tau_p = \frac{m_p}{6\pi\mu a_p} \qquad 5.4$$

Where m_p is the particle mass

Particle motion is only the first stage in modelling aggregation, the second stage focuses on collision processes. Within the literature there are a number of techniques used to calculate the likelihood of a collision occurring within a time step. (Henry *et al.*, 2013) and (Mohaupt, J. P. Minier and Tanière, 2011) utilise the diffusive bridge method in which a likelihood of collision is calculated for each particle within the domain and when a specific threshold is met then collision occurs. Alternatively, adaptive time step methods are used to explicitly model the collision point (Bolintineanu *et al.*, 2014). Though each of these techniques offers specific advantages and disadvantages it was decided that the collision detection here would be simplified and utilise the in-built agent procedure within NetLogo. Here the particles search for a particle within a radius equivalent to the magnitude of the two vectors produced by equation 5.2 and choose a random particle within that radius to collide with (Figure 5.1).

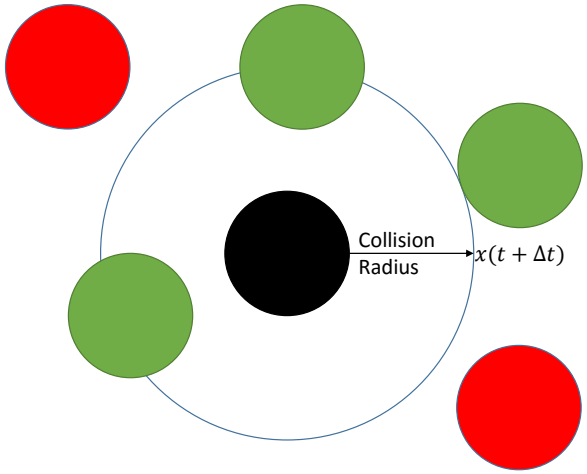

Figure 5.1 The collision detection technique used within NetLogo, where green highlights potential collision candidates and red highlights excluded candidates.

This agent then reports the other agent has its collision candidate and a collision is assumed to occur, each agent then sets a flag to state it has collided so that collisions are not double counted. To order the collision detection mechanism each of the agents were ordered by their respective unique identifier numbers (*who numbers*). The fully schematic of the particle motion and collision model can be seen in Figure 5.2, in which it is shown that the new particle conditions are created using equation 5.2, the collision detection step is run as an interim procedure. If a collision does not occur the particles carry on their trajectory and no collision is reported. If a collision does occur, new particle trajectories are calculated by using equation 5.2 and an adapted time step which equates to the full simulation time step

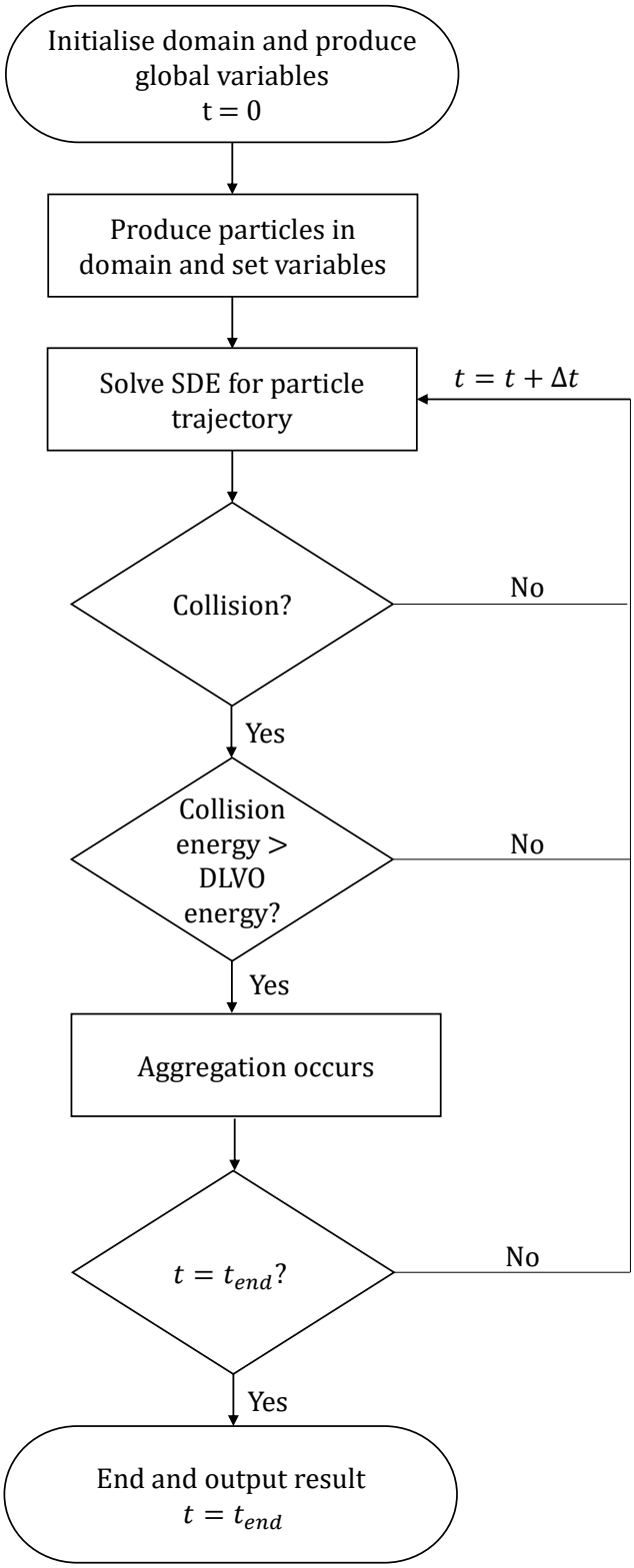

Figure 5.2 The Particle motion and collision schematic for colloidal aggregation within NetLogo

5.3 Model validation

To validate the aggregation model within NetLogo a three-stage process was undertaken, where each of these stages validates the accuracy of the model in comparison with either the analytical or experimental solution.

The first stage of the validation procedure consisted of comparing the diffusion limited aggregation data against the analytical solution of the discrete Smoluchowski equation as derived by Elimelech and O'Melia(1990)(see Chapter 2).

The second stage consisted of introducing the DLVO term, where effectively some stability is introduced to the model. The DLVO term modelled here was assumed to be sphere-sphere, however, it would be trivial to introduce a sphere-plate or plate-plate term dependent on the size range being studied. By varying the ionic strength or pH of the solution the ability of the colloidal particles to aggregate was examined. By introducing several different criteria, it is possible to establish a stability ratio and examine how this varies dependent upon the colloidal physical and chemical properties. The stability ratio of the model was then compared to experimental data for the same system.

The third stage of validation explores how the growth of the aggregate under varying chemical conditions directly effects its geometry. In this case, the particle ionic strength was varied so that the system either consisted of a purely diffusive system or a reactive system. The growth behaviour was the analysed using the fractal dimension and compared to experimental and analytical values found within the literature.

5.31 Comparison of a purely diffusive system

The simplest case to study aggregation within a colloidal system is to assume that the only controlling mechanism is transportation, commonly defined as diffusion limited aggregation (DLA). It is understood that this is synonymous to having a solute system which is highly attractive at small particle distances. As discussed in the Theory Chapter (Chapter 2) this is usually approximated by using the Smoluchowski equation for aggregation growth:

$$\frac{\delta n(x,t)}{\delta t} = \frac{1}{2}\int_0^x K(x-y,y)n(x-y,t)n(y,t)dy - \int_0^\infty K(x,y)n(x,t)n(y,t)dy \qquad 5.5$$

Where K is the collision kernel, n is the number of particles of specific size, t is time

Though equation 5.5 captures the continuous creation and destruction of particle complexes, it is more common to apply the discrete equation:

$$\frac{dn_k}{dt} = \frac{1}{2}\alpha\sum_{i+j=1}^{i}\beta(i,j)n_i n_j - \alpha n_k\sum_{i=1}^{\infty}\beta(i,k)n_i \qquad 5.6$$

Where n_k is the Aggregate size, α is the collision efficiency, β is the collision percentage

This population balance equation captures the relative change of particle complex concentrations, with the first term on the right, the promotion of the complexes. The secondary term on the right is reduction in the initial complexes.

By making a number of assumptions it is possible to produce a set number of equations which produce the analytical solution to diffusion limited aggregation. These assumptions can be synthesised as the following (Elimelech, 1997):

1 The limiting factor for colloidal movement is Brownian motion

2 Each collision results in attachment ($\alpha = 1$)

3 Particles are monodispersed

4 Particles are always spherical

5 2-particle only interactions

6 Particle breakage is excluded

These simplifications allow for the following equations to be produced:

$$n_k = \frac{n_0\left(\frac{t}{\tau}\right)^{k-1}}{\left(1+\left(\frac{t}{\tau}\right)\right)^{k+1}} \quad 5.7$$

$$\tau = \frac{\mu\pi a_p^3}{\phi k_B T} \quad 5.8$$

Where n_o is the initial concentration of monomers, k is the particle complex number, k_B is the Boltzmann constant, T is the absolute temperature, μ is the fluid viscosity ,τ is the relaxation time, a_p is the particle radius, ϕ is the volume fraction

Initial validation of the model within a diffusive only environment was undertaken using the following initial particle numbers; 500, 1000, 2000 particles (at 1μm). Each particle was tracked within a periodic box of the length 500μm. By setting T = 296.15K, μ = 0.89mPas^{-1}, this equates to an aggregation rate constant of 6.13x10^{-18} m^{3}s^{-1}, Δt was set to be >> τ to ensure that particle diffusion was captured within the system, here a time-step of 1s was used. To capture the random term within the particle motion equation (5.2) the in-built random-normal procedure was used within NetLogo, this produces a random number from Gaussian distribution using a Mersenne twister number generation. Table 1, shows the relevant initial volume densities of the particle domains being modelled.

Particle Number	Initial volume density (m^{-3})
500	2.01×10^{-6}
1000	4.19×10^{-6}
2000	8.38×10^{-6}

Table 5.3 Number of particles modelled within the NetLogo model and their representative initial volume density

Direct comparison of the models to the Elimelech analytical solutions shows good agreement in all 3 test cases (Figure 5.3). When only 500 particles are explicitly modelled it can be seen that the NetLogo model fluctuates around the analytical solution with the monomer model showing a slight under prediction to the decay curve. As the number concentration increases within the domain the accuracy of the system also significantly increases with the 2000 particle concentration showing to be only slightly divergent from the analytical solution (Figure 5.3c). Furthermore, convergence testing was undertaken on the number of runs needed to obtain an accurate description of the system being modelling with an initial particle number of 1000. Figure 5.4, shows that with only a single run of the model there is significant fluctuation of the model output compared to the analytical solution. In comparison, the mean value number for 100 runs shows a much closer convergence to the analytical solution. Though the model seems to converge much quicker even when repeated 10 times.

Finally, the difference between the analytical solution and 50 runs is also minimised, along with the accuracy increase between 50 and 100 runs. In this case all the models where repeated 50 times to increase the accuracy of the model without applying long run times. A similar extrapolation of the convergence could also be viewed from the

number of initial particles modelled within the system, as this is indicative of an increase in collisions which allows for increase in accuracy (figure 5.4).

Initially, the model can be seen to be performing well when predicting diffusion only aggregation with a much closer convergence rate when the system is repeated >50 times. For future runs, all modelling will be repeated at least 10 times and the mean results will be shown. It can also be seen that the collision algorithm for predicting collisions within a collision radius allows for accurate simulation of particle-particle collision mechanisms.

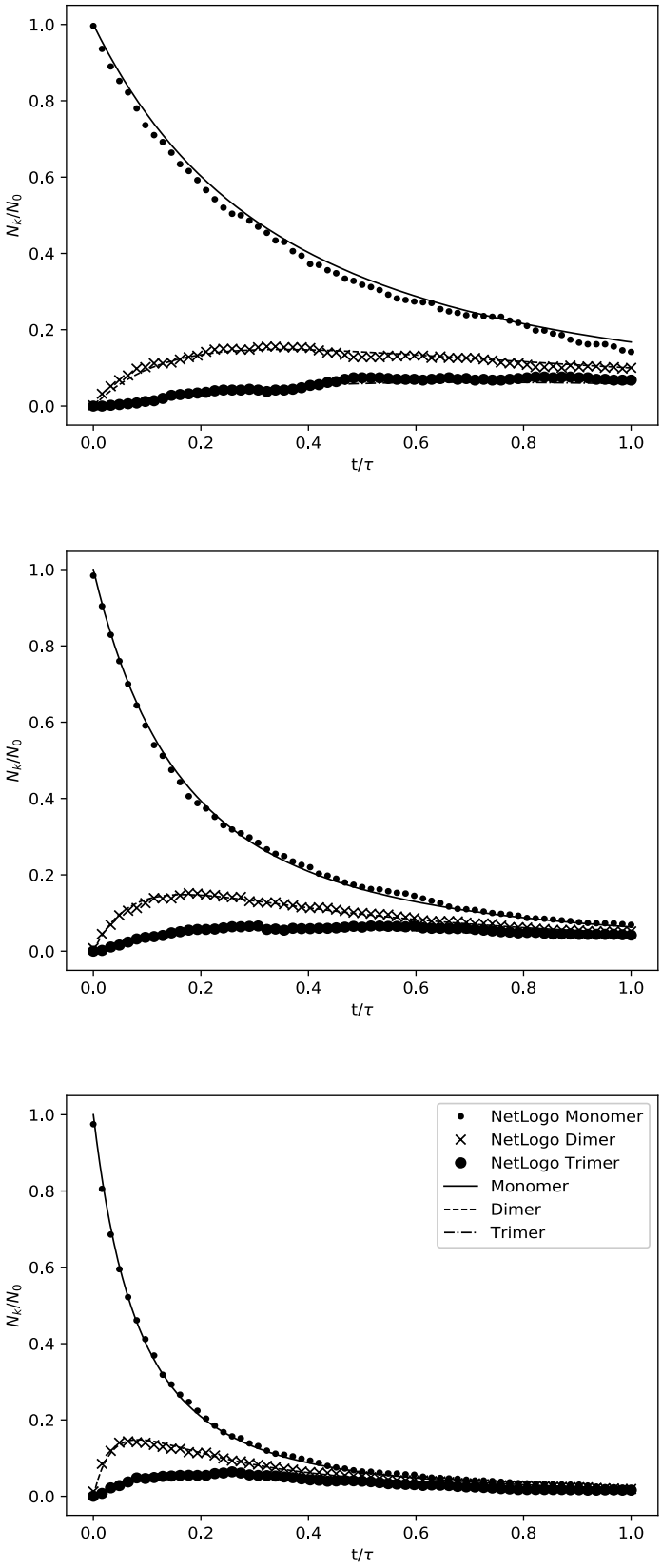

Figure 5.3 Theoretical aggregation sizes over normalised time as described by Smoluchowski compared to the NetLogo aggregation sizes A) 500 particles comparison B) 1000 particle comparison C) 2000 Particle comparison

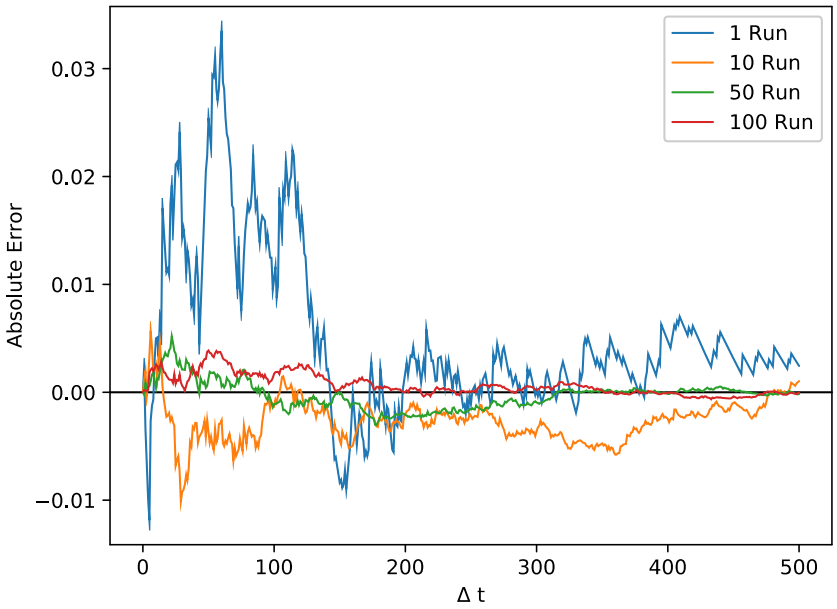

Figure 5.4 Absolute error of the mean monomer value at 1, 10, 50, 100 runs at 1000 particles

5.32 Reaction Limited Aggregation

Reaction limited aggregation (RLA) is the case when diffusion cannot be assumed to be the only limiting factor within colloidal aggregation. RLA is dependent on the both physical and chemical state of the system, as such, the particles are assumed to be influenced both by the temperature along with the chemistry of the system. Commonly, the inter-particle collision energy is calculated by utilising the DLVO equation for sphere-sphere interactions (Chapter 2). In this case, the limiting factor for particle-particle aggregation is the collision energy and the potential energy barrier. Figure 5.5, shows the variation in potential energy barrier for two colliding 1 μm polystyrene colloids at room temperature. It can be seen that the potential energy barrier decreases as a function of Ionic strength. In relation to RLA, at an ionic strength of 0.1 mMol it can be seen that the potential barrier is >60kBT and as such the system would be assumed to be stable meaning that aggregation only occurs over extremely long time scales, however, as ionic strength is increased the likelihood of particle-particle collisions resulting in aggregation increases until the potential barrier = 0, in which case diffusion limited aggregation is captured.

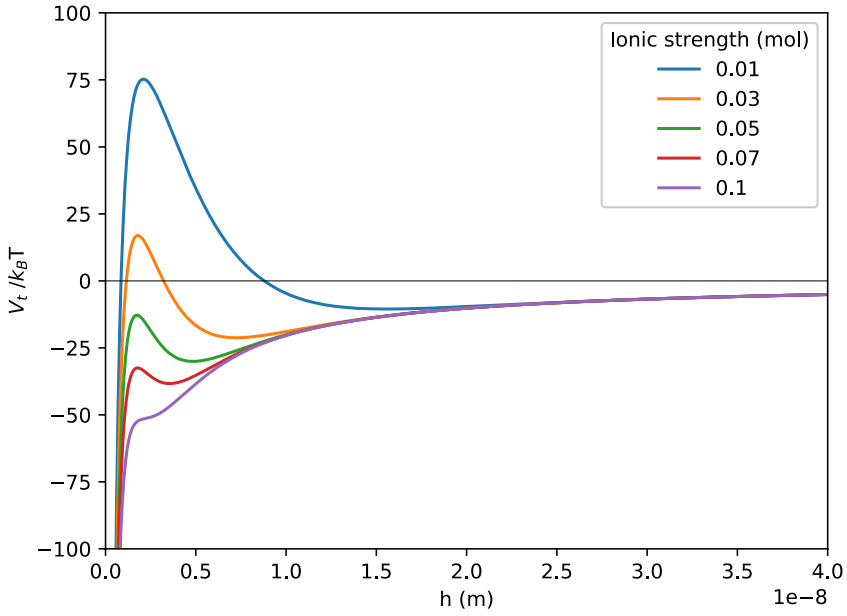

Figure 5.5 The DLVO profile for a 1µm polystyrene latex colloids with NaCl

Within the literature (Ball *et al.*, 1987; Berre, Chauveteau and Pefferkorn, 1998; Molina-Bolivar, Galisteo-Gonzalez and Hidalgo-Alvarez, 1999; Lattuada *et al.*, 2003; Tomilov *et al.*, 2013), it is common to model a system to understand the rate at which aggregation occurs as a function of the potential barrier height, this is usually captured using the stability ratio (W) (Table 2) which is dependent on the number of collisions resulting in aggregation to the number of unsuccessful collisions:

$$W = \frac{k_{fast}}{k_{DLVO}} \qquad 5.9$$

Where k_{fast} is the aggregation rate without a potential energy barrier, i.e. every collision results in an aggregate forming and k_{DLVO} is the number of collisions occurring when there is a potential barrier present.

Within a NetLogo context, this can be modelled using the following rule:

$$If\ Energy_{collision} > \Phi_{max}\ \ irreversible\ aggregation$$

$$If\ Energy_{collision} < \Phi_{max} \qquad no\ aggregation$$

If the collision energy is greater than the potential energy barrier then a successful collision is recorded, alternatively if the collision energy is less than the energy barrier than an unsuccessful collision is recorded. By monitoring the total collision along with the number of successful collisions it is possible to calculate the stability of the NetLogo model.

Author	Particle Type	Particle Diameter (nm)	Ionic Strength (mol)	Solution	Φ	W
(Sandkühler, Sefcik and Morbidelli, 2004)	Polystyrene latex	66	0.26	D_2O	0.05	$3.3x10^6$
(Behrens *et al.*, 2000)	Polystyrene latex	310 110	0.001 0.01 0.1	Deionized water	-	0.98 1.00 0.89 0.98 1.21 2.60 5.33 10.45 22.97 37.38 60.82 250.18
(Lattuada *et al.*, 2003)	Fluorinated-polymer latex	75	0.5 0.5 0.5 0.5 0.48 0.15	Deionized water	0.08 0.2 0.6 1.5 2 5	$2.6X10^5$ $9.50X10^5$ $2.00X10^6$ $1.04X10^6$ $1.94X10^6$ $4.41X10^6$
(Kim and Berg, 2000)	Polystyrene latex	98	1.5 0.93 0.75 0.5 0.3 0.15 0.1 0.08 0.07 005	D_2O	$1.47x10^{-6}$	4.4 4.2 4.6 5.3 4.8 6.6 8.1 7.7 20.0 28.5
(Burns *et al.*, 1997)	Polystyrene latex	330	0.4 0.5 0.6 0.7 0.85 1.00 1.25 1.5	Deionized water	0.0020 0.0035 0.0070	-

Table 5.4 Literature comparison of different stability ratios due to variations in ionic strength and size range

To validate the NetLogo model a comparison was undertaken against the experimental system developed by Behren's *et al*, which analysed the aggregation behaviour of two different sizes of carboxylated polystyrene latex spheres under varying pH at 3 different ionic strengths. The DLVO equation for sphere-sphere was implemented within NetLogo and the maximum potential energy barrier was set as a global variable to allow for easy access when a collision occurs. To capture the DLVO profile the zeta potentials where modelled using interpolation equation derived by Behren's *et al*. To increase the accuracy of the simulation further, a collision counter was used which incremented whenever a successful collision occurred allowing for a greater number of collisions to be sampled. To ensure double counting did not occur within the collision procedure only one agent reported a collision, and the other agent was excluded from any collision procedure for the time step (as described previously). Finally, the system being modelled was set at a particle radius of 155nm, a ionic strength of 10mM, periodic box of length 10 d_p, $\Delta t = 6.4x10^5 \cdot \tau_p \cong 0.2s$, which is significantly large enough to be considered diffusive behaviour.

The stability ratio can be seen to be captured accurately within the NetLogo model, particularly, when compared against the Behrens experimental results (Figure 5.6). At higher pH values it can be seen that the system becomes more stable, in particular, at a pH approaching 4 the likelihood of a successful collision occurring is significantly reduced. There is a transition period at a pH of approximately 3.6, in which the system goes from highly unstable (every collision results in aggregation) to stability. Within the context of colloidal sciences this is classed as the critical coagulation constant (CCC) which highlights the transition zone. Furthermore, it can be understood that

the system is highly sensitive to variations in ionic strength, at I > NUM there can be seen rapid increase in aggregation when compared to lower ionic strengths (Figure 5.7).

Finally, the NetLogo has captured both the DLA system and RLA system accurately for different physical and chemical conditions. Both analytically and experimentally the description of the particle motion using the Minier *et al* algorithm and the in-radius collision procedures captures the dynamics of colloidal systems in its most simplistic state.

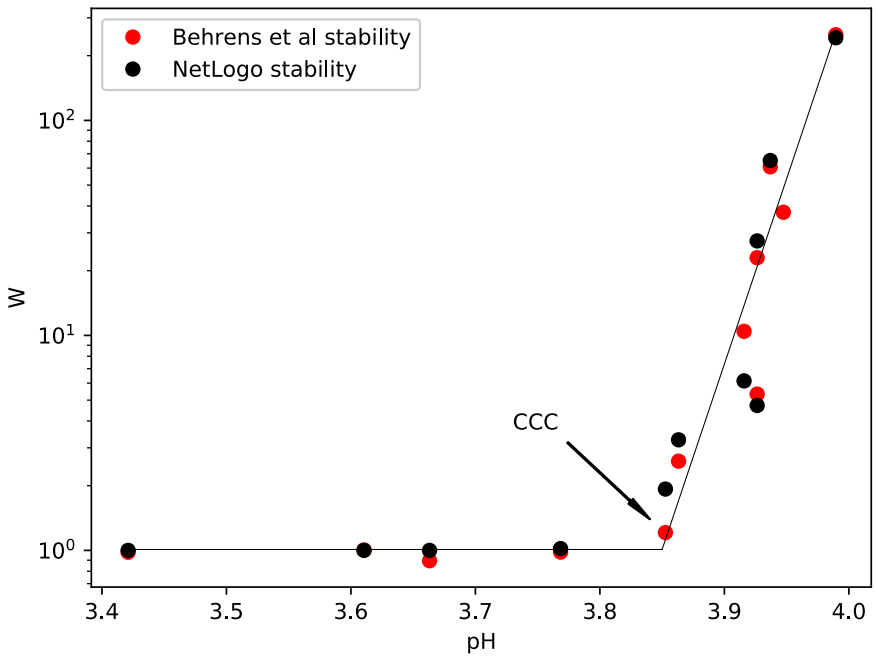

Figure 5.6 Comparison of NetLogo stability ratio to Behrens et al stability ratio for polystyrene latex colloids (310nm) at varying pH with the critical coagulation(CCC) point highlighted and a guideline placed to show the difference between the slow aggregation and fast aggregation zones around the CCC.

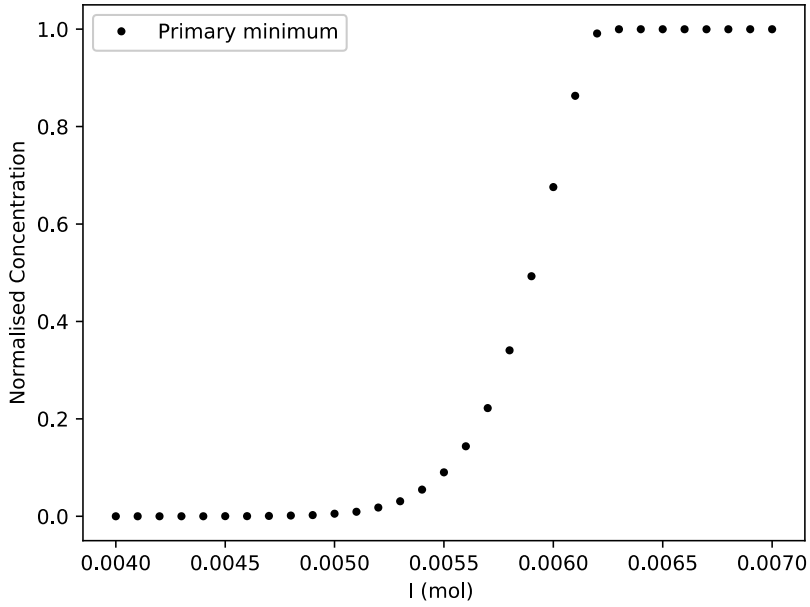

Figure 5.7 Sensitivity of 310nm colloidal particles to changes in ionic strength

5.33 Fractal dimensions

Previously, the system being modelled either ignored the particle aggregation shape, i.e. RLA, or else assumed an idealised aggregate shape as was the case in the DLA validation tests. In reality, it is understood that the particle aggregation structure plays an important role in the aggregation rate of the system. Within colloidal aggregation studies the fractal dimensions of particle aggregates are used to approximate the geometric shape of the aggregates as well as to state self-similarity irrespective of length scale (Schaefer *et al.*, 1984). For 3D aggregates a fractal dimension of 3 approximating to an exact sphere and a fractal dimension of <2 being associated with more dendrite like aggregates. It is well reported within the literature (Stankiewicz, Cabrerizo Vílchez and Hidalgo Alvarez, 1993) that the average fractal dimension for 3D aggregates due to DLA is ~1.8 whereas in RLA systems it is ~2.2. Furthermore, within the 2D system the fractal dimension is usually considered lower and for DLA is ~1.45 and for RLA is~1.8.

To understand the local aggregate structures of both diffusion limited aggregation (DLA) and reaction limited aggregation, fractal dimensions where taken from the cluster aggregates. This technique is commonly cited within the literature as a way of quantifying in which system an aggregate structure is placed. Application of the fractal dimension theory allows for the complex geometry of the structures to be defined and for a comparison of self-similarity to be approached (Chakrabarty *et al.*, 2011). By applying the following equation:

$$N = k_0 \left(\frac{R_g}{d_p}\right)^{1/D_f} \quad 5.10$$

Where N is the number of primary particles in the aggregate, k_o is the fractal prefactor, R_g is the radius of gyration, d_p the primary particle diameter, and D_f the mass fractal dimension.

Numerous techniques are reported within the literature when solving for the fractal dimensions, Chakrabarty *et al*, undertook a comprehensive analysis in determining the most suitable for calculating the fractal dimension in 2D and extrapolating to 3D cases. The ensemble method showed the most accurate comparison to the 3D solution from a 2D system, whereas alternative techniques offered less accurate approaches. As such, the approach undertaken here will centre on the ensemble method, though the system modelled is 2D this allows for extrapolation to the 3D case. The ensemble method is based on the following radius of gyration (R_g) equation:

$$R_g^2 = \frac{1}{N}\sum_{k=1}^{N}(r_k - r_{com})^2 \quad 5.11$$

Where r_k is the vector location of the particle and r_{com} is the centre of mass location.

This method can be described as a mass centric method, in comparison to the box counting method employed by the nested squares method and similar approaches. As

previously, mentioned in the diffusion limited aggregation the limiting factor is that of the diffusion of the particle. When the primary particle comes into contact with another primary particle or a cluster than instantaneous aggregation occurs, as a consequence of this is the production of "fluffy" aggregates in which the fractal dimension is <2. Alternatively, within a reaction limited regime, a particle may undergo multiple collisions before aggregation occurs. This results in particles travelling further into an aggregates structure before the necessary thermal excitation is great enough to overcome the repulsion barrier and result in attachment. With this case it is common to have a fractal dimension >2. In some cases, i.e. systems of emulsions, the fractal dimension can be equivalent to 3, which prescribes two spherical particles aggregating to form a single particle with the summation of the two primary particles. This approach was utilised in the previous section when calculating a direct comparison the Smoluchowski profiles (Figure 5.3).

Within the NetLogo environment both sets of systems where tested, along with a variation in the volume fraction. Diffusive behaviour was captured using the stochastic Langevin equations described in the previous section (5.2) along with the repulsive barrier being calculated from the DLVO equations. Alternatively, a probability of collision factor can be used to estimate the differences in fractal dimension. However, the approach of using the DLVO equations was used due to its ability to rapidly test difference pH and ionic strength conditions.

Within the NetLogo model the following conditions where assumed, a particle size of 300nm, NaCl conditions where varied from 0.11 and 1M to produce the necessary DLVO profiles, the time step used was set using the initial particle sizes, $\Delta t = 6.4x10^5 \cdot \tau_p \cong 0.2s$, the length of the domain was assumed to be 10 d_p.

Though similarity exists in this set up and the previous modelling criteria used in section 5.3, some changes were made to the particle motion procedure. The aggregate mass was used to calculate the new diffusion coefficient along with the hydrodynamic radius. Furthermore, the aggregates where only modelled as translating through the domain and rotation was neglected within the model. Finally, a leader was chosen within the aggregate to set the new particle motions. This leader was chosen using the recursion method described by Wilensky, 1999, which re-distributes the leader flag to the highest numbered particle. In this case it allows for explicit aggregate tracking. Within the aggregate group, the particles still exist and are all connected using the in-built link term within NetLogo which allows data transfer to occur. Also, in the case of reaction limited aggregation, the potential barrier was set above the mean kinetic energy of the particles, ensuring that only a limited number of successful collisions can occur.

Finally, the data was analysed using the least-squares fit model within the SciPy model library within the Python programming language to analyse the behaviour of the fractal dimension as a function of the ionic strength within the system. The data set was then compared to the literature value of the fractal dimension in 2D produced by Chakrabarty *et al*.

The aggregate geometry of the behaviour produced within NetLogo for RLA resulted in a fractal dimension of 1.8 produced from the radius of gyration and number of particles within the aggregate (Figure 5.8). It can be seen that this fractal dimension is equivalent to the literature derived result. As previously discussed, this is due to the particle having a much longer time to diffuse into the centre of the aggregate. In this case, if a particle enters the aggregate structure it is likely to undergo a number of collisions until the collision energy is large enough for aggregation to occur. In

comparison, the DLA system produced a fractal dimension of 1.4, implying loose aggregates with a highly fractal nature (Figure 5.9). This fractal dimension is also closely related to the literature derived value, implying that the collision mechanism within NetLogo and the aggregate recursion procedure allows for complex structures to be captured.

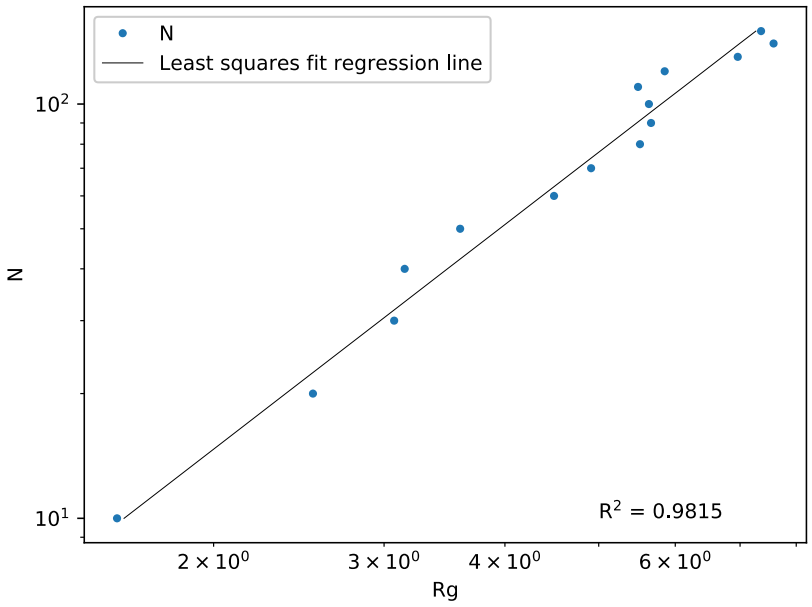

Figure 5.8 Radius of gyration for reaction limited aggregation with least squares fit with an $R^2 = 0.9815$

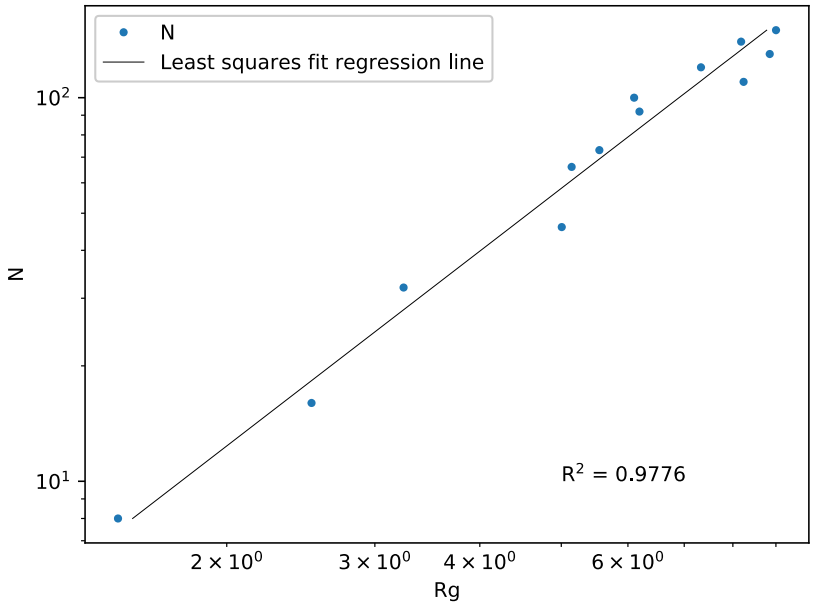

Figure 5.9 Radius of gyration of diffusion limited aggregation with least squares fit with an $R^2 = 0.9776$

5.4 Sensitivity of colloidal particles to secondary minima aggregation

Until recently the role of the secondary minima was neglected when modelling particle aggregation, however, it is now understood that the secondary minima is particularly important when understanding colloidal stability (Wu and Lai, 2005).Due to the well depth in the primary minimum, colloidal aggregation is usually considered irreversible. In comparison, when colloids attach within the secondary minima they are considered reversible with a number of studies recently being undertaken in predicting how long these particles reside in the well and as such how long they are aggregated for (Kovalchuk and Starov, 2012). This residence time is understood to be a function of internal diffusion within the aggregate whereas when the kinetic energy of the particle is large enough to overcome the secondary minima the particle is released back into the solution. Furthermore, when particles reside in the secondary minima, systems which were previously considered stable are now unstable. Figure 5.11B, shows the relative depth of the secondary minima to variations in ionic strength, whereas figure 5.11A shows the decrease in the potential height barrier. It can be seen that at lower ionic strengths there is rapid decrease from the positive value in which even including the secondary minima the system is considered stable. Once the ionic strength increases there is a linear well depth decrease. At approximately I = 0.05 Mol the potential barrier height is around 50 kBT, in traditional colloidal dynamics this would imply a stable solution, however, including the secondary minima shows that colloids are likely to remain in an aggregate for long time scales due to the well depth ~3 kBT in this case the solution would be assumed pseudo-stable.

It has also been noted that for small particles the DLVO and single Minimum assumption holds true, however, for larger particles the assumption does not. In this case it is important to know not only how long the particles reside within the secondary

minima but also the sensitivity of particle aggregation within the secondary minima to ionic strength. By understanding the behaviour of secondary minima aggregation, in particular the sensitivity of the aggregate to different ionic strengths it allows for a greater optimisation of experimental setup when understanding aggregation behaviour.

Implementation of the secondary minima model within NetLogo followed the same procedure outlined previously, in which the DLVO equation was used to produce a maximum potential energy measure. However, this was extended to take the secondary minima value which was also set as a global variable to increase the model run speed. The rule for aggregation was also update from equation 5.6 to equation 5.7. In this case and extra term was incorporated which allowed for the particles to be captured within the secondary minima.

$$If\ Energy_{collision} > \Phi_{max}\ \ irreversible\ aggregation$$

$$If\ Energy_{collision} < \Phi_{\sec min}\ reversible\ aggregation$$

$$If\ \Phi_{\sec min} < Energy_{collision} < \Phi_{max}\ no\ aggregation$$

To increase the accuracy of the simulation and to ensure that a suitable number of collisions where included the same collision procedure was utilised as in section 5.3.2 (RLA) in which the number of collision which would have resulted in a secondary minima aggregate forming along with primary aggregate and the total number of collisions where recorded. Furthermore, the particles in the system where assumed to be polystyrene latex, similar to all previous studies with a radius of 330 nm and as such the zeta potentials where calculated using the Behren's interpolation method (Behrens *et al.*, 2000)and assuming a KCl electrolyte. Finally, the system box length was set to 100 d_p and the time step was set to 0.2s ensuring that the system was modelling diffusive behaviour only.

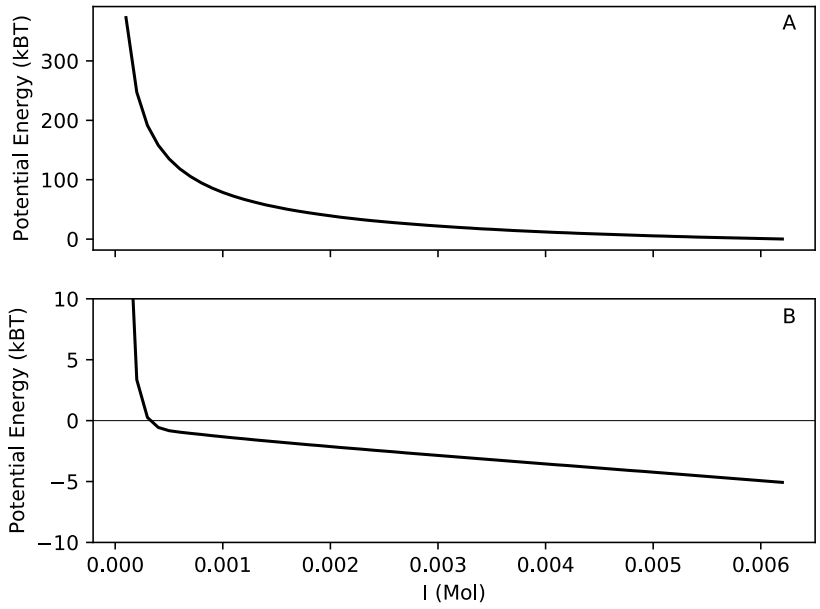

Figure 5.10 Comparison of primary well depth and secondary well depth as a function of ionic strength when using the DLVO theory equation. A) Shows the primary maximum potential energy due to ionic strength. B) Shows the secondary minima energy barrier due to ionic strength

Sensitivity of aggregation within the secondary minima can be seen to be captured in Figure 5.11. The behaviour of particle aggregation can be seen to be highly sensitive to both low ionic strengths and high ionic strengths. In the case of low ionic strength few particles aggregate though this is can be seen to be a function of the vertical asymptote in Figure 5.10A, where at this stage either the secondary minima does not exists or else the well depth is smaller than the mean collision energy (Figure 5.10B). However, as the ionic strength is increased to 0.003 mol the majority of the particles in the system are associated with secondary minima aggregation. Furthermore, at a well depth of 0.005 mol the system would be considered pseudo-stable as the well depth can be seen to be approximately 5kBT as such, it is highly unlikely that particles would be able to escape from the potential well. At around 0.0055 there is a rapid drop off in the number of particles being aggregated within the secondary minima, this is due to the primary

minimum barrier being reduced enough for a large number of particles to be deposited in the primary minimum instead of the secondary minima. At 0.006 and greater nearly all colloids undergo primary aggregation due to there being no potential barrier, at this point the system is purely undergoing DLA.

In Figure 5.11, there can be seen a lag between the aggregation of particles within the secondary minima and the primary minimum. As the ionic strength is increased it can be seen that the number of primary minimum aggregations increases at the same rate as the decrease rate of the secondary minima. Thus, it can be understood that colloidal aggregation both in terms of rate of aggregation along with stability of the system is highly sensitive to the ionic strength of the system. Furthermore, the actual point in which primary minimum aggregation is no longer negligible is approximately 0.004 mols, in which the aggregation rate is significantly faster than that of the secondary minima aggregation (figure 5.11). Here, the rate of secondary minima can be seen to be observing an almost logarithmic profile in comparison to that of the primary maximum.

Finally, by neglecting the secondary minima for large particles, i.e. particles > 50nm, there will be an underestimation of the rate of aggregation along with the number of aggregates formed. Though at low ionic strength it can be assumed that secondary minima aggregates are short lived and it is highly unlikely that aggregates larger than dimers would form due to the secondary minima depth being significantly shallower than the average collision energy or even the average kinetic energy of the colloid particles.

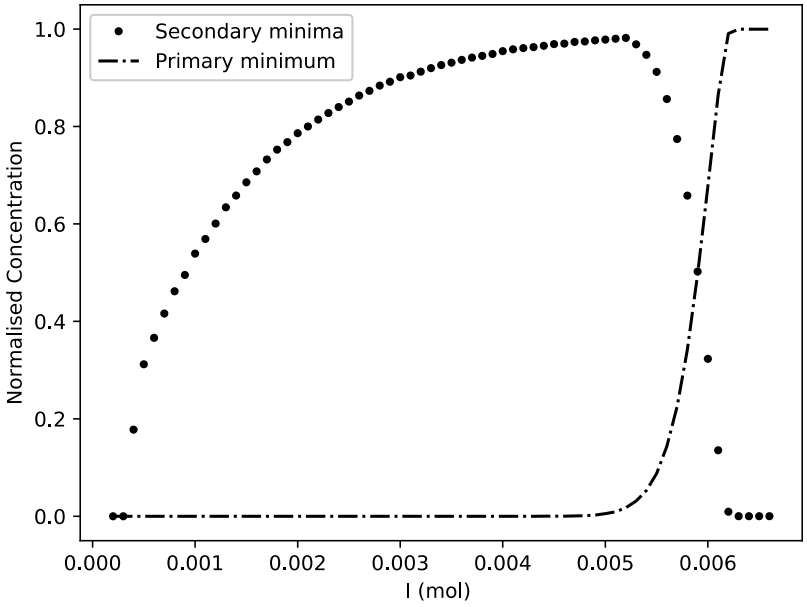

Figure 5.11 The normalised concentration of collisions which result in both secondary minima and primary minimum aggregation

5.5 Conclusions

The agent based modelling technique used in conjunction with the stochastic particle motion tracking equation produced by Minier *et al*, was successful in capturing diffusion aggregation for simplified colloidal particles. In particular, the use of a simple rule based aggregation procedure was used. In this case, the traditional potential approach utilised within the context of alterative colloidal particle modelling techniques was used with the rule based approach in which the processes where simplified.

It can be seen that NetLogo is a useful simulation suite for understanding colloidal aggregation in different physical and chemical conditions. Here a range of validation exercises have been undertaken in which various areas of colloidal aggregation have been modelled. It has been shown that the model performs well against the bench mark validation studies and can be extended to analyse more complex environmental conditions. Though there are some drawbacks in terms of performance at higher particle concentrations due to NetLogo's inherent memory usage.

Furthermore, it has also been shown that colloidal aggregation is inherently sensitive to changes surface chemistry conditions and that the rate of aggregation cannot be solely modelled as a function of primary minimum aggregation. Incorporation of the secondary minima principle allows for a more accurate understanding of colloidal aggregation and the influences that changes in temperature and surface chemistry have on both rates of aggregation and disaggregation.

Finally, by using the agent based modelling paradigm the incorporation of the secondary minima influence is easily achieved by inputting a new "rule" within the model at very little computational cost, hence showing the versatility and importance

of agent based modelling as an alternative modelling method for colloidal aggregation studies.

5.6 References

Ball, R. C. *et al.* (1987) 'Universal kinetics in reaction-limited aggregation', *Physical Review Letters*, 58(3), pp. 274–277. doi: 10.1103/PhysRevLett.58.274.

Behrens, S. H. *et al.* (2000) 'Charging and Aggregation Properties of Carboxyl Latex Particles: Experiments versus DLVO Theory', *Langmuir*, 16(6), pp. 2566–2575. doi: 10.1021/la991154z.

Berre, F. Le, Chauveteau, G. and Pefferkorn, E. (1998) 'Perikinetic and Orthokinetic Aggregation of Hydrated Colloids', *Journal of Colloid and Interface Science*, 199(199), pp. 1–12. doi: 10.1006/jcis.1997.5307.

Bolintineanu, D. S. *et al.* (2014) 'Particle dynamics modeling methods for colloid suspensions', *Computational Particle Mechanics*. Springer International Publishing, 1(3), pp. 321–356. doi: 10.1007/s40571-014-0007-6.

Burns, J. L. *et al.* (1997) 'A Light Scattering Study of the Fractal Aggregation Behavior of a Model Colloidal System', *Langmuir*, 13(24), pp. 6413–6420. doi: 10.1021/la970303f.

Chakrabarty, R. K. *et al.* (2011) 'Simulation of aggregates with point-contacting monomers in the cluster-dilute regime. Part 1: Determining the most reliable technique for obtaining three-dimensional fractal dimension from two-dimensional images', *Aerosol Science and Technology*, 45(1), pp. 75–80. doi: 10.1080/02786826.2010.520363.

Elimelech, M. and O'Melia, C. R. (1990) 'Langmuir 1990,6, 1153-1163', *Langmuir*, 6(6), pp. 1153–1163.

Henry, C. *et al.* (2013) 'A new stochastic approach for the simulation of agglomeration between colloidal particles', *Langmuir*, 29, pp. 13694–13707. doi: 10.1021/la403615w.

Henry, C. *et al.* (2014) 'A stochastic approach for the simulation of collisions between colloidal particles at large time steps', *International Journal of Multiphase Flow*. Elsevier Ltd, 61, pp. 94–107. doi: 10.1016/j.ijmultiphaseflow.2014.01.007.

Kim, A. Y. and Berg, J. C. (2000) 'Fractal aggregation: Scaling of fractal dimension with stability ratio', *Langmuir*, 16(5), pp. 2101–2104. doi: 10.1021/la990841n.

Kovalchuk, N. M. and Starov, V. M. (2012) 'Aggregation in colloidal suspensions: Effect of colloidal forces and hydrodynamic interactions', *Advances in Colloid and Interface Science*. Elsevier B.V., 179–182, pp. 99–106. doi: 10.1016/j.cis.2011.05.009.

Lattuada, M. *et al.* (2003) 'Aggregation kinetics of polymer colloids in reaction limited regime: Experiments and simulations', *Advances in Colloid and Interface Science*, 103(1), pp. 33–56. doi: 10.1016/S0001-8686(02)00082-9.

Minier, J.-P., Peirano, E. and Chibbaro, S. (2003) 'Weak first- and second-order numerical schemes for stochastic differential equations appearing in Lagrangian two-phase flow modeling', *Monte Carlo Methods and Applications*, 9(2). doi: 10.1515/156939603322663312.

Mohaupt, M., Minier, J.-P. and Tanière, a. (2011) 'A new approach for the detection of particle interactions for large-inertia and colloidal particles in a turbulent flow', *International Journal of Multiphase Flow*. Elsevier Ltd, 37(7), pp. 746–755. doi: 10.1016/j.ijmultiphaseflow.2011.02.003.

Mohaupt, M., Minier, J. P. and Tanière, A. (2011) 'A new approach for the detection of particle interactions for large-inertia and colloidal particles in a turbulent flow', *International Journal of Multiphase Flow*. Elsevier Ltd, 37(7), pp. 746–755. doi: 10.1016/j.ijmultiphaseflow.2011.02.003.

Molina-Bolivar, J. A., Galisteo-Gonzalez, F. and Hidalgo-Alvarez, R. (1999) 'Colloidal

aggregation in energy minima of restricted depth', *Journal of Chemical Physics*, 110(11), pp. 5412–5420. doi: 10.1063/1.478436.

Peirano, E. *et al.* (2006) 'Mean-field/PDF numerical approach for polydispersed turbulent two-phase flows', *Progress in Energy and Combustion Science*, 32(3), pp. 315–371. doi: 10.1016/j.pecs.2005.07.002.

Sandkühler, P., Sefcik, J. and Morbidelli, M. (2004) 'Kinetics of gel formation in dilute dispersions with strong attractive particle interactions', *Advances in Colloid and Interface Science*, 108–109, pp. 133–143. doi: 10.1016/j.cis.2003.10.016.

Schaefer, D. W. *et al.* (1984) 'Fractal Geometry of Colloidal Aggregates', *Physical Review Letters*, 52(26), pp. 2371–2374. doi: 10.1103/PhysRevLett.52.2371.

Stankiewicz, J., Cabrerizo Vílchez, M. A. and Hidalgo Alvarez, R. (1993) 'Two-dimensional aggregation of polystyrene latex particles', *Physical Review E*. American Physical Society, 47(4), pp. 2663–2668. doi: 10.1103/PhysRevE.47.2663.

Tomilov, A. *et al.* (2013) 'Aggregation in colloidal suspensions: Evaluation of the role of hydrodynamic interactions by means of numerical simulations', *Journal of Physical Chemistry B*, 117(46), pp. 14509–14517. doi: 10.1021/jp407247y.

Wu, K. L. and Lai, S. K. (2005) 'Theoretical studies of the early stage coagulation kinetics for a charged colloidal dispersion', *Langmuir*, 21(8), pp. 3238–3246. doi: 10.1021/la0476682.

Chapter 6. Modelling particle transport in pore scale systems using NetLogo and lattice Boltzmann

This chapter concentrates on the implementation of the stochastic differential equations for particle tracking within the NetLogo environment utilising the previously validated lattice Boltzmann technique. Extension of the model from purely diffusive to advective-diffusive is studied, along with analysis of deposition methods upon collector surfaces. A simple case study is first approximated in which only single particle deposition is modelled, this is then extended to incorporate multiple particle deposition. Finally, the deposition of particles within the secondary minima is studied in varying flow conditions.

6.1 Background and previous work

Behaviour of particles within porous media can be seen to be influenced by a number of forces; diffusion, advection, inertial, and gravitational (Gao *et al.*, 2008) . When the particle size is small enough the influence of gravitational force can be neglected. In this case, the dominating forces are diffusion and advection. Commonly, the weighted influence of these forces upon the particle trajectory is categorised using the non-dimensional Peclet number (Pe)(Li *et al.*, 2018):

$$Pe = \frac{U_{max} a_p}{B_x} \tag{6.1}$$

Where U_{max} is the maximum velocity of the system, a_p the particle radius and B_x is the Stokes-Einstein diffusion coefficient ($B_x = \frac{k_B T}{6\pi a_p \mu}$, k_B is the Boltzmann constant, T is the temperature, a_p is the particle radius, and μ is the fluid viscosity).

In systems where the advective term within the particle motion is dominating than Pe >> 1 and the influence of diffusion is minimal, as such the particles will adhere to the streamlines of the fluid. Whereas, in a diffusion dominated system the particles are likely to observe more of a random walk profile and not closely adhere to the streamlines of the fluid, in this case the Pe << 1. In some instances the Pe = 1, where the influence of the advective term and diffusive term are equal and as function of this, the system is usually termed as transient (Li *et al.*, 2017). Finally, in the unique case of Pe = 0 the system is termed as purely diffusional and the advective term can be neglected completely, this is analogous to a quiescent system. This is the case in which a particle random walk is influenced only by the thermal energy of the system (Chapter 5).

There are two fundamental procedures for particle behaviour within porous media, firstly the transport of the particle, whilst secondly how the porous media surface is modelled. This can be modelled using a Lagrangian technique and solving the forces being applied to the particle. Commonly, simple geometries are studied to simplify the fluid influence on the particle trajectory (Ma *et al.*, 2009). In particular, the use of the sphere in cell model allows for an analytical solution of the fluid flow within the Stoke's regimes. By using a simplified geometry the single collector efficiency (the ability of the collector to accept particles onto its surface) can be studied (N Tufenkji and Elimelech, 2004). The collector efficiency is understood to vary due to a number of different conditions, from a purely physical point of view it is dependent on the Pe number. In diffusive regimes the particle takes longer to be transported to the collector surface, however once there it has much longer contact time with the surface. In a purely advective system, the particle is transported much more rapidly to the collector system, however, as it adheres more closely to the streamlines of the fluid it is less likely to come into contact with the collector surface. In the advective case, the most likely

influence of particles colliding with the collector surface is particle size, as particle size increases contact is more likely to occur (Elimelech and O'Melia, 1990a).

Once the particle has reached the surface of the collector the hydrodynamic and diffusional forces are replaced with the particle-wall forces. These are commonly resolved using the DLVO approach (Chapter 2). Particles can be captured on the wall if their kinetic energy is great enough to overcome the potential energy barrier between the particle and the wall (Saiers, Hornberger and Liang, 1994). In the simplest case the collector surface can be treated as attractive and any particle which comes into contact with the collect is irreversibly stuck (primary minimum attachment), in this case it is assumed that the adhesive forces are significantly greater than the hydrodynamic forces. Recently, it has been understood that there is also the contribution of the secondary minima in particle attachment to the collector surface, in this case the particles are captured in a much shallower potential well and as such are more readily influenced by changes in hydrodynamic and chemical conditions of the system (Kuznar and Elimelech, 2007).

If the physico-chemical conditions are such that particle-collector collisions are attractive and particle-particle collisions are repulsive, then a single layer of deposition occurs on the collector surface (Henry, Minier and Lefèvre, 2012). As such, any particle coming into contact with the deposited particle is reflected back into the flow and either finds unoccupied site or else is removed from the system. The ability of a particle to come into contact with multiple depositions sites is dictated by the flow conditions of the system. In a highly advective regime once the particle is reflected back into the flow channel then it is unlikely to be captured. In comparison, in a diffusion dominated system the likelihood of a particle coming into an unoccupied site is greatly increased. This is commonly understood to greatly influence the collector efficiency, as in an

advective regime the collector efficiency is reduced even though unoccupied depositions sites may still be available particles are unlikely to come into contact with them (Ko, Bhattacharjee and Elimelech, 2000). Whereas, in a diffusion dominated system the collector efficiency is maximised as particles have a much greater chance of being deposited. In reality, it is unlikely that single layer deposition will occur, especially over heterogeneous particle systems. If the particle-particle interaction is not assumed to be repulsive then multiple deposits can occur. In this case the influence of the hydrodynamic forces on the deposited particles is important. In reasonably advective systems, Pe > 1 then the deposited particles may be removed either out of the system or else to an area of low flow (Shen *et al.*, 2010).

The collector efficiency is usually predicted using a simplified sphere model in which surfaces are assumed smooth and homogeneous (Auset and Keller, 2006). In reality collector surfaces are rarely uniform and are rough. If a rough collector is assumed then deposition may not be as readily predicted due to heterogeneous physico-chemical conditions on the surface(Dagaonkar and Majumdar, 2018). As such, collector efficiency may offer an estimate as to the likelihood of deposition depending on the localised DLVO potential energy.

The deposition of particles in porous media is thus dependent on a number of criteria; the particle size, fluid flow, diffusive properties of the particle, chemistry of the system, collector geometry, and collector roughness. Each of these directly influence the collector efficiency and as a consequence of this the overall collector efficiency of the full porous media system. Each of these variables can be complex to model using traditional modelling techniques (sphere in cell), in particular, collector geometry and collector roughness (Auset and Keller, 2006).

By analysing each of these properties and understanding the sensitivity of the collector efficiency term this will allow for a greater assessment of how removal of particles within porous media is modelled and the rate of particle breakthrough can be better understood.

6.2 Methodology

6.21 Particle transportation

Transportation of the colloidal particle can be captured using a variety of different techniques, however, in an advection-diffusion regime it usually captured using the following stochastic differential equation (SDE):

$$dx(t) = U_p\big(x(t)\big)dt + B_x dW(t) \qquad 6.2$$

Where $U_p(x(t))$ is the velocity of the particle, and dW(t) is the Weiner process.

There are numerous techniques for evaluating the above SDE, with different variations starting from the Langevin view in which the accumulation of the forces acting upon the particle are calculated and solved using either an Euler or higher integration technique (Paquet and Viktor, 2015). With these techniques there are temporal issues associated with the integration method resulting in a time step equivalent to or less than the particle relaxation time. Alternatively, (Minier, Peirano and Chibbaro, 2003) proposed a view which uses Ito calculus to derive a number of approximate solutions to particle transportation in varying time scale regimes, under certain constraints. If the time step is assumed greater than the particle Brownian relaxation time (Peirano *et al.*, 2006):

$$\tau_p = \frac{\rho_p}{\rho_f}\frac{4d_p}{3C_d|\boldsymbol{U_r}|} \qquad 6.3$$

Where ρ_p is the particle density, ρ_f is the fluid density, d_p is the particle diameter, C_d is the drag coefficient, a non-linear function of the particle's Reynolds number $Re = |\boldsymbol{U_r}|d_p/\nu_f$ (U_r is the instantaneous velocity which is $U_r(t) = U_p(t) - U_s(t)$ and ν_f is the fluid kinematic viscosity).

However, in a Stoke's regimes with small particles the following particle Brownian relaxation time can be seen to be equivalent to (Nelson and Ginn, 2005):

$$\tau_p = \frac{m_p}{6\pi\mu a_p} \tag{6.4}$$

Where m_p is the particle mass, μ is the dynamic fluid viscosity and a_p is the particle radius

Along with the assumption that the fluid flow field is deterministic, i.e. is in steady state. Then the following expression can be derived from the SDE (as previously utilised in Chapter 5):

$$x(t + \Delta t) = U_p(t) + U_s(\mathrm{t})\Delta t + B_x\sqrt{\Delta t}\,\xi_x \tag{6.5}$$

Where,U_p is the particle velocity, U_s is the fluid velocity, ξ_x a random number sampled from a zero-mean Gaussian distribution, B_x is the diffusion term ($\sqrt{\frac{k_B T}{6\pi\mu a_p}}$ where k_B is the Boltzmann constant and T temperature).

Further, the particle velocity is (Henry *et al.*, 2013):

$$U_p(t + \Delta t) = U_s(t) + B_x\sqrt{1/2\tau_p}\xi_v \tag{6.7}$$

Where ξ_v is a random number sampled from a zero-mean Gaussian distribution

Here it can be seen that the particle position is solely a function of the fluid velocity and Brownian fluctuation of the system. To resolve the fluid velocity of the system a lattice Boltzmann simulation is run until convergence (Chapter 4), this produces the

necessary flow field for the U_s term to be interpolated from. At convergence it is assumed that the flow field is steady state and as such deterministic or can be considered "frozen". As the lattice Boltzmann model is fixed to a discrete nodal grid, if the particle is based anywhere apart from on the node then the velocity value will need to be interpolated from the 4 nearest neighbours using a bi-linear interpolation technique (Gao *et al.*, 2008). It is assumed here that the particle-fluid interaction is one-way and as such the influence of the particles on the fluid is not important. This remains true for dilute concentrations, however, if the concentration increases then two-way coupling needs to be taken into account (Peirano *et al.*, 2006).

A suitable choice of time-step is also considered which maintains the integrity of the particle trajectory equation (6.5). However, the time-step should also maintain that the movement of the particle is not any greater than the grid size, otherwise overstepping may occur. To account for this the following time-step analysis is used:

$$U_{max}\Delta t + B_x\sqrt{\Delta t} \leq dx \qquad 6.8$$

Where U_{max} is the maximum fluid velocity, dx is the dimensionalised grid spacing.

Finally, it is worth noting that the model solely concentrates on translational motion and rotation is neglected. This is assumed as the particles modelled are idealised circles in 2D and as such rotation can be neglected. If non-circular geometries where being modelled the rotational behaviour of the particle would need to be accounted for.

6.22 Particle collision

Particle collision can be treated in two ways depending on the system being modelled. In the initial system in which a particle may collide with the surface of a collector and be deposited, this is assumed inelastic and as such the particle stays on the surface of the collector. In this case it is relatively simple to model and as such the deposited

particle becomes part of the surface. In the secondary case, where a site is already occupied then the collision is assumed elastic to reduce computation time. In this case the particle is treated as being reflected back into flow stream and either comes into contact with an unoccupied site or else exits the domain (Figure 6.1).

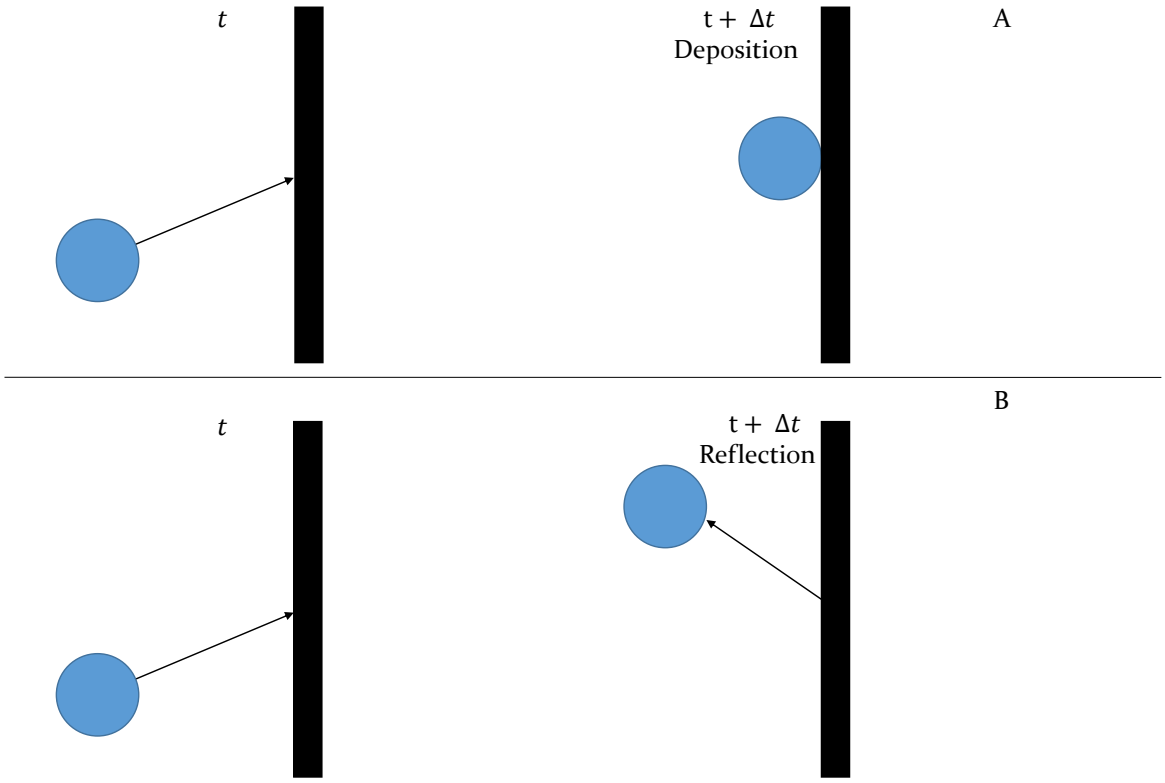

Figure 6.1 Behaviour of the particle at the wall depending on if the particle is being deposited (A) or being reflected (B).

In the case where multiple depositions can occur and growth can be instigated then the following situation is simulated:

$$E_k > E_{tot} : Deposition\ occurs$$
$$E_k < E_{tot} : Reflection\ occurs \qquad 6.9$$

Here the kinetic energy is derived from equation 6.5 and is compared to the value of the DLVO potential energy profile for particle-particle collisions or in the case where the wall is not assumed to be attractive the particle-wall equation (Chapter 2).

6.23 Modelling the domain using lattice Boltzmann

A lattice Boltzmann model was produced which modelled a single collector within the domain using the techniques described in Chapter 4. The domain consists of an inlet and outlet in the x direction and periodic boundaries in the y direction (Figure 6.2). The model is then run until the fluid is at steady state, at which point the model is then saved and exported as csv file to allow for faster modelling in later studies. The flow conditions are fixed such that the Re < 1, to capture creep flow. Thus the reference time in which a particle is within the regime if no collision occurs and the system is advective can be calculated as:

$$\tau_r = \frac{\delta x}{2U_{max}} \qquad 6.10$$

Where δx is the lattice spacing

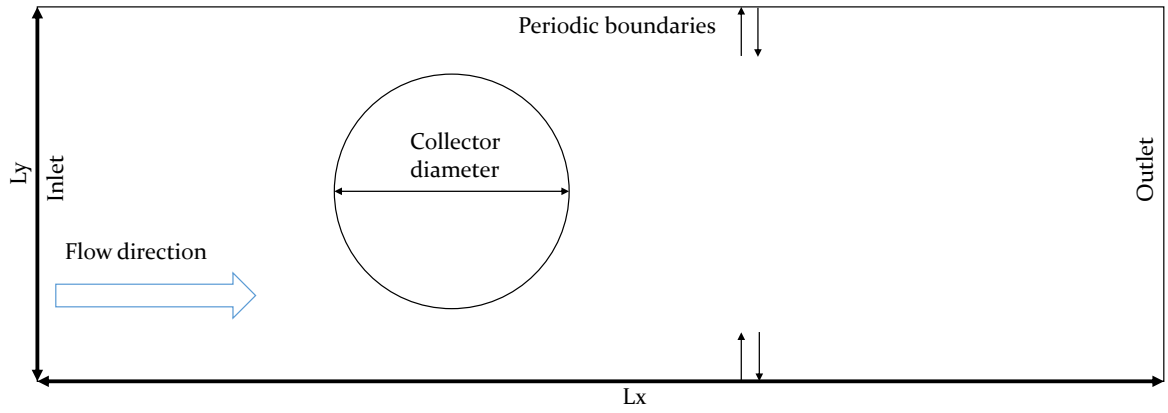

Figure 6.2 The domain setup for the lattice Boltzmann model

6.24 Modelling the particle transport in NetLogo

Due to the lattice Boltzmann model being based in LB units it is first required for the fluid velocity and the particle mesh size to be converted back into dimensionalised units. This allows for a suitable particle time step to be chosen which honours the criteria set out in equation 6.8. After this a single particle is modelled where x coordinate is set to 0 and the y co-ordinate is created using the random number generator in NetLogo. Once the particle has been created the particle trajectory algorithm is introduced and the particle is modelled under varying flow conditions. A new particle is generated when the current particle has either left the domain or else has been deposited upon the collector surface. This is run until the Nth particle has been modelled within the domain (Figure 6.3).

In the initial occupied site model, the particle is transported to surface of the collector and then a sub-routine checks to see if site is occupied. In terms of NetLogo this equates to the agent checking if patch ahead is occupied by another agent. If this is the case then another subroutine called reflection is run and the agent is reflected back into the flow. In the unlikely chance that a particle is produced which follows a streamline into the centre of the collector (Figure 6.4) and this site is already occupied then this agent is removed from the system straight away. This is to remove any likelihood of the reflection/SDE routine being caught in an infinite loop, though this should only occur during purely advective systems as within diffusive systems the particle should move away from the streamline over time.

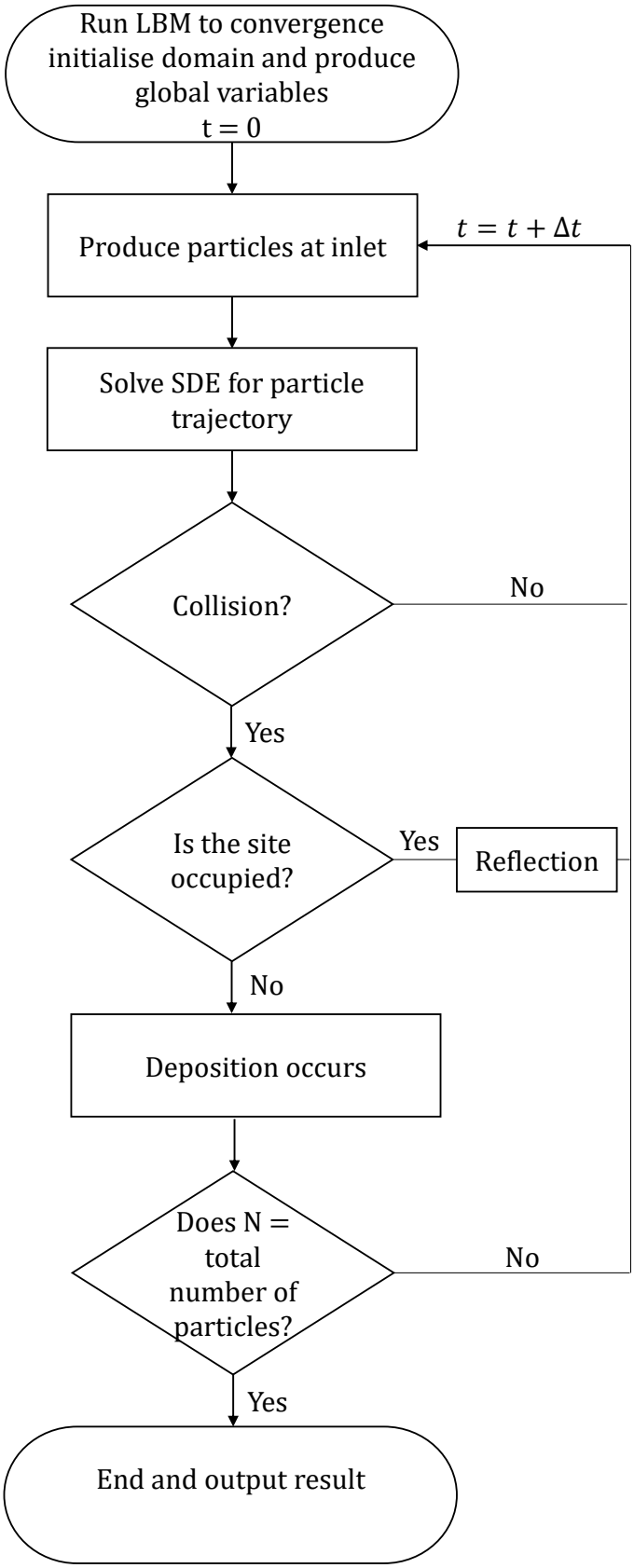

Figure 6.3 The programme schematic for implementing the particle trajectory and deposition in NetLogo for the occupied site model

For a collector which is not assumed attractive then a new sub-routine is used which checks the particles kinetic energy against the particle-collector potential energy (potential energy is calculated at the initialisation step). The criteria in equation 6.9 is evaluated and if the kinetic energy is not enough to overcome the potential barrier the reflection sub-routine is used. However, if the kinetic energy is greater than the potential energy barrier but the site is already occupied then once again the reflection sub-routine is utilised.

Finally, in the case of particle-particle deposition, potential energies are calculated at the initialisation step one for particle-wall interaction and the other for particle-particle interaction. In this case equation 6.9 is utilised in both and the particles are either deposited or reflected.

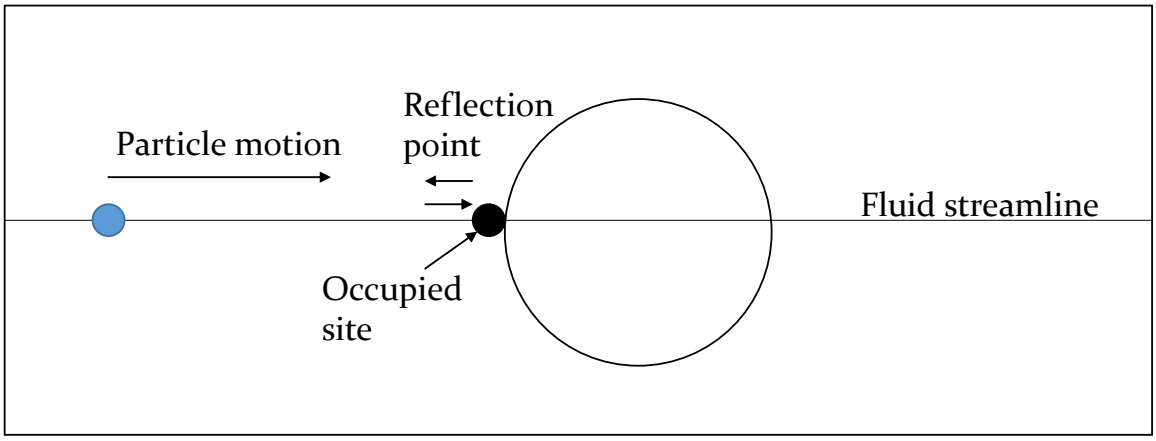

Figure 6.4 The possible infinite reflection of the particle on the horizontal streamline if the site is already occupied in the case of a purely advective system.

6.3 Deposition in attractive collector conditions and repulsive particle conditions and effect on collector efficiency

The first conditions to be tested within the NetLogo model is a variation in Peclet number as a function of the flow velocity along with particle size. Here, an infinite sink

model is used for when a particle collides with the collector surface, thus allowing for its removal from the domain and the successful trajectory is reported. After a large number of trajectories have been sampled, the collector efficiency can be estimated, here 6000 is used as both Nelson & Ginn (2005) describe this to be the necessary number of trajectories needed to estimate the collector efficiency.

Parameter	**Minimum value**	**Maximum**
Particle Size (a_p)	0.1 μm	2 μm
Fluid approach velocity (V_o)	1×10^{-6}m/s	1×10^{-3}m/s
Ionic strength (IS)	1 mMol	7 mMol
Temperature (T)	287K	300K

Table 6.1 The parameters used within the modelling to validate the NetLogo transportation model against the collector efficiency produced by Nelson & Ginn.

Table 6.1, shows the criteria set within the NetLogo model to analyse the collector efficiency of the system. This efficiency is then compared to the Smoluchwoski-Levich approximation of collector efficiency as described by Nelson & Ginn. In this case, the number of successful trajectories are compared to the particles sampled which allows for the collector efficiency to be calculated (Li, Xie and Ghoshal, 2015).

In the initial model the domain is set such that the collector has a diameter $100 \cdot d_p = 100\mu m$, each patch within NetLogo has a length of $1d_p = 1\mu m$ with the total domain length $120 \cdot d_p = 120\mu m$. The time step (Δt) is varied between 0.1 and 0.001 to ensure that a large enough number of trajectories were captured in each simulation whilst also maintaining the criteria set in equation 6.8. Finally, the vertical boundaries are set to periodic to capture an infinite flow field in the y-direction. The inlet and outlet are set

at a constant pressure gradient to capture the flow dynamics of the system and to ensure that the flow does not exceed a Re of 1.

The collector efficiency is calculated using the following equation:

$$Collector\ efficiency = \frac{successful-trajectories}{N} \quad 6.11$$

Where N is the total number of particles in the system

Flow Number	Flow Velocity (m/s)	Peclet Number
1	1×10^{-3}	1024.6
2	1×10^{-4}	102.5
3	1×10^{-5}	10.3
4	1×10^{-6}	1.03

Table 6.2 Variation of Peclet numbers transitioning from advective to diffusive with a particle radius of 0.5μm

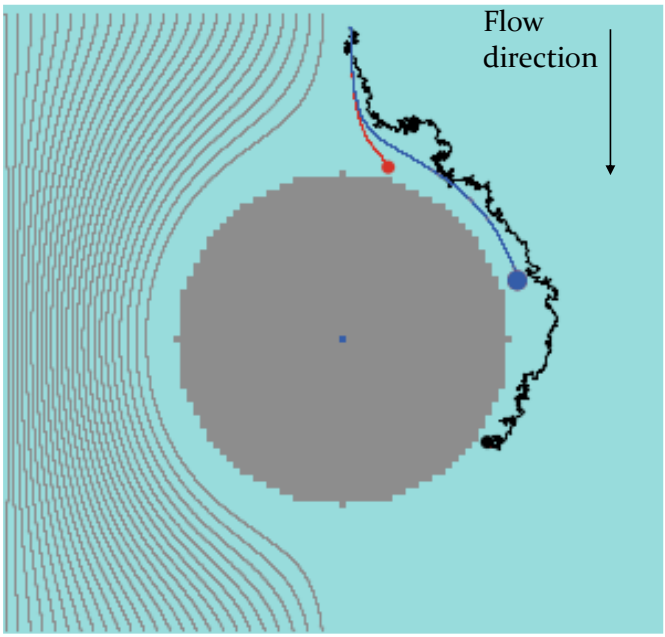

Figure 6.5 Trajectories of particles and interception of particles due to diffusion (black), interception (blue), and gravity (red) with the fluid streamlines shown in grey for reference.

The various mechanisms in which a particle can interact with the collector is show in Figure 6.5, where it can be seen that the when the flow is strongly advective then particle sticks to the streamlines and interception due to size is the dominating mechanism. In comparison, when the flow is approaching a Pe = 1, then the particle undergoes advective-diffusive behaviour and only follows the streamlines loosely and as such can deposit much further along the collector surface. Finally, if the dominating mechanism is gravitational then the particle rapidly diverges from the idealised flow lines to deposit onto the collector surface (Figure 6.5).

After the infinite sink model, deposition conditions are kept constant and single layer deposition is modelled; this is analogous to the Langmuir deposition described earlier. Furthermore, modelling the particles singularly is analogous to a dilute flow and allows for surface coverage to be analysed in more detail.

There is a significant change in deposition locations between a system which is diffusion dominated and that of one which is dominated by advection. In the case of diffusion dominated deposition, the collector surface is more evenly spread as particles have the opportunity to interact more frequently with the collector surface, irrelevant of their initial position when entering the system (Figure 6.6A). Whereas, when advection is the dominating condition, particles are limited in their interactions with the collector, only a narrow concentration of particles occupy the relevant flow fields for successful collision to occur with the collector surface. In this case, deposition occurs around the stagnation point in which the controlling force rapidly changes from the advection to diffusion. This process can be seen in figure 6.6B where the majority of deposition occurs around the stagnation point, any particles which cannot find an unoccupied deposition point are then captured by the flow field and removed from the system.

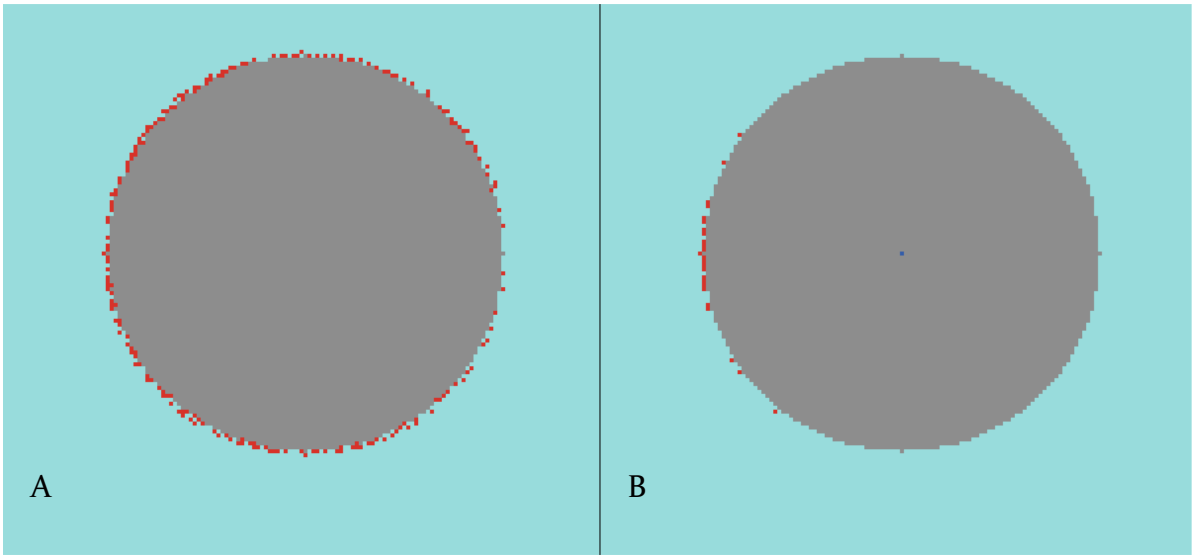

Figure 6.6 The deposition of the particles on the collector surface as a function of diffusive behaviour (A) and advective diffusive behaviour (B)

To capture the process of particle interception with the collector surface it is common to use the collector efficiency (You-Im and Jue-Joan, 1999). This efficiency is dependent on the number of forces in which the particle is being subjected too. Commonly these forces are gravitational, inertial, and diffusion where depending on the particle and flow conditions individual forces can be considered "switched off" (Long and Hilpert, 2009). In the case of small particle sizes gravitational and inertial forces become secondary to diffusive forces and the collision efficiency is reasonably high (c. 40%), in comparison when only inertial forces are implemented the collision efficiency rapidly decreases to >5%. Finally, as the particle size is increased alternative mechanisms come into play, in particular, interception where particles are large enough to come into contact with the collector surface. Furthermore, gravitational effects also come into place and as such particles are more likely to deviate away from the streamlines and come into contact with the collector surface, as shown in figure6.6B in which the collision efficiency can be seen to be approaching c.60%.

Analytical solutions exist within the literature to compare collector efficiencies against, when the results from the NetLogo model are compared against the Nelson and Ginn (2005) solution there can be seen to be a good relationship at smaller particle sizes, however, as larger particle sizes are introduced the collision efficiency starts to deviate, which can be seen to show a slower increase than predicted by the Nelson and Ginn solution (Figure 6.6A). This is due to the lack of a gravitational term incorporated in the trajectory equation (equation 6.6). When the gravitational term is included within the model it can be seen that the collision efficiency adheres to the analytical solution (Figure 6.6B).

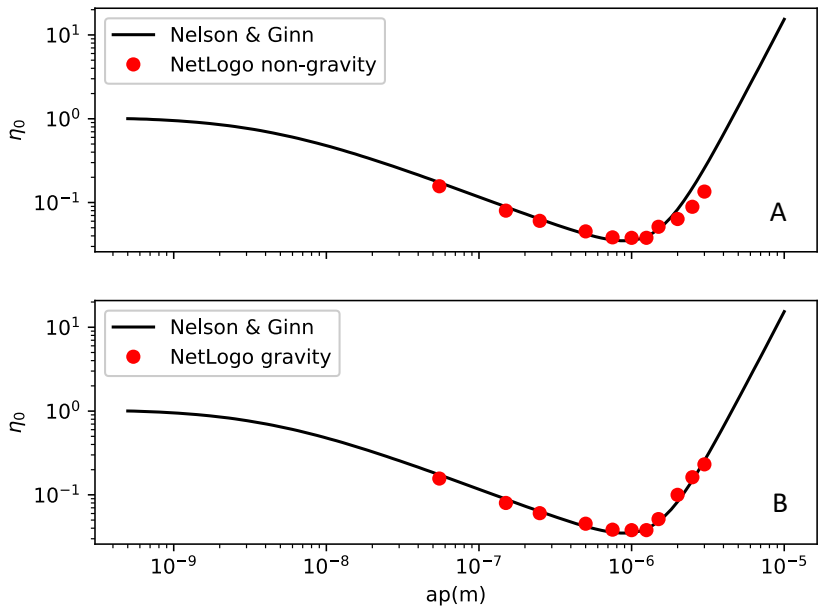

Figure 6.7 A) NetLogo collision efficiency compared to the analytical solution derived by Nelson & Ginn without a gravity term B) Collision efficiency with gravity term incorporated in the particle trajectory equation $\left(F_g = \frac{(\rho_p - \rho_f)g}{9\mu U}\right)$

Sensitivity of the surface collector coverage to Peclet number shows that as the transition between advection to diffusion becomes pronounced the total available sites occupied by particles increases significantly (Figure 6.8). Transitioning from an

advective-diffusive system to an advective system can be seen to have a significant influence on the likelihood of a deposition taking place and as a consequence of this the surface coverage is reduced from c.70% in a diffusion dominated environment to >5% in advection. Indeed, even in the change from a Pe ≅ 1 to Pe ≅ 10, there is a significant reduction in coverage of the collector. This is indicative of the importance of flow conditions on the deposition of particles within the domain. This also concurs with the results of collector efficiencies within the literature, in which the likelihood of a collision occurring is dependent on the flow velocity. As previously discussed, this is a consequence of particle adherement to the streamlines in highly advecting flows, and as flow velocity reduces the likelihood of particles transferring between streamlines is increased as shown in the exponential decrease in figure 6.8.

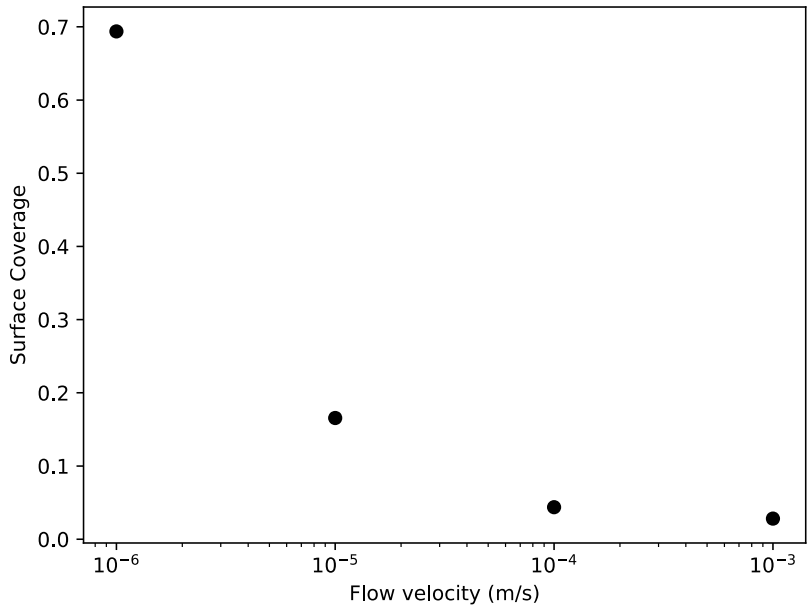

Figure 6.8 Surface coverage of single layer deposits as a function of flow velocity in an attractive system

6.4 Sensitivity of attachment efficiency and surface coverage due to variations in surface chemistry at varying flow conditions for particle size of 0.5 µm

There are two primary mechanisms associated with particle deposition, firstly particle transportation to the collector surface, and secondly the deposition of the particle onto the surface of the collector is controlled both by hydrodynamic forces and chemical forces (Henry, Minier and Lefèvre, 2012). In particular, the surface chemistry between the particle and collector surface is usually simplified using the DLVO equation (discussed in Chapter 2). The accumulation of both the transportation step and the attachment efficiency once the particle reaches the surface, can be extrapolated out for the full porous media using the following equation (Tufenkji, 2007):

$$\eta = \eta_0 \alpha \qquad 6.12$$

Where η_0 is the single collector efficiency and α is the attachment efficiency between the particle and the collector surface.

Recently, it has been shown that the standard approach to understanding attachment efficiency between colloidal particles and the collector surface significantly underestimates the amount of retained particles (Tosco, Tiraferri and Sethi, 2009). Indeed, using standard DLVO equations the primary mechanism for deposition is particle capture within the primary well. However, by solving the standard sphere-sphere DLVO equation using the Derjaguin approximation (Chapter 2) the necessary kinetic energy to overcome the potential barrier is large (c. 1000 KbT) for some solution chemistries. In this case, using particle trajectory techniques and modelling this behaviour results in no particles being deposited on the collector surface. Experimental models show that this is not the case and particle retention is observed (Tosco, Tiraferri and Sethi, 2009). It is now understood that this mechanism is a consequence of the

secondary minima, as such, particles are being deposited onto the surface of the collector even when the potential barrier is high, to model this the DLVO equations can be used and the secondary minima depth can be extracted.

Within NetLogo the deposition mechanism and location of particles within the primary and secondary minima can be accounted for by using a simple logic statement:

$$E_{tot} \geq E_k : Secondary\ Minimum\ attachment$$

$$E_{tot} \geq E_k : Primary\ minimum\ Attachment$$

$$E_{tot} > Ek > Sec_{well} : Reflection$$

The kinetic energy of the particle is calculated using equation 6.6. The surface energy is explicitly calculated using the well depths described by Tosco *et al*, 2009 and deposition is assumed to have occurred if the particle is located either within the secondary or primary minima. Commonly, Lagrangian particle tracking explicitly calculates all the forces applied to the particle, including the van Der Waals and electrostatic forces. However, these forces are only significant at small spatial scales i.e. nm range, as such, within the NetLogo model the above criteria is only calculated when the particle is within a set distance from the collector surface. This is assumed appropriate due to the spatial scale chosen within the modelling domain, as each patch within the domain is assumed to be 1μm². In this case, it is assumed that particle-collector collision occurs instantaneously. This method of interaction was previously validated in Chapter 5 for particle-particle aggregation.

The attachment efficiency within the model can be calculated by using the following equation:

$$\alpha = \frac{successful\ collision}{unsuccessful\ collisions} \qquad 6.13$$

The particle radius is set to 1μm and the temperature is 297.15K using this along with the Stokes-Einstein equation gives a diffusion coefficient $2.44x10^{-13}$ m^2/s. The Peclet number is produced using equation 6.1 and the full modelling conditions are shown in table 2. Varying the Peclet number from ~1 to ~1000, there can be seen a transition from extremely advective to diffusive behaviour. The surface chemistry of the system is calculated by varying the ionic strength and using the data provided by Tosco *et al* (2009).

Ionic strength(mMol)	**Primary height (kBT)**	**Secondary minima depth (kBT)**
1	2549	0
3	2327	-0.6
10	1887.2	-2.3
30	1310.7	-8.2
100	400.4	-32.6

Table 6.3 Primary barrier height and secondary minima depth dependence on Ionic strength taken from Tosco et al, 2009.

In the initial model the domain is set such that the collector has a diameter $50 \cdot d_p = 100\mu m$, each patch within NetLogo has a length of $1d_p = 2\mu m$ with the total domain length $120 \cdot d_p = 200\mu m$. The minimum time step (Δt) is set to 0.001 which allows for the criteria of equation 6.8 to be met, for diffusive behaviour the time step is increased to 0.1 to ensure that the number concentration of particles within the system is comparable. Finally, the vertical boundaries are set to periodic to capture an infinite flow field in the y-direction. The inlet and outlet are set at a constant pressure gradient

to capture the flow dynamics of the system and to ensure that the flow does not exceed a Re of 1.

Though the influence of the secondary minima cannot be neglected it can be seen that for low ionic strengths it does not, or exists at a significantly reduced depth (Table 6.3), furthermore, the height of the primary barrier can be seen to be large and as such in this condition particles would be reflected back into the flow stream and significant breakthrough would occur. However, at high ionic strengths the depth of the secondary minima barrier is important, at an I = 3mMol there can be seen to be a large primary minimum barrier (c.2327 kBT) and a small secondary minima well depth (-0.6 kbT). When this system was modelled it can be seen that for flow regimes with a high Peclet number the deposition likelihood within the minima is reduced, this is due to the a limited number of particles coming into contact with the necessary kinetic energy. In this case, when a particle is approaching the collector surface and is not on a direct collision course then the kinetic energy is larger than the secondary minima barrier. In comparison, for a low Peclet number system there can be seen to be a greater percentage of successful deposits in the secondary minima (>35%), indicating that a larger number of particles do not have sufficient energy to overcome the secondary minima. Though not tested here, the residence time of particles within the secondary minima has been tested in previous studies (Kovalchuk *et al.*, 2008)and shows that for such a weak secondary minima depth even diffusion deposited particles would rapidly escape due to the thermal excitation and secondary collisions. Hence, the reason why secondary deposition is considered reversible and particles captured within the secondary minima can be removed.

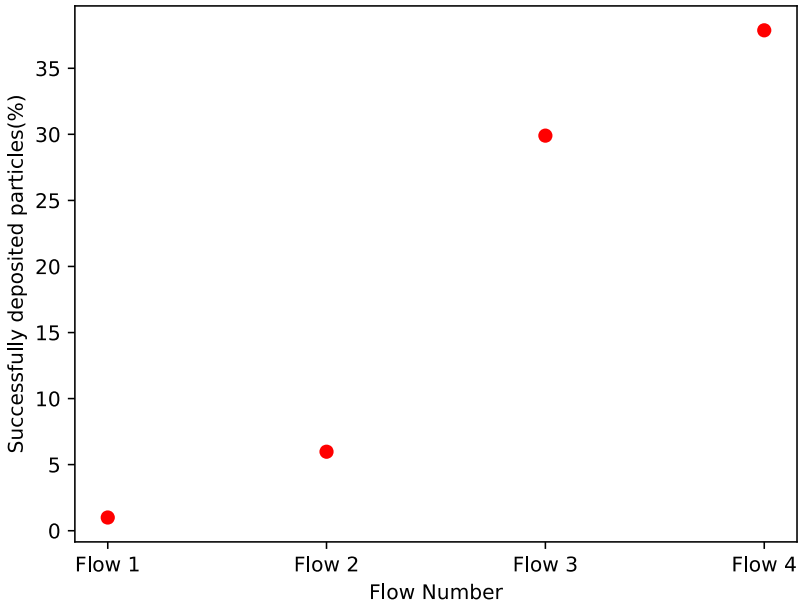

Figure 6.9 Number of successfully deposited particles in a secondary minima depth of -0.6 kBT

In comparison to the low well depth of I = 3mMol, the well depths of I = 10, 30, 100 are significantly deeper indicating that particles captured within these secondary minima are more likely to remain captured. When a diffusive system is studied Pe ≅ 1, then the likelihood of any particles having sufficient energy to escape the secondary minima decreases, particularly, for the well depths of 30mMol and 100mMol which equal -8.2 kBT and -32.6 kBT, respectively. This is shown in figure 6.10, where the number of successful particle deposits can be seen to be 100% for these ionic strengths indicating that the particles are more easily captured. With the ionic strength of 10mMol there is a successful capture of c.80% indicating that some particles had significant energy to overcome the secondary minima depth of c.-2.3 kBT, this is reasonable to assume as the thermal excitation of the particles is commonly modelled as a normal distribution (and is modelled as such within the NetLogo model) as such there is a probability that particles exhibit a kinetic energy of > 2.3 kBT. Whereas for higher ionic strengths it is unlikely for these particles to have sufficient thermal excitation. Tosco *et al* (2009),

found that there was a significant change in particle breakthrough time depending on the ionic strength of the system, for lower ionic strengths breakthrough was almost instantaneous, implying as found with the NetLogo model that particles were being reflected by the collector. In comparison, for lower ionic strengths the particles were being released much later as a function of collision or thermal excitation, also in agreement with the results from the NetLogo model.

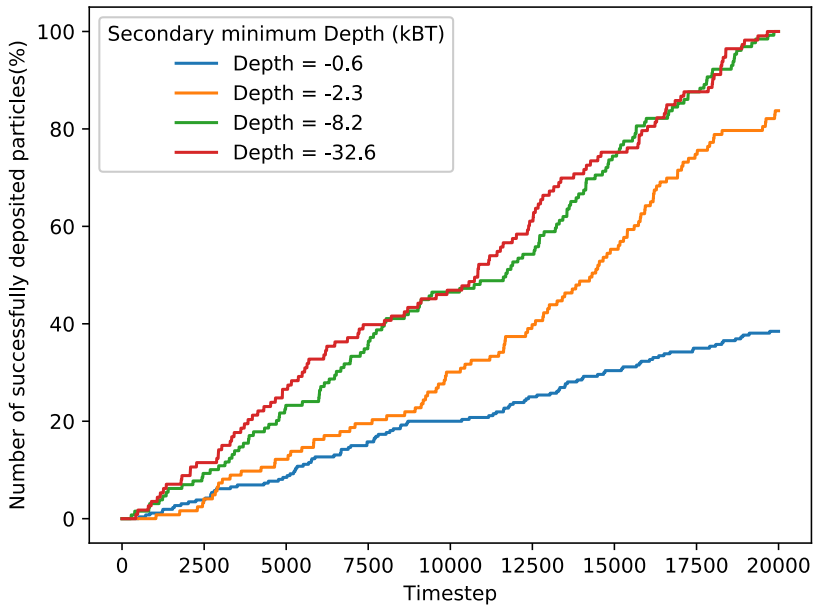

Figure 6.10 The percentage of successful deposited particles in the secondary minima and diffusion dominated flow field (1x10-6 m/s)

6.5 Growth size of deposited particles in varying particle-particle surface chemistry and attractive particle-wall surface chemistry in diffusive and advective regimes

In the two previous case studies, emphasis was placed upon the collector-particle interactions by analysis of the transportation of particles or subsequent surface deposition. In both of these cases the particle-particle deposition case was ignored, which is assumed for highly repulsive interaction chemistry. In reality, the growth on the collector surface is the dominating mode of particle removal in the system (Henry,

Minier and Lefèvre, 2012). Furthermore, the growth mechanism can be seen as entering a later stage of deposition in which the collector is said to be undergoing ripening (Gitis *et al.*, 2010). In this case, the breakthrough of the particles is significantly reduced. However, there are some caveats to this system the attachment efficiency of particle deposition onto an already deposited particle is subject to the same surface chemistry conditions as the previous case study, i.e. modelled via the DLVO equation.

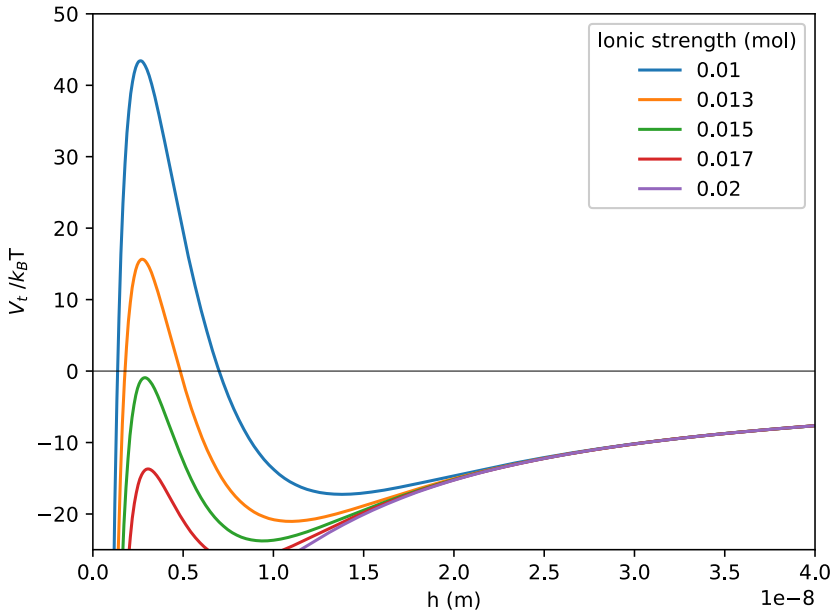

Figure 6.11 DLVO profiles for sphere interactions as a function of Ionic strength with the potential energy barrier shown

Modelling of these dendrite growths on the collector surface are particularly important for understanding the clogging mechanism of the whole porous media. As these growths increase in size the likelihood of clogging of the pore space also increases. In turn, this means that oversaturation of the porous media may occur. In the simplified case where it is assumed that if a deposition occurs, the particle is placed within the primary minimum and as such is irreversibly bound this results in a redistribution of the flow through the bed. However, in the secondary minima case where particles are

not irreversibly bound, there is a greater chance for the pressure build up caused by the clogging to incur mass re-entrainment with the final consequence of complete breakthrough.

This is the simplified case and as such emphasis is placed on the build-up of dendrites on the collector surface, the secondary minima effects will be neglected and only primary minimum deposition will be studied. In this case the following modelling conditions have been chosen, again polystyrene latex has been chosen has the particle with a particle radius set at 0.5μm. The domain size is set such that the collector has a diameter $50 \cdot d_p = 50\mu m$, each patch within NetLogo has a length of $1d_p = 1\mu m$ with the total domain length $120 \cdot d_p = 60\mu m$. With once again the time step being set to ensure that equation 6.8 is always met ensuring that particles cannot "jump" over each other. To calculate the DLVO energies of the system the ionic strength is set assuming NaCl and the zeta potentials are calculated using the interpolation method produced by Behrens *et al.*(2000). Finally, successful collisions are assumed if the following criteria is met:

$$E_{tot} \geq E_k : Primary\ minimum\ Attachment$$

The size of the dendrites is calculated simply by asking the primary deposited particle (particle deposited on collector surface) to count the number of particles associated to itself. Within NetLogo this is achieved using a recursive procedure which ensures that all particles associated with an initially deposited particle are accounted for accurately. To test the growth of dendrites on likelihood of pore blocking the y-axis boundary conditions are set to periodic which allows for an evenly spaced infinite pore space to be modelled. Finally, simulations are run until a chosen number concentration of particles have passed through the domain to allow for comparison between different flow conditions.

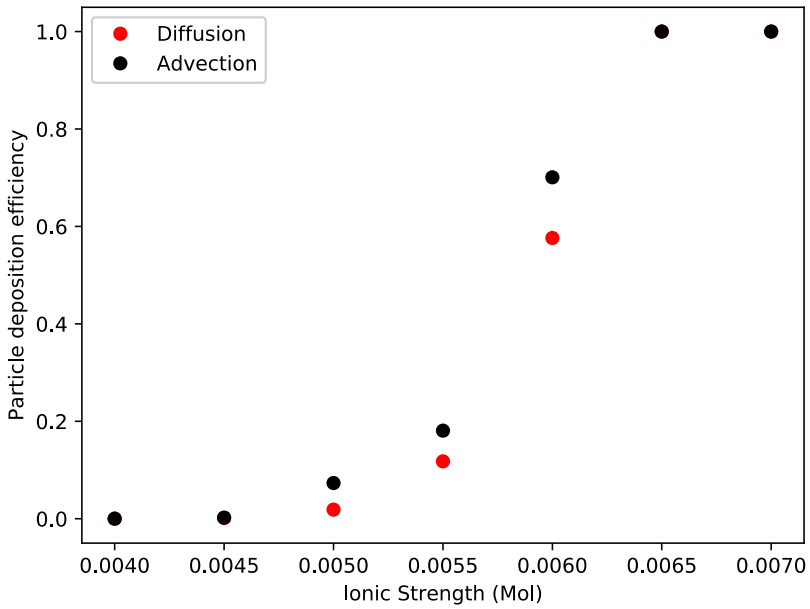

Figure 6.12 Stability ratio of particles dependent on flow velocity with Pe = 1.03 and Pe = 1023 showing advection and diffusion respectively

To model the stability of the system, the ionic strength was varied resulting in highly repulsive to highly attractive conditions between particles (Figure 6.12). To reduce the complexity within the system it is assumed that any particle which interacts with the surface of the collector is deposited in the primary minimum. As such, the interaction mechanism focused on here is particle-particle collision. The stability ratio can be seen to be influenced by the flow velocity, Figure 6.12. The number of successful collisions due to ionic strength can also be seen to be sensitive to the flow conditions. The deciding factor when dealing with these systems is dependent on the kinetic energy and as such higher flow velocities result in greater collision energies. The rate at which particle-particle deposition can also be seen to be significantly influenced by flow velocity, in the case of the advection dominated flow there is a much more rapid increase in particle deposition when compared to that of the diffusion dominated flow. This is due to later deposited particles having a greater kinetic energy as they are

deposited in an area of greater flow rate, in comparison to the initially deposited particles.

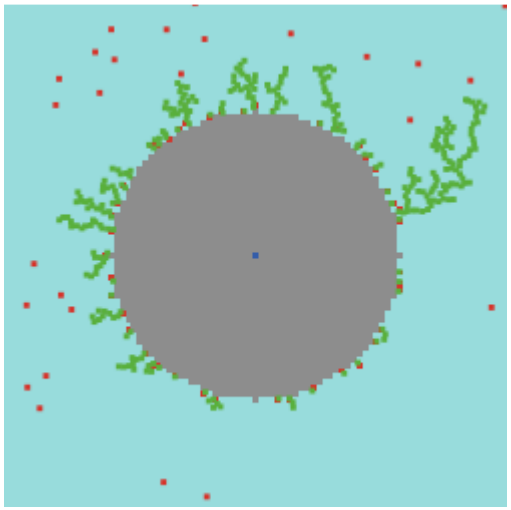

Figure 6.13 Large dendrite growth on the surface of the collector in a diffusion dominated domain

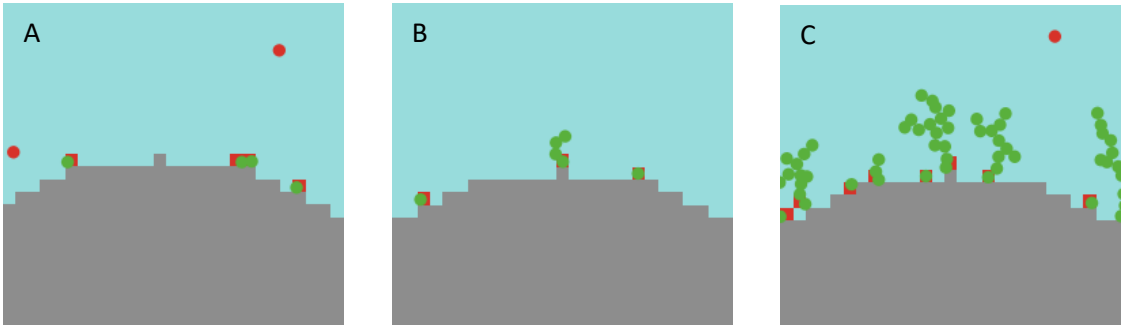

Figure 6.14 Growth of dendrites on collector surface at different particle-particle surface chemistry regimes; Repulsive (A), Reduced Attractive (B), Attractive (C)

When particle-particle system is highly repulsive it can be seen that apart from the initial deposition on the collector surface, all other particles are removed from the system, in this case only a single layer of deposited particles are produced (figure 6.14A). When particle-particle interaction is predominately attractive the number of particles which are removed from the system are significantly increased, in particular, particles which would not usually come into contact with the collector surface are

captured by the dendrite growths from the surface of the collector (Figure 6.13). This process can be seen in figure 6.14, where the growth of dendrite can be seen to be affected by the chemistry of the system, in relation to maximum growth size the more attractive the larger the dendrite growth (figure 6.14C)

Thus, as ionic strength is increased within the system the breakthrough number is reduced. This is a consequence of the high ionic strength as particles are more likely to successfully deposit on previously deposited particles. When coupled with low flow velocities the particles have a greater amount of time within the pore structure to come into contact with the dendrite growths and are captured more easily (Figure 6.13).

Finally, the sensitivity of the dendrite size can be seen to be influenced by both the flow regime along with the chemistry of the system (Figure 6.15). At lower ionic strengths the likelihood of successful collision is muted, however, at the transition zone from repulsive the likelihood of successful collision increases. In the case of Pe ≅ 1, there is a lag in growth at an ionic strength of 0.06 mol, in comparison, to the advective flow Pe ≅ 1000, indicating that the advecting particles have greater kinetic energy than that of the diffusing particles. However, when the system is purely attractive there can be seen to be a limit to the growth size of the particles within an advection dominated regime, this is due to the number of available sites for initial deposition to occur. As such, the number of dendritic growths are limited. Further, even within transition regimes (Pe approaching 1) there are a limit to number of initial seeding points for dendrite growth. As particles deposit and dendrites start to grow, shadow zones form behind the growth in which particle deposition is reduced. In the case of diffusion, this is slightly offset by the ability of the particles diffuse more readily through the system (Figure 6.16). However, in the case of the alternative flow regimes this significantly reduces anymore growth on the collector surface (Figure 6.17). The rate of the dendrite

growth increases rapidly once it gets beyond more than two particles as the likelihood of capture increases irrelevant of the system chemistry.

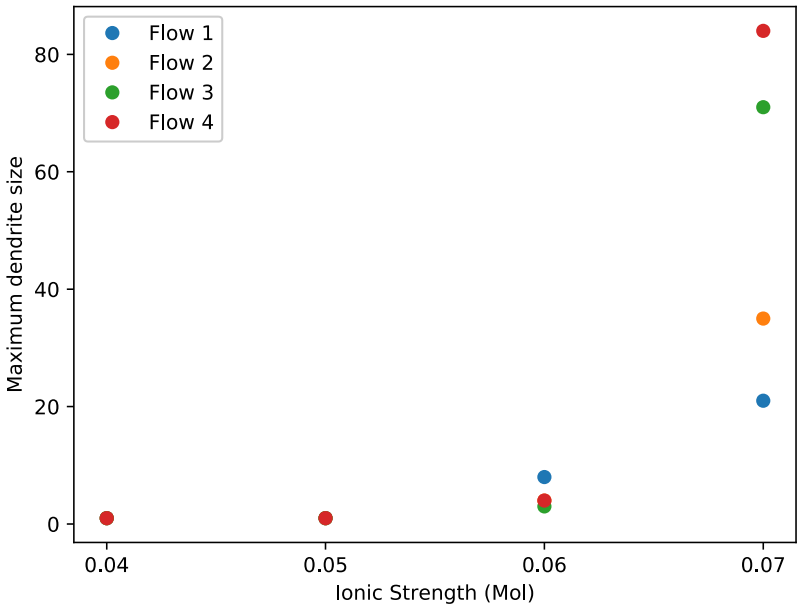

Figure 6.15 Dendrite size sensitivity dependent on ionic strength and flow velocity

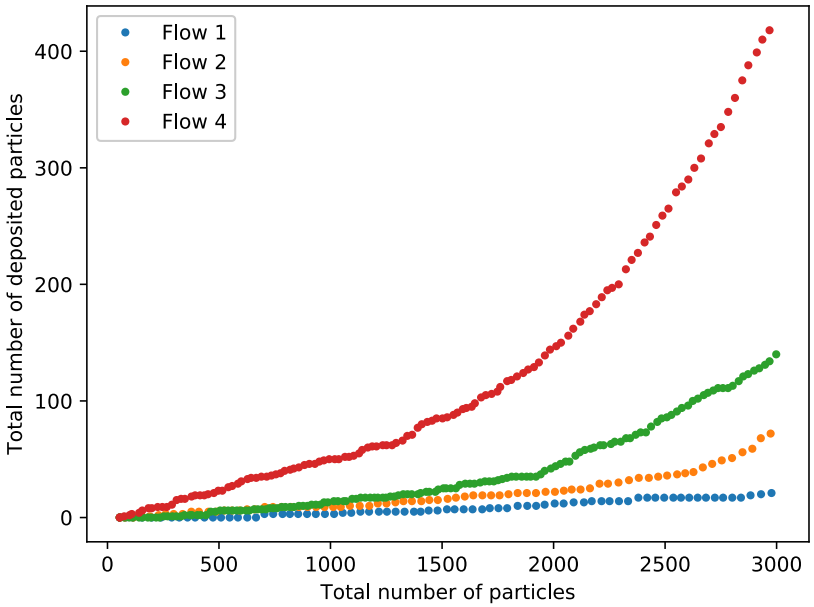

Figure 6.16 Deposited number of particles in purely attractive regime for varying flow conditions

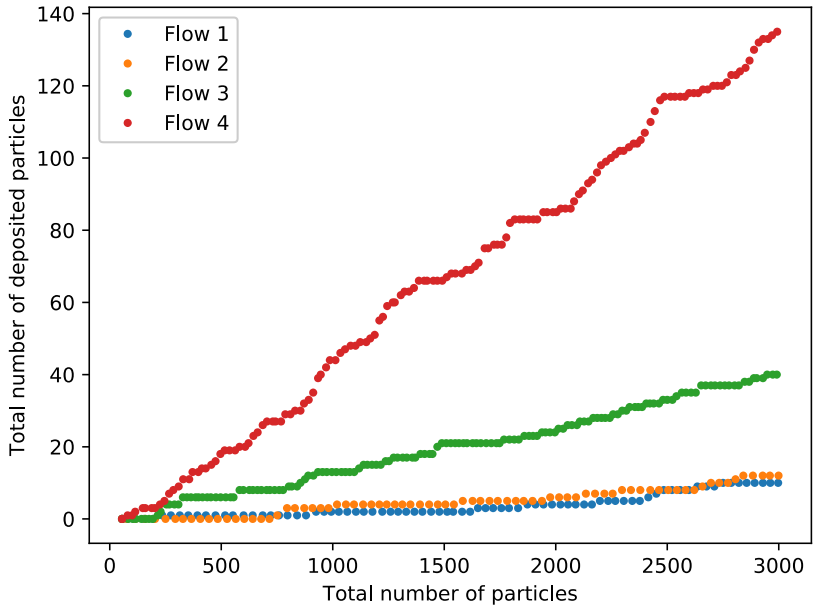

Figure 6.17 Deposited number of particles in a repulsive regime for varying flow conditions

6.6. Conclusions

Behaviour of particles around a single collector within varying flow environments was captured using the NetLogo modelling suite. It can be seen that the model accurately captures transportation to the surface of the collector, when compared to the collector efficiency produced by Nelson and Ginn there is a good agreement between the NetLogo efficiency and their efficiencies. Furthermore, it is understood that the likelihood of deposition upon the collector surface is unlikely within the primary minima as predicted by the DLVO theory, however, breakthrough experiments regularly find that particles still attach even under traditionally highly repulsive environments. Here it can be seen that this deposition is a function of the secondary minima depth, the model presented here captured the likelihood of deposition within the secondary minima for a number of different well depths.

With low flow environments in which the system is transitioning from advective to diffusive, particles are captured within shallow secondary minima well depths, though this is not irreversible as the diffusive behaviour of the particles along with collisions with incoming particles may result in sufficient energy to escape. As the ionic strength is increased the secondary well depth also increases and it can be understood that the likelihood of particles being captured even for higher flow velocities increased significantly, conforming to experimental observations found within the literature.

Particle-particle deposition is inherently sensitive to changes in surface chemistry within the system resulting in the number of deposited particles varying significantly. In particular, in low ionic strength environments particle-particle deposition was reduced, this can also be observed within the literature for flow through experiments in porous media.

Finally, the NetLogo model along with the lattice Boltzmann model can be seen to accurately portray the transportation and deposition of colloidal particles in simple fluid systems. This shows that by using agent based modelling alternative routes can be taken in studying and understanding colloidal depositions. Furthermore, by using this “rule” based method changes in the environment can be rapidly undertaken without the need for any additional changes to the fundamental system.

6.7 References

Auset, M. and Keller, A. A. (2006) 'Pore-scale visualization of colloid straining and filtration in saturated porous media using micromodels', *Water Resources Research*, 42(12), pp. 1–9. doi: 10.1029/2005WR004639.

Behrens, S. H. *et al.* (2000) 'Charging and Aggregation Properties of Carboxyl Latex Particles: Experiments versus DLVO Theory', *Langmuir*, 16(6), pp. 2566–2575. doi: 10.1021/la991154z.

Dagaonkar, M. and Majumdar, U. (2018) 'Effect of Fluid Flow, Solution Chemistry and Surface Morphology of Fibrous Material on Colloid Filtration', *Journal of Engineered Fibers and Fabrics*, 7(3), p. 155892501200700. doi: 10.1177/155892501200700309.

Elimelech, M. and O'Melia, C. R. (1990) 'Kinetics of Deposition of Colloidal Particles in Porous Media', *Environmental Science and Technology*, 24(10), pp. 1528–1536. doi: 10.1021/es000080a012.

Gao, H. *et al.* (2008) 'Modelling microscale flow and colloid transport in saturated porous media', *International Journal of Computational Fluid Dynamics*, 22(7), pp. 493–505. doi: 10.1080/10618560802238259.

Gitis, V. *et al.* (2010) 'Deep-bed filtration model with multistage deposition kinetics', *Chemical Engineering Journal*. Elsevier B.V., 163(1–2), pp. 78–85. doi: 10.1016/j.cej.2010.07.044.

Henry, C. *et al.* (2013) 'A new stochastic approach for the simulation of agglomeration between colloidal particles', *Langmuir*, 29, pp. 13694–13707. doi: 10.1021/la403615w.

Henry, C., Minier, J. P. and Lefèvre, G. (2012) 'Towards a description of particulate fouling: From single particle deposition to clogging', *Advances in Colloid and Interface*

Science, 185–186(October), pp. 34–76. doi: 10.1016/j.cis.2012.10.001.

Ko, C.-H., Bhattacharjee, S. and Elimelech, M. (2000) 'Coupled Influence of Colloidal and Hydrodynamic Interactions on the RSA Dynamic Blocking Function for Particle Deposition onto Packed Spherical Collectors', *Journal of Colloid and Interface Science*. Academic Press, 229(2), pp. 554–567. doi: 10.1006/JCIS.2000.7062.

Kovalchuk, N. *et al.* (2008) 'Colloidal dynamics: Influence of diffusion, inertia and colloidal forces on cluster formation', *Journal of Colloid and Interface Science*, 325(2), pp. 377–385. doi: 10.1016/j.jcis.2008.06.017.

Kuznar, Z. A. and Elimelech, M. (2007) 'Direct microscopic observation of particle deposition in porous media: Role of the secondary energy minimum', *Colloids and Surfaces A: Physicochemical and Engineering Aspects*, 294(1–3), pp. 156–162. doi: 10.1016/j.colsurfa.2006.08.007.

Li, J., Xie, X. and Ghoshal, S. (2015) 'Correlation Equation for Predicting the Single-Collector Contact Efficiency of Colloids in a Horizontal Flow', *Langmuir*, 31(26), pp. 7210–7219. doi: 10.1021/acs.langmuir.5b01034.

Li, Y. *et al.* (2017) 'Colloidal Particle Deposition in Porous Media Under Flow : A Numerical Approach To cite this version : HAL Id : hal-01636813 Colloidal particle deposition in porous media under flow : A numerical approach'.

Li, Y. *et al.* (2018) 'Three-dimensional microscale simulation of colloidal particle transport and deposition in model porous media with converging/diverging geometries', *Colloids and Surfaces A: Physicochemical and Engineering Aspects*. Elsevier, 544(December 2017), pp. 179–186. doi: 10.1016/j.colsurfa.2018.02.034.

Long, W. and Hilpert, M. (2009) 'A correlation for the collector efficiency of Brownian particles in clean-bed filtration in sphere packings by a Lattice-Boltzmann method',

Environmental Science and Technology, 43(12), pp. 4419–4424. doi: 10.1021/es8024275.

Ma, H. *et al.* (2009) 'Hemispheres-in-Cell Geometry to Predict Colloid Deposition in Porous Media', *Environmental Science & Technology*. American Chemical Society, 43(22), pp. 8573–8579. doi: 10.1021/es901242b.

Minier, J.-P., Peirano, E. and Chibbaro, S. (2003) 'Weak first- and second-order numerical schemes for stochastic differential equations appearing in Lagrangian two-phase flow modeling', *Monte Carlo Methods and Applications*, 9(2). doi: 10.1515/156939603322663312.

Nelson, K. E. and Ginn, T. R. (2005) 'Colloid filtration theory and the happel sphere-in-cell model revisited with direct numerical simulation of colloids', *Langmuir*, 21(6), pp. 2173–2184. doi: 10.1021/la048404i.

Paquet, E. and Viktor, H. L. (2015) 'Molecular Dynamics, Monte Carlo Simulations, and Langevin Dynamics: A Computational Review', *BioMed Research International*. Hindawi, 2015, pp. 1–18. doi: 10.1155/2015/183918.

Peirano, E. *et al.* (2006) 'Mean-field/PDF numerical approach for polydispersed turbulent two-phase flows', *Progress in Energy and Combustion Science*, 32(3), pp. 315–371. doi: 10.1016/j.pecs.2005.07.002.

Saiers, J. E., Hornberger, G. M. and Liang, L. (1994) 'First- and second-order kinetics approaches for modeling the transport of colloidal particles in porous media', *Water Resources Research*. John Wiley & Sons, Ltd, 30(9), pp. 2499–2506. doi: 10.1029/94WR01046.

Shen, C. *et al.* (2010) 'Predicting attachment efficiency of colloid deposition under unfavorable attachment conditions', *Water Resources Research*. John Wiley & Sons, Ltd, 46(11). doi: 10.1029/2010WR009218.

Tosco, T., Tiraferri, A. and Sethi, R. (2009) 'Ionic Strength Dependent Transport of Microparticles in Saturated Porous Media: Modeling Mobilization and Immobilization Phenomena under Transient Chemical Conditions', *Environmental Science & Technology*. American Chemical Society, 43(19), pp. 7592–7593. doi: 10.1021/es902084v.

Tufenkji, N. (2007) 'Modeling microbial transport in porous media : Traditional approaches and recent developments', 30, pp. 1455–1469. doi: 10.1016/j.advwatres.2006.05.014.

Tufenkji, N. and Elimelech, M. (2004) 'Correlation Equation For Predicting Single-Collector Eficiency in Physiochemical Filtration in Saturated Porous Media', *Environmental Science & Technology*, 38(2), pp. 529–536. Available at: http://pubs.acs.org/doi/abs/10.1021/es034049r.

You-Im, C. and Jue-Joan, W. (1999) 'Particle deposition behavior simulated by the stochastic method', *Journal of Petroleum Science and Engineering*, 22(1–3), pp. 189–203. doi: 10.1016/S0920-4105(98)00068-0.

Chapter 7. Conclusions and further work

The original aim of this thesis was to analyse the use of agent based modelling as an alternative way to further understand particle deposition and aggregation with porous media. To accomplish this four objectives were highlighted which focussed on two systems. Firstly, the aggregation system, this resulted in a suitable agent based modelling framework to be developed and tested along with the incorporation of a particle trajectory algorithm. Secondly, deposition within porous media, this allowed for the development of a suitable fluid solver to be developed to capture flow dynamics within the medium and then the incorporation of both particle trajectory and fluid solver in understanding the sensitivities of key colloidal deposition variables.

7.1 Summary and Conclusions

In Chapter 2, the current field of colloid filtration theory was addressed and key problem areas were discussed. In particular, the current development of deposit geometry as well as sensitivities in rates of deposition and re-entrainment within porous media. This analysis showed that there is currently a lack of understanding in deposit morphology and location on the collector surface. As such, a new style of modelling is needed to analyse these localised phenomena and address how they affect the macroscale.

Chapter 3, analysed the current literature on particle dynamics within porous media along with current agent based modelling methods and addressing the most suitable agent based modelling simulation suite (objective 1). By addressing various methods, such as, continuum models and molecular dynamics there can be seen to be a lack of attention given to meso-scale processes. By utilising the agent based modelling paradigm it was found that there was less restriction on spatio-temporal processes associated with molecular dynamics. In particular, the use of a “rule” based system over

potential based modelling allows for a large range of environments to be tested allowing for parameter sweeping to occur and key sensitivities to be extracted. Furthermore, the introduction of agents as autonomous interacting particles allows for deposition geometries to be developed without the use of complex mathematical formulae, this also allows for the study of particle removal from deposit or aggregate complexes more easily. However, there are a number of draw backs associated with agent based models by undertaking the rule based approach to problem solving the decision is in the hands of the modeller on which parameters are key in the "rules" and which can be neglected or have little influence on the emergent phenomena. In comparison, molecular dynamic based models solve potential interactions allowing for parameters to be incorporated when and where they are needed. Furthermore, a suitable implementation environment needs to be fully understood when developing agent based models. Currently, there are a number of environments which allow for rapid implementation of agent based models. These environments range from little programming knowledge to complete programming knowledge. After a search of the literature in regards to the most commonly used ABM suites, NetLogo was chosen for its easy learning curve, large amount of learning materials in the form of tutorials and examples, and its validation within the literature. When using NetLogo there are some caveats which must be observed due to the models conversion from Logo to Java there is limited memory storage, hence, agent numbers are limited in comparison to other suites. Furthermore, debugging can be an issue as Java based issues result in the model shutting down without any error messages.

After addressing the suitable choice of ABM suite in Chapter 3, Chapter 4 focussed on implementing the lattice Boltzmann model within agent based modelling and analysing its uses as a suitable fluid solver in approximating fluid flow within porous media (objective 2). Here the lattice Boltzmann method was chosen to implement the

flow field. This was due to how boundary conditions are implemented in comparison to alternative fluid solver methods. Furthermore, this method inherently behaves like an ABM in effect localised interactions at the mesoscale produce emergent phenomena in macroscale in the way of key parameters fluid velocity and density. To ensure that the lattice Boltzmann method could be incorporated within NetLogo a series of validation exercises were undertaken. The first validation exercise was the traditional Poiseuille flow, which captures a gravity drive flow between two plates. This was chosen as it has an analytical solution and as such convergence testing can be undertaken relatively easily. The results showed good agreement between the NetLogo data and that of the analytical solution. Furthermore, when the lattice size is reduced there is a significant reduction in the L^2 norm error. The second validation test, Lid driven cavity flow, incorporated a moving boundary along with reflective boundaries within the cavity. Due to a lack of an analytical solution the NetLogo model was compared to the FEM model produced by Ghia *et* al, which is traditionally used as benchmarking test in fluid dynamics. It could be seen that the difference between the two models was nominal indicating that the flow boundary and reflective boundaries captured this phenomena well. Finally, flow around a cylinder at various Reynolds numbers was tested and compared against a number of literature and experimental derived results. Here, it could be seen that the drag coefficients perform well compared to the literature derived results. Furthermore, the Strouhal number also compared well against the Grucelski & Pozorski results. However, the inherent issue within NetLogo was grid refinement. Due to the nature of NetLogo refinement of the grid occurs over the whole domain this can be costly in terms of computational run time. Furthermore, the implementation of this method is not optimised compared to alternative LB solvers. By implementing the LBM in NetLogo it allows all modelling to remain in-house at the cost of computational run time. Alternatively, a traditional LB solver could be utilised

and the flow field converted into NetLogo parameters though this would require extra computation within the NetLogo model.

Chapter 5, focussed on choosing a suitable particle trajectory equation and using this equation to address the suitability of agent based modelling in the role of understanding particle aggregation (objective 3). After a literature search it became apparent that the algorithm developed by Minier *et* al, was most suited for this role due to its large time stepping capabilities, as well as previously being validated for wall boundary interactions. Validation of this method within NetLogo was achieved by simulating the behaviour of diffusing colloidal particles with collisions modelled using a simple set of rules which relied on NetLogo's own inbuilt primitives. This allowed for a significant reduction in run times where agents within the model did not need to test their likelihood of collision with all of agents in the domain but only the closest ones within a defined region. Furthermore, the collision energy was simplified to a simple IF/OR statement allowing for a more efficient calculation of collisions between particles. These rules were shown to capture colloidal aggregation well when compared to the analytical solutions produced by Elimelech. Furthermore, when reaction limited system modelled by Behrens was included in our model there could be seen to be good agreement between the two. Finally, when the geometric radius of gyration was calculated for the two systems, there was good agreement between the NetLogo model and that of the literature described values. After validation of the particle tracking method was undertaken extensions were made to be incorporate the secondary minima term and explore the likelihood of particle aggregation and disaggregation when captured within this minima. The results showed that particle aggregation within the secondary minima is inherently sensitive to ionic strength highlighting the need for more research in the dynamics of particles captured within the secondary minima. Overall, the particle tracking algorithm and agent based rule system showed good

agreement with other modelling techniques whilst also allowing an exploration of the secondary minima problem within colloidal aggregation. There were some drawbacks with the model; namely focussed on limited sample size numbers, and the use of homogenous particles within the system. This could be addressed by scaling the model in an alternative modelling suite which allows for high performance computing capabilities.

In chapter 6, the incorporation of both the particle tracking algorithm along with the LB model was undertaken to analyse the key deposition behaviour of particles (objective 4). This was achieved by analysing particle-surface deposition and then secondary particle-particle deposition in varying physical and chemical conditions. Particle transportation and deposition was analysed initially by the collector efficiency term (η), this was compared against the literature derived value. Interestingly within the collector efficiency term was calculated correctly until a large particle size was introduced ($d > 1x10^6$ μm) in which case the model results diverged from the empirical solution. However with the incorporation of the gravity term within the particle trajectory algorithm the collector efficiency was correctly calculated within the model. Once validation of the transportation of the particles was undertaken, incorporation of the DLVO equation was used to understand how surface chemistry affects deposition. It could be seen that deposition is inherently unachievable within the primary minimum and as such deposition can be considered to solely consist in the secondary minima. With low flow environments in which the predominant transportation mechanism is diffusion there can be seen to be a large uptake in particle deposits even in shallow secondary minima wells, though these particles cannot be considered irreversibly captured. Furthermore, a particle-particle deposition model was explored which allows for key sensitivities in deposit profiles and locations to be understood. This showed that particle-particle deposition is inherently sensitive to both physical

and chemical systems. However, the focus on this model was to understand how homogeneous particles interact in an idealised collector without any emphasis on particle-fluid interactions or particle transportation on the collector surface (rolling & tumbling). By incorporation of surface dynamics, particle-fluid dynamics, and heterogeneous particles within the model a more complete system could be developed.

Overall, NetLogo as a viable simulation suite for studying and understanding colloidal behaviour, in both purely aggregating systems and depositing systems, is well founded. Not only does the simulation suite offer a much easier learning curve than alternative modelling suites along with its large database of extensions allowing for compatibility with a number of more traditional modelling platforms. It also makes an ideal choice for analysing the sensitivities of particle aggregation and deposition as well as bridging the gap between molecular dynamics and continuum dynamics.

7.2 Further work

The current model focuses on single collector processes in a 2D domain utilising homogeneous colloidal populations, this was undertaken to both simplify the problem and analyse the performance of agent based modelling as suitable modelling platform for colloidal processes. In reality, these problems are multi-facetted in which populations of colloidal particles are highly heterogeneous and are influenced by a number of parameters within the 3D domain. As such, a number of extensions could be undertaken to model these processes in 3D. Firstly, NetLogo does offer a 3D version of its modelling system with the caveat that there are less inbuilt primitives and modelling time is longer.

Alternative agent-based modelling suite such as RePast may also be used; this would offer greater computation performance due to its use of traditional languages in

comparison to NetLogo, however, at the cost of simplicity. The current version of RePast allows for importation of NetLogo models allowing for the ease of NetLogo and the robustness of RePast to be utilised. Furthermore, the use of RePast would allow access to high performance computing which would allow for much larger concentrations of particles to be studied and the full emergence of porous media could be fully understood. Indeed, microfluidic experiments could be exactly replicated within the modelling environment and variation in flow dynamics, surface structures, and surface chemistry could be more extensively studied in a 3D environment.

The techniques used to model the flow field focused on the lattice Boltzmann model, in particular, the use of the D2Q9 model which uses a single relaxation term and a fixed grid approach for modelling fluid flow. Alternative methods exist which utilise a multiple relaxation method on a varying grid resolution allowing for more accurate capture of flow dynamics around collector surfaces.

Recent pilot studies using microfluidic flow experiments undertaken by the author have found that the behaviour of the particle around the collector is highly dynamic and sensitive to local flow conditions. Therefore, a two-way couple LB model would allow for a more realistic reflection of the system. In particular, re-entrainment and particle growth dynamics could be analysed in much greater detail. By using NetLogo's ability to important images into the domain direct comparison of colloidal deposition could be undertaken along with parameter sweeping to capture interesting model dynamics.

Appendix A. NetLogo code for Poiseuille flow

The below code shows the implementation of the lattice Boltzmann method within NetLogo:

```
Globals [uMax Re nu tau omega t1 t2-5 t6-9 new-ux old-ux max-
modulus]

Patches-own[new-rho rho u-f ux uy solid f1i f2i f3i f4i f5i f6i f7i
f8i f9i f1o f2o f3o f4o f5o f6o f7o f8o f9o cx1 cx2 cx3 cx4 cx5 cx6
cx7 cx8 cx9 cy1 cy2 cy3 cy4 cy5 cy6 cy7 cy8 cy9]

to setup

  clear-all

 ;;General flow constants

  let lx world-width

  let ly world-height

  ask patches [if pycor = min-pycor [set pcolor grey set solid 1]]

  ask patches [if pycor = max-pycor [set pcolor grey set solid 1]]

  set new-ux 0

  set uMax 0.065

  set tau 0.73

  set Re uMax * world-height / ((tau - 0.5) / 3)

  set nu uMax * world-width / Re

  set omega 1 / tau;1 / ( 3 * nu + 1 / 2)

  initial-conditions ;; sets up the fluid domain

  reset-ticks

end


to initial-conditions ;; D2Q9

  set t1 4 / 9 set t2-5 1 / 9 set t6-9 1 / 36

  ask patches [set cx1 0 set cx2 1 set cx3  0 set cx4  -1 set cx5 0
set cx6  1 set cx7  -1 set cx8 -1 set cx9 1

  set cy1 0 set cy2 0 set cy3  1 set cy4  0 set cy5 -1 set cy6  1
set cy7  1 set cy8 -1 set cy9 -1

  if pcolor = grey [set solid 1]]
```

```
  ask patches [ if solid != 1 [

    let L  world-height - 2

  let y_phys pycor - 1.5

    set ux 0

    set uy 0

    set rho 1

    set f1i rho * t1   ;* (1 + (3 * (cx1 * ux + cy1 * uy)) + 1 / 2
* ((3 * (cx1 * ux + cy1 * uy)) * (3 * (cx1 * ux + cy1 * uy))) - 3 /
2 * (ux ^ 2 + uy ^ 2))

    set f2i rho * t2-5 ;* (1 + (3 * (cx2 * ux + cy2 * uy)) + 1 / 2
* ((3 * (cx2 * ux + cy2 * uy)) * (3 * (cx2 * ux + cy2 * uy))) - 3 /
2 * (ux ^ 2 + uy ^ 2))

    set f3i rho * t2-5 ;* (1 + (3 * (cx3 * ux + cy3 * uy)) + 1 / 2
* ((3 * (cx3 * ux + cy3 * uy)) * (3 * (cx3 * ux + cy3 * uy))) - 3 /
2 * (ux ^ 2 + uy ^ 2))

    set f4i rho * t2-5 ;* (1 + (3 * (cx4 * ux + cy4 * uy)) + 1 / 2
* ((3 * (cx4 * ux + cy4 * uy)) * (3 * (cx4 * ux + cy4 * uy))) - 3 /
2 * (ux ^ 2 + uy ^ 2))

    set f5i rho * t2-5 ;* (1 + (3 * (cx5 * ux + cy5 * uy)) + 1 / 2
* ((3 * (cx5 * ux + cy5 * uy)) * (3 * (cx5 * ux + cy5 * uy))) - 3 /
2 * (ux ^ 2 + uy ^ 2))

    set f6i rho * t6-9 ;* (1 + (3 * (cx6 * ux + cy6 * uy)) + 1 / 2
* ((3 * (cx6 * ux + cy6 * uy)) * (3 * (cx6 * ux + cy6 * uy))) - 3 /
2 * (ux ^ 2 + uy ^ 2))

    set f7i rho * t6-9 ;* (1 + (3 * (cx7 * ux + cy7 * uy)) + 1 / 2
* ((3 * (cx7 * ux + cy7 * uy)) * (3 * (cx7 * ux + cy7 * uy))) - 3 /
2 * (ux ^ 2 + uy ^ 2))

    set f8i rho * t6-9 ;* (1 + (3 * (cx8 * ux + cy8 * uy)) + 1 / 2
* ((3 * (cx8 * ux + cy8 * uy)) * (3 * (cx8 * ux + cy8 * uy))) - 3 /
2 * (ux ^ 2 + uy ^ 2))

    set f9i rho * t6-9 ;* (1 + (3 * (cx9 * ux + cy9 * uy)) + 1 / 2
* ((3 * (cx9 * ux + cy9 * uy)) * (3 * (cx9 * ux + cy9 * uy))) - 3 /
2 * (ux ^ 2 + uy ^ 2))

  set new-rho f1i + f2i + f3i + f4i + f5i + f6i + f7i + f8i + f9i

  ]]
```

```
end


to main-cycle
  set old-ux new-ux
  ask patches [ ;;Macroscopic variables
    if solid != 1 [
      set rho f1i + f2i + f3i + f4i + f5i + f6i + f7i + f8i + f9i
      set ux  ((f1i * cx1) + (f2i * cx2) + (f3i * cx3) + (f4i *
cx4) + (f5i * cx5) + (f6i * cx6) + (f7i * cx7) + (f8i * cx8) + (f9i
* cx9)) / rho
      set uy  ((f1i * cy1) + (f2i * cy2) + (f3i * cy3) + (f4i *
cy4) + (f5i * cy5) + (f6i * cy6) + (f7i * cy7) + (f8i * cy8) + (f9i
* cy9)) / rho
      ]
]
      ;;Equilbrium distribution and collision steps
     ask patches [ if solid != 1 [
      let ux1 ux + (6.37867E-05 * tau) ;; Forcing term incorporated
here
     let feq1 rho * t1   * (1 + (3 * (cx1 * ux1 + cy1 * uy)) + 1 /
2 * ((3 * (cx1 * ux1 + cy1 * uy)) * (3 * (cx1 * ux1 + cy1 * uy))) -
3 / 2 * (ux1 ^ 2 + uy ^ 2))
     let feq2 rho * t2-5 * (1 + (3 * (cx2 * ux1 + cy2 * uy)) + 1 /
2 * ((3 * (cx2 * ux1 + cy2 * uy)) * (3 * (cx2 * ux1 + cy2 * uy))) -
3 / 2 * (ux1 ^ 2 + uy ^ 2))
     let feq3 rho * t2-5 * (1 + (3 * (cx3 * ux1 + cy3 * uy)) + 1 /
2 * ((3 * (cx3 * ux1 + cy3 * uy)) * (3 * (cx3 * ux1 + cy3 * uy))) -
3 / 2 * (ux1 ^ 2 + uy ^ 2))
     let feq4 rho * t2-5 * (1 + (3 * (cx4 * ux1 + cy4 * uy)) + 1 /
2 * ((3 * (cx4 * ux1 + cy4 * uy)) * (3 * (cx4 * ux1 + cy4 * uy))) -
3 / 2 * (ux1 ^ 2 + uy ^ 2))
     let feq5 rho * t2-5 * (1 + (3 * (cx5 * ux1 + cy5 * uy)) + 1 /
2 * ((3 * (cx5 * ux1 + cy5 * uy)) * (3 * (cx5 * ux1 + cy5 * uy))) -
3 / 2 * (ux1 ^ 2 + uy ^ 2))
```

```
    let feq6 rho * t6-9 * (1 + (3 * (cx6 * ux1 + cy6 * uy)) + 1 /
2 * ((3 * (cx6 * ux1 + cy6 * uy)) * (3 * (cx6 * ux1 + cy6 * uy))) -
3 / 2 * (ux1 ^ 2 + uy ^ 2))

    let feq7 rho * t6-9 * (1 + (3 * (cx7 * ux1 + cy7 * uy)) + 1 /
2 * ((3 * (cx7 * ux1 + cy7 * uy)) * (3 * (cx7 * ux1 + cy7 * uy))) -
3 / 2 * (ux1 ^ 2 + uy ^ 2))

    let feq8 rho * t6-9 * (1 + (3 * (cx8 * ux1 + cy8 * uy)) + 1 /
2 * ((3 * (cx8 * ux1 + cy8 * uy)) * (3 * (cx8 * ux1 + cy8 * uy))) -
3 / 2 * (ux1 ^ 2 + uy ^ 2))

    let feq9 rho * t6-9 * (1 + (3 * (cx9 * ux1 + cy9 * uy)) + 1 /
2 * ((3 * (cx9 * ux1 + cy9 * uy)) * (3 * (cx9 * ux1 + cy9 * uy))) -
3 / 2 * (ux1 ^ 2 + uy ^ 2))


    set f1o f1i - (f1i - feq1) / tau

    set f2o f2i - (f2i - feq2) / tau

    set f3o f3i - (f3i - feq3) / tau

    set f4o f4i - (f4i - feq4) / tau

    set f5o f5i - (f5i - feq5) / tau

    set f6o f6i - (f6i - feq6) / tau

    set f7o f7i - (f7i - feq7) / tau

    set f8o f8i - (f8i - feq8) / tau

    set f9o f9i - (f9i - feq9) / tau

    ]]

   ;; bounce-back (mid-plane for walls)



;   7         3        6

;   4         1        2

;   8         5        9


 ask patches [  if solid = 1 [

     if pycor = min-pycor     [   ;dx dy

       set f3o [f5i]  of patch-at 0 1
```

```
        set f6o [f8i]  of patch-at 1 1
        set f7o [f9i]  of patch-at -1 1
    ]

   if pycor = max-pycor     [   ;dx dy
        set f5o [f3i]  of patch-at 0 -1
        set f8o [f6i]  of patch-at -1 -1
        set f9o [f7i]  of patch-at 1 -1
    ]
    ]
  ]

    ;;streaming step
  ask patches[  if solid != 1  [
        set f1i f1o
        set f2i [f2o] of patch-at -1 0
        set f3i [f3o] of patch-at 0 -1
        set f4i [f4o] of patch-at 1 0
        set f5i [f5o] of patch-at 0 1
        set f6i [f6o] of patch-at -1 -1
        set f7i [f7o] of patch-at 1 -1
        set f8i [f8o] of patch-at 1 1
        set f9i [f9o] of patch-at -1 1
  ]
    set u-f sqrt (ux ^ 2 + uy ^ 2)
  ]
  ask patches [if solid != 1 [set pcolor scale-color blue ux 0.065
0]]
  set new-ux sum [ux] of patches
  tick
end
```

Appendix B. NetLogo code for implementation of diffusion limited aggregation

```
;;;
 This model analyses the behaviour of particle aggregation between
homogeneous and heterogeneous particles, using standard DLVO and
stochastic solutions to the equation of motions
;;;
;; Constants, particle, and fluid variables


globals [kB T nu-f rho-f I delta-t stick-counter collision-counter
non-stick-counter]
patches-own[]
turtles-own[r rho-p mp Ek u ux uy tau Bx me collide]


;; initialise phase;;


to initialise
  clear-all   ;; removes any legacy coding
  constants   ;; introduces constants
  particles   ;; sets up particles
  fluids      ;; ses up fluid
  DLVO        ;; produces initial DLVO curve
  reset-ticks ;; resets the iterator
end


to constants        ;; units
  set kB 1.38e-23   ; m^2.kg.s^-2.K^-1
  set T  296.15      ; K
  set nu-f 1.83e-5  ; Pa / s
  set rho-f 1000    ; kg/m^3
end


to particles
```

```
  ask n-of n patches [sprout 1]
  ask turtles [
    set shape "circle"
    set me who ;; is set to the turtle identifier
    set collide 1
    set r 0.5e-6    ; m
    set rho-p 1000  ; kg/m^3
    let vp (4 / 3) * pi * (r) ^ 3 ; m ^ 3
    set mp rho-p * vp ; kg
    set tau mp / (6 * pi * nu-f * r) ; s, particle relaxation time
    set Bx sqrt(2 * kB * T * (tau / mp)) ; m^2/s
  ]
  ask turtle 0 [
    type "my relax time =" print tau
    type "my mass =" print mp
    type "my diffusion co-eff =" print Bx
    type "suggested delta t =" print ((tau) * 1e6)
  ]
  set delta-t (max [tau] of turtles * 1e5) ;; time step must be
greater than relaxation time for diffusion
end


;; Simulation phase ;;


to go
  ask turtles
  [
    random-motion ;; solves the stochastic equation using Milner et
al technique
    collision     ;; checks the DLVO MAX against the collision
energy
    aggregation   ;; determines whether aggregation has occurred
  ]
  tick
```

```
end


to random-motion
  set xcor xcor + (Bx * sqrt(delta-t) * random-normal 0 1) * 1e6
  set ycor ycor + (Bx * sqrt(delta-t) * random-normal 0 1) * 1e6
  set ux Bx * sqrt(1 /(2 * tau)) * random-normal 0 1
  set uy Bx * sqrt(1 /(2 * tau)) * random-normal 0 1
  set u sqrt((ux * ux) + (uy * uy))
  set Ek (0.5 * (mp) * (u) ^ 2) /(kb * T)


end


to collision
 if (count other turtles in-radius 1 with [me != [me] of myself] >
0)
  [
    let candidate one-of other turtles in-radius (r * 1e6) with [me
!= [me] of myself]
    set collision-counter collision-counter + 1
    ifelse  (candidate != nobody) and (0 <= ek)
    [
      let new-r (([r] of candidate) ^ 3 +  r ^ 3) ^ (1 / 3)
      let new-vp (4 / 3) * pi * (new-r) ^ 3
      let new-mp rho-p * new-vp
      let new-tau new-mp / (6 * pi * nu-f * new-r)
      let new-Bx sqrt(2 * kB * T * (new-tau / new-mp))
      set r new-r  set mp new-mp set tau new-tau set Bx new-bx
      ask candidate [die]
      set size 1 + (2 * r)
      set collide collide + 1
      set stick-counter stick-counter + 1
    ]
     [set non-stick-counter non-stick-counter + 1]
   ]
```

```
end
;; Produces the DLVO plot for particles
to DLVO
clear-plot
let Na 6.022e23
let el 1.602e-19
let epi_r 80.2
let epi_0 8.8e-12
set phi 0.0192 * (I) ^ (-0.245)
let A 1e-20
let r1 (1 * 1e-6) / 2
let k1 1 / sqrt((epi_r * epi_0 * kb * T) / ((2e3) * Na * el ^ 2 *
I))
let elv 0.5 * (epi_r * epi_0) * r1 * phi ^ 2


let h 6e-10
let sep_count 1
let sep_dist 1 * 10 ^ -10
set sep_list n-values 1 [0]
set energy_list n-values 1 [0]
while [sep_count < 1000]
  [
    set sep_dist (sep_count * (1 * 10 ^ -10))
    set sep_list lput sep_dist sep_list
    set Vh   -1 * (A * r1 / ( 12 * sep_dist))
    set vd elv * log( 1 +  exp ( - k1 * sep_dist)) 10
    set vt (Vh + vd)/ ( Kb * T)  ;; this plots the total energy in
the system
    set energy_list lput vt energy_list
    set sep_count sep_count + 1
  ]
  ;;Sets the maximum energy required to overcome potential barrier
```

```
  ask turtles [set rep-en (max energy_list)]
  set maxenergy max energy_list
  set new_max position (max energy_list) energy_list

;; Sets the secondary minima depth
  ifelse new_max = 0 [
    set min_list sublist energy_list 8 (length energy_list)
  ][
  set min_list sublist energy_list new_max (length energy_list)
  ]

  set sec_min min min_list
  set sec_max max min_list
  type "sec min = " print sec_min

end
```

Appendix C. NetLogo code for implementation of particle trajectories around a single collector

```
breed [stayers stayer]

globals [primary-min secondary-min primary-agg secondary-agg]

patches-own [ vel lead-turtle stucked theta-p growth-count ux uy]

turtles-own [xc yc  sticks stucks d df r u v x-vel y-vel ek r-c
theta rc1 a1  r-c-list  leader counts linked?]

;; This imports the fluid field from the LB model and converts the
fluid flow back to dimensionlised units;;

to setup-fluid-domain

  ;; uMax values: 1.6333E-4 8.16667E-5 1.63333E-5 8.16667E-6
1.63333E-6 8.16667E-7 1.63333E-7 8.16667E-8 1.63333E-8


  import-fluid

  convert-velocity

end


to convert-velocity

  ask patches [

    set ux ux * 6.12244898


    set uy uy * 6.12244898


    set stucked false

  ]

end

;; Imports the fluid field

to import-fluid

  let filetemp word "Fluid-new " field-number

  let filename word  filetemp".csv"

  import-world filename

end


;; This sets up the agents and incorporates their variables;;
```

```
to setup
 clear-all
  set primary-agg 0
  set secondary-agg 0
  setup-fluid-domain
  random-seed new-seed
  set  primary-min 0 set secondary-min 0
  set breakthrough 0
  set collision 0
  set stuck 0
  set T 297.15 ;; absolute Temp
  set kB 1.38e-23;; Boltzmann constant
  set eta 0.000018 ;; viscosity of water in SI units
  ;; Remember at around 2 microns gravity is not minimized
  let rm (dp * 1e-6) / 2
  let n-r rm
  set mp (1055) * ((4 * pi * (n-r) ^ 3) / 3)
  set tau-p 6.58552E-08
  ;;sets a suitable time step depending on the flow field
  ifelse dp < 1
  [
  if field-number = 5 or field-number = 9[set dt 0.01]
  if field-number = 4 or field-number = 8[set dt 0.01]
  if field-number = 3 or field-number = 7[set dt 0.001]
  if field-number = 2 or field-number = 6[set dt 0.001]
  if field-number = 1 or field-number = 11[set dt 0.00001]
  ]
  [
    if field-number = 5 or field-number = 9[set dt 0.1]
    if field-number = 4 or field-number = 8[set dt 0.1]
    if field-number = 3 or field-number = 7[set dt 0.01]
    if field-number = 2 or field-number = 6[set dt 0.01]
```

```
    if field-number = 1 or field-number = 11[set dt 0.0001]
  ]
  set-default-shape turtles "circle"
  ask patches
  [ if solid != 1 [set pcolor 87]]
  ask n-of 50   patches with [pxcor = 5 ] ;; This asks a random
patch at the inlet to produce a turtle
  [
    sprout  1


  ]
  ask turtles [
    set stucks false
    set sticks 0
      set color red
      set shape "circle"
      set ycor random-float world-height
      set r n-r
      set size dp
      set Df  sqrt((kB * T) / (6 * pi * 8.9e-4 * r))   ;; This is
the area which the Stokes-Einstein diffusion coefficient is
calculated
      set xc xcor - 51
      set yc ycor - 51
      set ek random-float 1.5
      set r-c sqrt((xc * xc) + (yc * yc))
      set theta atan yc xc
      set linked? false
      set leader  self
  ]
  DLVO
  set total-agents count turtles
  reset-ticks
end
```

```
;; Change this to the SDE solution
to go
  let test count (turtles with [color = green and xcor < 2])
  ifelse test <= 0 [

    let concs count turtles with [color = red]
    if concs < 50 [create-new-agent]
    foreach sort turtles [ the-mover -> ask the-mover [move] ]
    tick
  ]

  [
    stop
  ]
end
to move
  if color = red [
;; This uses the bilinear interpolation call function
    let ux-part interpolate-x [patch-at 1 1 patch-at -1 1 patch-at
-1 -1 patch-at 1 -1]
    let uy-part interpolate-y [patch-at 1 1 patch-at -1 1 patch-at
-1 -1 patch-at 1 -1]
  set u ((ux-part * dt)  + ((random-normal 0 1) * df * sqrt(dt)))
* 1e6
  set v ((uy-part * dt) + ((random-normal 0 1) * df * sqrt(dt))) *
1e6
  set x-vel ux-part +  Df * sqrt(1 / (2 * tau-p)) * random-normal 0
1
  set y-vel uy-part +  Df * sqrt(1 / (2 * tau-p)) * random-normal 0
1
  set heading atan v u
  set vel sqrt((x-vel * x-vel) + (y-vel * y-vel))
  set ek 0.5 * mp * (vel * vel)
  set ek ek / (kb * T)
  collisions
  setxy (xcor + u) (ycor + v)
```

```
  if xcor > 95  [
    set break break + 1
    create-new-agent
    die
  ]
  ]
end


to collisions
  let candidates min-one-of (turtles in-radius (size) with [color =
green])
  [size]
  if (candidates != nobody)
  [
    if ek > rep-en
    [
      set u 0 set v 0
      create-link-with candidates [tie]
      ask candidates
      [
        merge
      ]
      set counts count turtles with [leader = myself]
      set color green
      set primary-min primary-min + 1
    ]
    if ek < sec-min
    [
      set u 0 set v 0
      create-link-with candidates [tie]
      ask candidates
      [
        merge
      ]
```

```
      set counts count turtles with [leader = myself]
      set color green
      set secondary-min secondary-min + 1
    ]
    if ek > sec-min and ek < rep-en
    [
      set u u * -1
      set v v * -1
      set reflection reflection + 1
    ]

  ]
  if any? patches in-radius (size) with [solid = 1]
  [
    set color green
    set sticks 1
    set u 0 set v 0
    ask patch-here [set pcolor red set stucked true set theta-p
atan y x ]
    set counts count turtles with [leader = myself]
    create-new-agent
    die
  ]

  ask turtles with [color = green][set counts [counts] of leader]

end
to create-new-agent
  ask n-of 1 patches with [pxcor = 1 ] ;; This asks a random patch
at the inlet to produce a turtle
  [
    sprout  1
    [
      set leader self
```

```
       set sticks 0
      set r (dp * 1e-6) / 2
     set ycor random-float world-height
      set color red
      set shape "circle"
      set size dp
      set Df  sqrt((kB * T) / (6 * pi * 8.9e-4 * r))
      set xc xcor - 51
      set yc ycor
      set r-c sqrt((xc * xc) + (yc * yc))
      set theta atan yc xc
      set ek random-float 1.5
    ]
  ]
  set total-agents total-agents + 1
end
;; Solves the DLVO equation for particle-particle interaction, in
this model deposition on the collector surface is assumed
attractive
to DLVO


let Na 6.022e23
let el 1.602e-19
let epi_r 80.2
let epi_0 8.8e-12
let phi 0.0192 * (I) ^ (-0.245)
let A 1e-20
let r1 dp * 0.5e-6
let k1 1 / sqrt((epi_r * epi_0 * kb * T) / ((2e3) * Na * el ^ 2 *
I))
let elv 0.5 * (epi_r * epi_0) * r1 * phi ^ 2


let h 6e-10
let sep_count 1
```

```
let sep_dist 1 * 10 ^ -10
set sep_list n-values 1 [0]
set energy_list n-values 1 [0]
while [sep_count < 1000]
  [
    set sep_dist (sep_count * (1 * 10 ^ -10))
    set sep_list lput sep_dist sep_list
    let Vh   -1 * (A * r1 / ( 12 * sep_dist))
    let vd elv * log( 1 +  exp ( - k1 * sep_dist)) 10
    let vt (Vh + vd)/ ( Kb * T)  ;; this plots the total energy in
the system
    set energy_list lput vt energy_list
    set sep_count sep_count + 1
  ]
  set rep-en (max energy_list)
  type "Max energy = "  print max energy_list
  let new_max position (max energy_list) energy_list
  ;print length energy_list
  let new_list sublist energy_list new_max (length energy_list)
  ;print length new_list
  set sec-min min new_list



end


to merge
  set leader [leader] of myself
  set color green
  set stucks true
  ask link-neighbors with [who < [who] of myself]
  [merge]


end
;; Bilinear interpolation mechanism for fluid velocity
```

```
to-report interpolate-ux

  let Q11 [ux] of p1

  let Q21 [ux] of p2

  let Q12 [ux] of p3

  let Q22 [ux] of p4

  let int-1 (([xcor] of p2) - xcor)*([ycor] of p2) - ycor))/([xcor]
of p2) - [xcor] of p1)*([ycor] of p2) - [ycor] of p1)) * Q11

 let int-2 ((xcor) - [xcor] of p1)*([ycor] of p2) - ycor))/([xcor]
of p2) - [xcor] of p1)*([ycor] of p2) - [ycor] of p1)) * Q21

 let int-3 (([xcor] of p2) - xcor)*([ycor] of p2) - ycor))/([xcor]
of p2) - [xcor] of p1)*([ycor] of p2) - [ycor] of p1)) * Q12

 let int-4 ((xcor) - [xcor] of p1)*([ycor] of p2) - ycor))/([xcor]
of p2) - [xcor] of p1)*([ycor] of p2) - [ycor] of p1)) * Q22

report int-1 + int-2 + int-3 + int-4

end


to-report interpolate-uy

  let Q11 [uy] of p1

  let Q21 [uy] of p2

  let Q12 [uy] of p3

  let Q22 [uy] of p4

  let int-1 (([xcor] of p2) - xcor)*([ycor] of p2) - ycor))/([xcor]
of p2) - [xcor] of p1)*([ycor] of p2) - [ycor] of p1)) * Q11

 let int-2 ((xcor) - [xcor] of p1)*([ycor] of p2) - ycor))/([xcor]
of p2) - [xcor] of p1)*([ycor] of p2) - [ycor] of p1)) * Q21

 let int-3 (([xcor] of p2) - xcor)*([ycor] of p2) - ycor))/([xcor]
of p2) - [xcor] of p1)*([ycor] of p2) - [ycor] of p1)) * Q12

 let int-4 ((xcor) - [xcor] of p1)*([ycor] of p2) - ycor))/([xcor]
of p2) - [xcor] of p1)*([ycor] of p2) - [ycor] of p1)) * Q22

report int-1 + int-2 + int-3 + int-4


end
```